NPS ARCHIVE
1964
MLEKUSH, M.

Thesis
M655

Library
U. S. Naval Postgraduate School
Monterey, California

TRANSMISSION AND REFLECTION OF DEEP WATER WAVES FROM A SUBMERGED BREAKWATER

by

Matt Clarence Mlekush

B.S., United States Naval Academy, 1955

B.S.(C.E.), Rensselaer Polytechnic Institute, 1959

A Thesis submitted to the Faculty of the Graduate School of the University of Colorado in partial fulfillment of the requirements for the Degree

Master of Science

Department of Civil Engineering

1964

NPS ARCHIVE
1964
WILEKUSH, M

Library
U. S. Naval Postgraduate School
Monterey, California

This Thesis for the M.S. degree by

Matt Clarence Mlekush

has been approved for the

Department of

Civil Engineering

by

Mlekush, Matt Clarence (M.S., Civil Engineering)

Transmission and Reflection of Deep Water Waves from a Submerged Breakwater

Thesis directed by Associate Professor J. Ernest Flack

Laboratory research on the characteristics and motion of gravity waves has not kept pace with the theoretical treatment of wave phenomena. Only a limited amount of research has been performed on the reflection and transmission of waves from submerged objects. When a wave impinges on a submerged object only part of the original wave is transmitted beyond the object, the rest is either reflected or dissipated.

The primary purpose of this investigation was to relate the effects of the incident wave characteristics, and the height and width of the submerged structure to the reflection and transmission of waves. The basic submerged structure used in this investigation was a quarter cylinder. The width was changed by installing additional structures. The height of the breakwater was varied in three-inch increments. A reciprocating plunger type wave generator located at one end of the channel produced the periodic progressive two-dimensional gravity waves. Only deep water waves, i.e. waves in which the stillwater depth is greater than one-half the wave length, were studied.

The height of the transmitted wave and the height of the superimposed reflected and incident waves were measured by means of variable resistance gauges. A continuous record was produced by an optically recording oscillograph.

The results of the experiments indicate that the breakwater

height has the greatest effect on the transmission and reflection of waves. At low breakwater heights, most of the original wave is transmitted, while at high breakwater heights, most is reflected. However, when the breakwater height equalled the stillwater depth the incident wave broke at the upstream face of the breakwater resulting in less reflection. Waves of low steepnesses are reflected more than steep waves, other things being equal. Increasing the width of the breakwater decreased the amount of transmission.

This abstract of about 250 words is approved as to form and content.

TO MY WIFE

TABLE OF CONTENTS

CHAPTER		PAGE
I.	INTRODUCTION	1
II.	REVIEW OF PREVIOUS WORK	4
III.	THEORETICAL DEVELOPMENT	14
IV.	EXPERIMENTAL APPARATUS	26
	Wave Tank and Generator	26
	Recording Apparatus	27
	Breakwater	28
V.	EXPERIMENTAL PROCEDURE	34
VI.	EXPERIMENTAL RESULTS	39
VII.	CONCLUSIONS	44
	BIBLIOGRAPHY	92

LIST OF FIGURES

FIGURE		PAGE
1.	Beach Erosion Board Models	5
2.	Graphical Summary of Priest's Investigation for Smooth Waves	9
3.	Graphical Summary of Priest's Investigation for Breaking Waves	9
4.	Theoretical Reflection and Transmission Coefficient Values for a Thin Vertical Barrier Obtained by Ursell,	12
5.	Theoretical Reflection and Transmission Coefficient Values for a Thin Vertical Barrier Obtained by Dean.	12
6.	Theoretical Reflection and Transmission Coefficient Values for Vertical Reef Obtained by Fuchs and Lamb.	13
7.	Definition Sketch	15
8.	Variation in Amplitude for Partial Clapotis	24
9.	Cone of Influence of Wave Motion	25
10.	Wave Tank	29
11.	Wave Filter	30
12.	V-Shaped Plunger-type Generator	31
13.	Variable Resistance Probes and Carriage	32
14.	Visicorder Oscillograph Recorder	33
15.	Wave Action Over the Submerged Breakwater	33
16.	Breakwater Configurations.	34
17.	Example of Calibration Trace	35
18.	Sample of Wave Record Trace	37

FIGURE PAGE

19. Reflection Coefficient vs. Submergence Ratio for Relative Depths and Wave Steepnesses, Breakwater A . . 49

20. Reflection Coefficients vs. Submergence Ratio for Relative Depths and Wave Steepnesses, Breakwater B . . 50

21. Reflection Coefficients vs. Submergence Ratio for Relative Depths and Wave Steepnesses, Breakwater C . . 51

22. Reflection Coefficients vs. Submergence Ratio for Relative Depths and Wave Steepnesses, Breakwater D . . 52

23. Transmission Coefficients vs. Submergence Ratio for Relative Depths and Wave Steepnesses, Breakwater A . . 53

24. Transmission Coefficients vs. Submergence Ratio for Relative Depths and Wave Steepnesses, Breakwater B . . 54

25. Transmission Coefficients vs. Submergence Ratio for Relative Depths and Wave Steepnesses, Breakwater C . . 55

26. Transmission Coefficients vs. Submergence Ratio for Relative Depths and Wave Steepnesses, Breakwater D . . 56

27. Reflection Coefficients vs. Submergence Ratio for Relative Widths, $H_i/L = 0.0222$ 57

28. Reflection Coefficients vs. Submergence Ratio for Relative Widths, $H_i/L = 0.0333$ 58

29. Reflection Coefficients vs. Submergence Ratio for Relative Widths, $H_i/L = 0.0455$ 59

30. Reflection Coefficients vs. Submergence Ratio for Relative Widths, $H_i/L = 0.0675$ 60

31. Transmission Coefficients vs. Submergence Ratio for

FIGURE PAGE

Relative Widths, H_i/L = 0.0222 61

32. Transmission Coefficients vs. Submergence Ratio for Relative Widths, H_i/L = 0.0383 62

33. Transmission Coefficients vs. Submergence Ratio for Relative Widths, H_i/L = 0.0455 63

34. Transmission Coefficients vs. Submergence Ratio for Relative Widths, H_i/L = 0.0675 64

35. Reflection Coefficients vs. Submergence Ratio, Comparison of Breakwaters C and D, Low Wave Steepnesses 65

36. Reflection Coefficients vs. Submergence Ratio, Comparison of Breakwaters C and D, High Wave Steepnesses 66

37. Transmission Coefficients vs. Submergence Ratio, Comparison of Breakwaters C and D, Low Wave Steepnesses 67

38. Transmission Coefficients vs. Submergence Ratio, Comparison of Breakwaters C and D, High Wave Steepnesses 68

39. Transmission Coefficient vs. Submergence Ratio, Comparison of Quarter Cylindrical Shape and Trapezoidal Shape, High Wave Steepness 69

40. Transmission Coefficient vs. Submergence Ratio, Comparison of Quarter Cylindrical Shape and Trapezoidal Shape, Low Wave Steepness. 70

FIGURE PAGE

41. Transmission Coefficient vs. Submergence Ratio Comparison of Quarter Cylindrical Shape and Triangular Shape, High Wave Steepness 71

42. Transmission Coefficient vs. Submergence Ratio, Comparison of Quarter Cylindrical Shape and Triangular Shape, Low Wave Steepness 72

43. Reflection Coefficients vs. Effective Wave Motion Ratio, For Different Wave Steepnesses, Breakwater A . . 73

44. Reflection Coefficients vs. Effective Wave Motion Ratio, For Different Wave Steepnesses, Breakwater B . . 74

45. Reflection Coefficients vs. Effective Wave Motion Ratio, For Different Wave Steepnesses, Breakwater C . . 75

46. Reflection Coefficients vs. Effective Wave Motion Ratio, For Different Wave Steepnesses, Breakwater D . . 76

47. Transmission Coefficients vs. Effective Wave Motion Ratio, For Different Wave Steepnesses, Breakwater A . . 77

48. Transmission Coefficients vs. Effective Wave Motion Ratio, For Different Wave Steepnesses, Breakwater B . . 78

49. Transmission Coefficients vs. Effective Wave Motion Ratio, For Different Wave Steepnesses, Breakwater C . . 79

50. Transmission Coefficients vs. Effective Wave Motion Ratio, For Different Wave Steepnesses, Breakwater D . . 80

LIST OF TABLES

TABLE		PAGE
I.	EXPERIMENTAL DATA - SUBMERGENCE RATIO BREAKWATER A	81
II.	EXPERIMENTAL DATA - SUBMERGENCE RATIO BREAKWATER B	82
III.	EXPERIMENTAL DATA - SUBMERGENCE RATIO BREAKWATER C	83
IV.	EXPERIMENTAL DATA - SUBMERGENCE RATIO BREAKWATER D	84
V.	EXPERIMENTAL DATA - SUBMERGENCE RATIO BREAKWATER HEIGHT EQUALS STILLWATER DEPTH.	85
VI.	EXPERIMENTAL DATA - EFFECTIVE WAVE MOTION RATIO BREAKWATER A	86
VII.	EXPERIMENTAL DATA - EFFECTIVE WAVE MOTION RATIO BREAKWATER B	87
VIII.	EXPERIMENTAL DATA - EFFECTIVE WAVE MOTION RATIO BREAKWATER C	88
IX.	EXPERIMENTAL DATA - EFFECTIVE WAVE MOTION RATIO BREAKWATER D	89
X.	EXPERIMENTAL DATA - EFFECTIVE WAVE MOTION RATIO BREAKWATER HEIGHT EQUALS STILL WATER DEPTH	90
XI.	LIST OF SYMBOLS.	91

CHAPTER I

INTRODUCTION

Since the beginning of time man has depended upon the sea for much of his livelihood. At times the sea was his greatest friend and yet sometimes his worst enemy. The rise and fall of the tide, the movement of the waves to shore and their ultimate breaking and power to shape the shoreline has always fascinated man. However, relatively little research was undertaken in an effort to understand the structure and characteristics of waves until after the beginning of the twentieth century.

Wind-generated waves are the most common waves that exist in nature. The most destructive waves, however, are those generated by earthquakes. These seismic waves, referred to as "tsunamis", travel great distances at an average velocity of over 450 miles per hour. Just recently (May 1964) the tsunamis generated by the Alaskan earthquake caused the loss of many lives and property damage estimated in the millions of dollars in Crescent City, California which was over 1500 miles from the epicenter of the quake. It has been noted that the presence of a wide continental shelf provides a reasonable degree of protection of the coastline against the full impact of these seismic waves.

The everyday problems confronting the coastal and hydraulic engineers center around harbor protection and beach erosion.

Structures, thought to be capable of withstanding the force of water waves, have been completely destroyed or rendered useless by wave action. In an effort to duplicate the effects of the continental shelf, engineers turned their attention to the employment of submerged breakwaters. A submerged breakwater is a barrier so constructed that its top is at the same elevation, or slightly below, the still-water level. These barriers, either partially or completely, reflect and/or transmit the incident wave energy or dissipate the incident wave energy at the barrier.

Various geometric shapes and kinds of structures have been investigated to determine their effectiveness in reducing the wave energy which is transmitted shoreward. However, little attention has been given to the reflective effect of these structures. The author of this paper has attempted to investigate various factors relating to the effectiveness of a particular submerged breakwater in the transmission and reflection of gravity water waves.

It is impossible to duplicate natural conditions in a laboratory since natural waves are the result of the intersection of many wave trains which have differing wave-lengths and directions. These wave trains are usually formed in the generating area. The intersection of these multiple waves gives rise to an extremely wide spectrum of waves. However, as waves move away from their source of generation they become more symmetrical in form and therefore can be reasonably duplicated in a long channel. This experiment was confined to two-dimensional deep water waves. The effectiveness of the test structure, for various degrees of submergence and width, was determined by relating the amount of reflection and transmission to

the original incident wave.

For this investigation the reflection coefficient was defined as the ratio of maximum height of the superimposed reflected and incident waves to the height of the incident wave. The transmission coefficient was defined as the ratio of the height of the transmitted wave to the incident wave.

CHAPTER II

REVIEW OF PREVIOUS WORK

Rigorous theoretical treatment of gravity waves has been known for many years, but it was only recently that the phenomenon of gravity waves was studied in laboratory experiments. The complexity of the theoretical treatment, even after utilizing simplifying assumptions, gives rise to a variety of solutions concerning the motion and paths of water particles in a progressive wave train.

One of the earliest laboratory investigations reporting on the effectiveness of submerged breakwaters was published in 1940 by the Beach Erosion Board.[1*] This paper provided reliable data on the damping effectiveness of three cross-sectional configurations; namely, trapezoidal, triangular and a thin vertical flat plate. The water depths used in the experiments varied from 0.9 to 1.5 times the height of the structures. The data gathered, which included wave period, height, length and celerity, were the averages of 10 to 30 measurements. The ratio of the shoreward wave height, H_l , to the seaward wave height, H_s, was used to indicate the effectiveness of the structures in stilling the waves. A plot of the ratio of H_l/H_s versus the submergence ratio, which was defined as the ratio of the

---

* Superscripts refer to references listed in Bibliography.

stillwater depth to the height of the structure, was used to summarize the results. The vertical plate was most effective in stilling the waves, for submerging ratio over 1.1. The trapezoidal shape was more effective than the vertical plate at the low submergence ratios. Neither the trapezoidal or triangular shapes were effective at the high submergence ratios.

The Beach Erosion Board[2] also reported on experiments in 1944, however, these investigations were primarily concerned with the change in wave length after waves passed over a submerged reef. The three reef configurations used in the experiment are shown in Figure 1. The results of the experiment established a criteria for determining whether a wave would pass over a reef as a single wave or break into a multiplicity of waves. The parameter $\sqrt{H_o L_o / a}$ was used as the criteria, where H_o is the wave height in deep water, L_o is the wave length in deep water and a is the depth of barrier below still-water level. When the ratio was less than 2.0 the transition was regular. When the ratio was greater than 2.0, the wave passing over the reef broke into a number of waves.

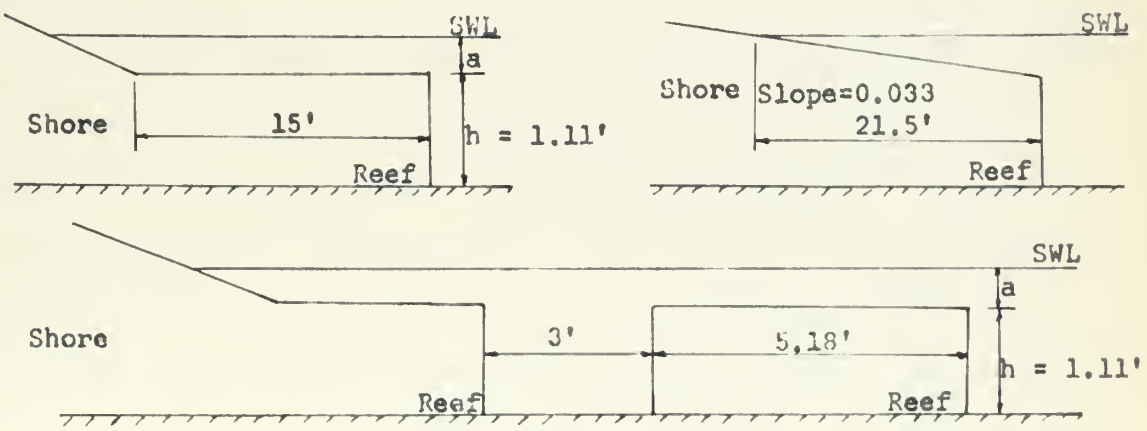

FIGURE 1

BEACH EROSION BOARD MODELS

The damping action of plane sloping surfaces which extended below the still water level only a portion of the total depth was investigated by Hamilton[3] in 1950. For this type barrier installation some of the wave energy was transmitted shoreward by the waves passing under the structure. The author defined the transmission coefficient as the ratio of the height of the wave inshore from the barrier to the height of the wave seaward from the barrier. The barrier was positioned, at two different angles of inclination, such that the upper edge of the plane surface was located above, at, and below the still water level. It was concluded that the transmission coefficient was a function of the relative width of the surface (wave length seaward from barrier to width of sloping barrier, L_s/B) with the angle of inclination of the surface as a parameter. Neither the wave steepness, H/L_s, or relative depth, d/L_s, were considered as possible parameters in the experiments. The completely submerged plane was found to be relatively ineffective in damping the waves, whereas when the upper edge of the sloping plane was at or above the stillwater level effective damping action was obtained.

In 1951 Johnson, Fuchs, and Morison[4] extended the work of the Beach Erosion Board. Their investigation was conducted to determine the reduction of wave heights beyond a submerged breakwater. The transmission coefficient was defined as the ratio of the wave height inshore from barrier, H_i, to the wave height seaward from barrier, H_s. The primary submerged breakwater used in the experiment was a simple rectangular sill. Wave heights were measured by means of resistance wire gauges placed three feet on either side of

the breakwater. The inshore wave height, H_i, was taken as the average of the fifth through tenth waves as measured on the oscillograph record. The wave length and period of the incident wave was measured by these two gauges without the breakwater in place.

It was determined that the transmission coefficient was a function of wave steepness (ratio of wave height seaward from barrier, H_s, to wave length, L_s), degree of submergence (ratio of height of breakwater, h, to still water depth, d), and relative depth (ratio of still water depth, d, to wave length, L_s), and relative barrier width (ratio of width of barrier, W, to wave length, L_s). The following dimensionless groupings were used to represent the relationship between the transmission coefficient, H_i/H_s, and the other variables; $H_i/H_s = f(H_s/L_s, h/d, d/L_s, W/L_s)$.

It was concluded that, in general, the transmission coefficient increased for decreasing wave steepness and increasing relative depths. The effect of increasing the width of the breakwater was an increase in wave reduction. The 1940 investigations of the Beach Erosion Board were also re-analyzed to conform to the method utilized for the rectangular barriers. The authors concluded that with the trapezoidal and triangular barriers a greater degree of damping was observed for the lower wave steepness values than for the steeper waves.

Another laboratory investigation considering the reduction of waves by submerged breakwater, using both smooth and breaking waves, was conducted by Priest[5] and published in 1958. Seven different breakwaters were used in the investigation: (1) a thin vertical flat plate (height 7 inches), (2) a dentated plate (one-inch

dentations, height 7 inches), (3) six rows of one-inch O.D. tubing (height 6-5/16 inches), (4) 1/2 inch rod jacks (height 3-1/4 inches), (5) flexible 16 mesh screen (height 7 inches), (6) flexible 8 mesh screen (height 7 inches), (7) a broom with coarse, stiff, fibrous bristles (height 7-3/4 inches, top width 5-1/2 inches). The experiment was limited to shallow water waves, in which the water depth was small compared to the wave length. The wave lengths averaged between 10 and 12 feet.

To determine the effect of each test structure on the wave height the incident wave was measured 7.5 feet upstream and 7.5 feet downstream from the location at which the structures were to be installed. The incident wave height upstream of the structure location was designated H_a. The incident wave height downstream of the structure location was designated H'. The height of the wave downstream of the structure location, after installation of the test structure, was designated H. The experimental data for the smooth waves were presented through the use of two dimensionless parameters. These parameters were the relative reduction in wave height, $\frac{H' - H}{H_a}$, and the ratio of the height of the test structure to the still-water depth, h/D. The results are summarized in Figures 2 and 3 from Priest's Report. Figures 2 and 3 show the damping effectiveness of each submerged structure for smooth waves and breaking waves respectively. Structures 1 and 7 produced the greatest change in the incident wave heights for a small change in the h/D parameter. Priest noted that very strong surface currents existed over and near these two test structures.

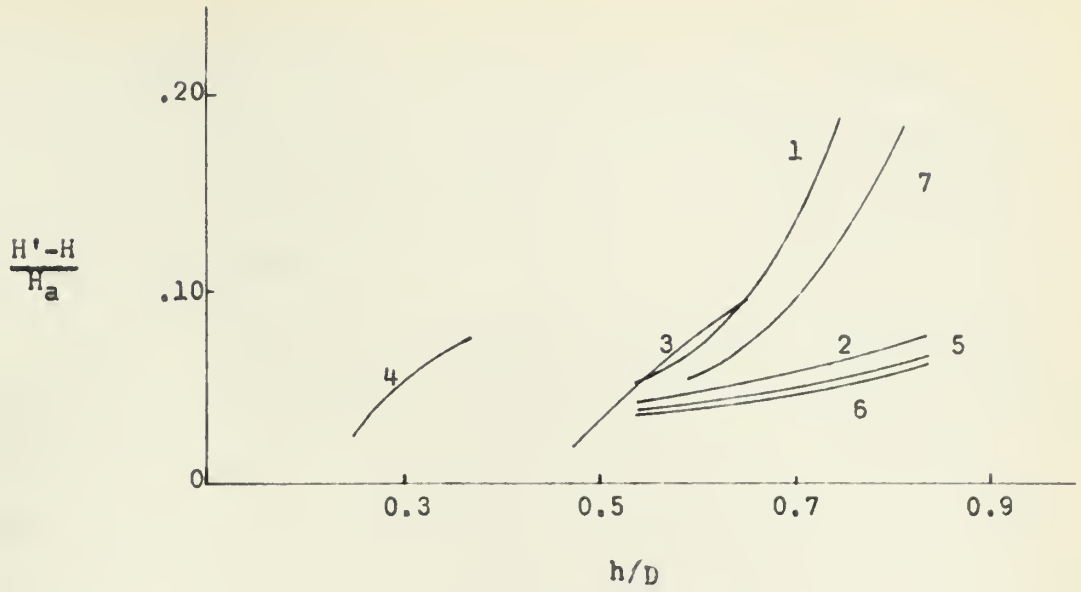

FIGURE 2

RELATION BETWEEN $(H'-H)/H_a$ AND h/D
SMOOTH WAVES

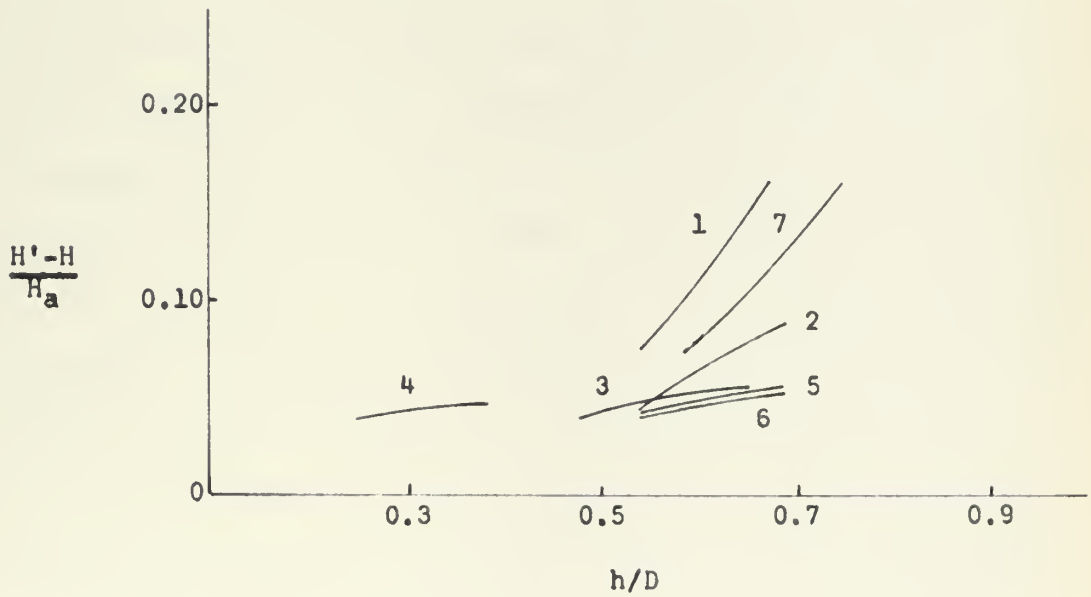

FIGURE 3

RELATION BETWEEN $(H'-H)/H_a$ and h/D
BREAKING WAVES

Priest's investigation was devoted to the determination of the changes in wave heights for the various test structures. The author did not attempt to give any special consideration to changes in wave energy. He concluded, however, that the relative change in wave energy was appreciably greater than the associated relative change in wave height.

One of the most recent laboratory experiments investigating wave action over submerged barriers was undertaken by May[6] in 1964. May's investigation was limited to deepwater waves. The author used a thin vertical barrier and an eight foot long vertical sill. The depth of the water was maintained at 24 inches. The height of each structure was varied from 15 to 24 inches to obtain different degrees of submergence. The submergence ratio was defined as the ratio of the still-water depth, D, to the structure height, h. The height of the transmitted wave and the magnitude of the superimposed reflected and incident waves were measured by means of a variable resistance probe. The height of the incident wave was determined without the structure in the wave tank. The transmission coefficient was defined as the ratio of the height of the transmitted wave to the height of the incident wave. The reflection coefficient was defined as the ratio of the height of the reflected wave to the height of the incident wave. The height of the reflected wave was taken as the difference between the magnitude of the superimposed reflected and incident waves and the height of the incident waves.

May introduced a stilling factor which was defined as the ratio of landward to seaward wave heights. The landward wave height was taken as the height of the transmitted wave. The seaward

wave height was taken as the height of the superimposed reflected and incident waves seaward of the barrier. The stilling factors and transmission coefficients were plotted against the depth of submergence. The stilling factor curves were similar to the transmission coefficient curves.

May determined that the variable which had the greatest effect on the results was the degree of submergence. May concluded that for identical degrees of submergence and structure geometry the transmission and reflection coefficients were smaller for the higher wave steepnesses. May also stated that the difference in reflection and transmission between the vertical barrier and the eight foot long vertical sill was very small. In addition, his study indicated that low submergence ratios proved to be most effective in reducing the height of waves beyond the structure.

A very thorough study covering the basic theories of two-dimensional periodic progressive gravity waves was published in 1960 by Dr. Bernard Le Mehaute.[7] In January 1961, Dr. B. Le Mehaute[8] published a study of the hydrodynamic relationships for the height of a standing wave, or clapotis, at a breakwater. Both of these reports were of significant help to the author of this paper.

A highly theoretical study of the reflection of surface waves by a submerged cylinder was undertaken by W. R. Dean[9] and published in 1948. He showed that the coefficient of reflection (the ratio of the amplitudes, at a great distance from the barrier, of the reflected and incident waves) was zero. The only effect of the obstacle at a great distance was that there existed a phase difference between the incident and transmitted waves with their

amplitudes being the same.

A graphical summary of the theoretical treatment of wave action over submerged barriers by Dean[10], Ursell[11], Fuchs[12], and Lamb[13] is presented in Figures 4, 5, and 6.

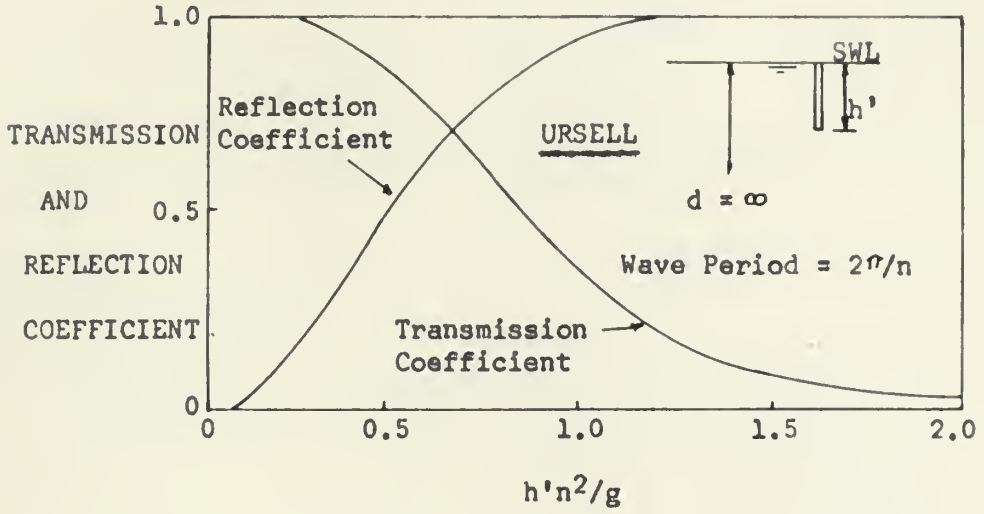

FIGURE 4

THEORETICAL REFLECTION AND TRANSMISSION COEFFICIENTS FOR A THIN VERTICAL BARRIER

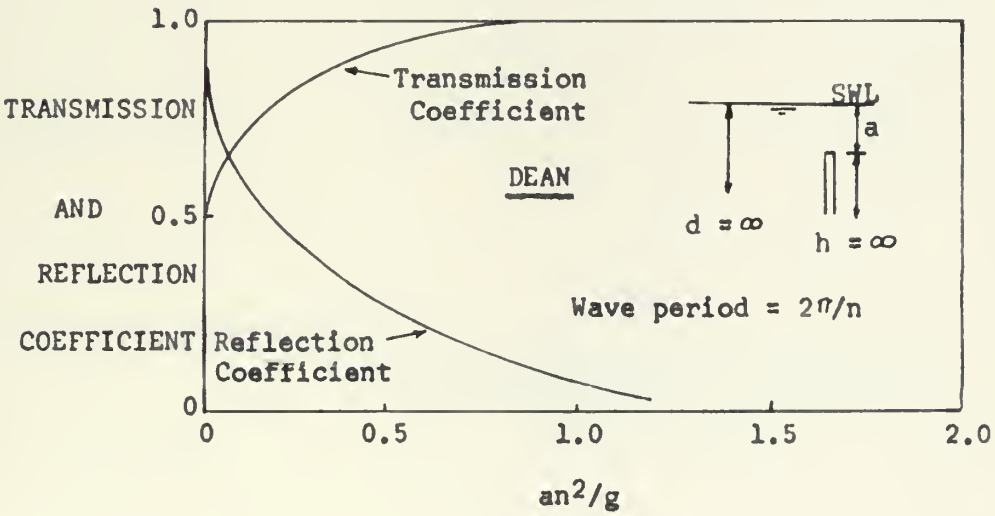

FIGURE 5

THEORETICAL REFLECTION AND TRANSMISSION COEFFICIENTS FOR A THIN VERTICAL BARRIER

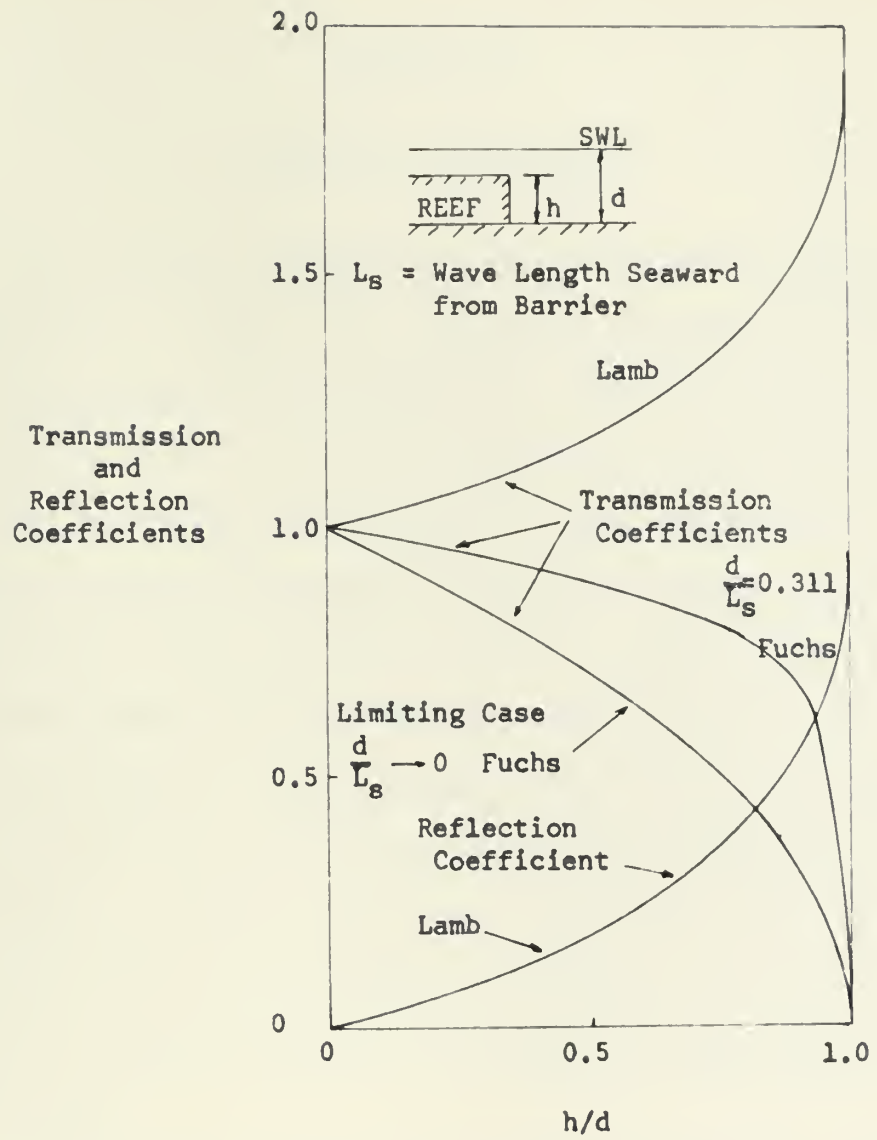

FIGURE 6

THEORETICAL REFLECTION AND TRANSMISSION COEFFICIENTS FOR WAVE ACTION ON A VERTICAL REEF

CHAPTER III

THEORETICAL DEVELOPMENT

The theoretical treatment of wave formation and motion is so complex that no single theory exists which considers all flow characteristics and fluid properties. Even after employing simplifying assumptions a variety of solutions have been developed.

The two-dimensional progressive gravity wave theories are the basis for many other theories, including the complex three-dimensional waves which exist in nature. Two-dimensional progressive gravity waves are defined as waves which travel in a definite direction without change in characteristics, are not affected by boundary conditions, and in which frictional decay is negligible. Although such waves do not exist in nature they can be produced with a reasonable degree of accuracy in a laboratory provided a long smooth channel with a properly designed wave generator[14] is utilized.

Gravity waves are divided into three categories: (1) Deep water waves, depth greater than one-half the wave length, $d > 0.5L$, (2) Intermediate water waves, $0.5L > d > 0.05L$, (3) Shallow water waves, $d < 0.05L$. This investigation was limited to deep water waves, since the depth of water was greater than one-half the wave length.

The gravity wave theories are based on the principle of continuity, Newtonian principle of force, boundary conditions and

periodicity of motion.

Since no fluid is being added or subtracted during wave-motion the quantity of fluid involved remains constant. Considering a two-dimensional rectangular fluid element, as indicated in Figure 7, the amount of fluid entering the element must equal the amount of fluid leaving.

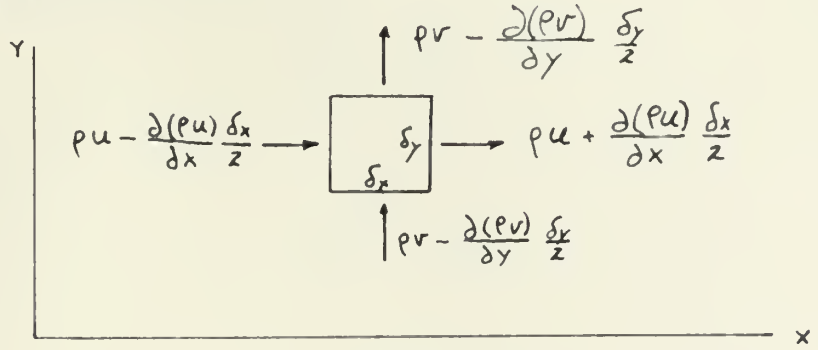

If ρ denotes the density at the center of the element, u the velocity in the x-direction and v the velocity in the y-direction then the total mass influx is

$$\left(\rho u - \frac{\partial(\rho u)}{\partial x}\frac{\delta_x}{2}\right)\delta_y + \left(\rho v - \frac{\partial(\rho v)}{\partial y}\frac{\partial y}{2}\right)\delta_x .$$

The total mass efflux is

$$\left(\rho u + \frac{\partial(\rho u)}{\partial x}\frac{\delta_x}{2}\right)\delta_y + \left(\rho v + \frac{\partial(\rho v)}{\partial y}\frac{\delta_y}{2}\right)\delta_x .$$

The rate of change of mass in the element is

$$\frac{\partial(\rho\,\delta_x\,\delta_y)}{\partial t} .$$

Since the mass influx minus the mass efflux must equal the rate of change of mass in the element this may be expressed as

$$\frac{\partial(\rho u)}{\partial x} + \frac{\partial(\rho v)}{\partial y} + \frac{\partial \rho}{\partial t} = 0 .$$

For an incompressible fluid

$$\frac{\partial u}{\partial x} + \frac{\partial v}{\partial y} = 0 .$$

Since

$$\vec{V} = \vec{u} + \vec{v}$$

then

$$\nabla V = \frac{\partial u}{\partial x} + \frac{\partial v}{\partial y} = 0 .$$

Assuming that viscous forces are negligible and that the flow is irrotational a velocity potential, ϕ, can be introduced such that

$$u = \frac{\partial \phi}{\partial x}$$

and

$$v = \frac{\partial \phi}{\partial y} .$$

Therefore,

$$\vec{u} + \vec{v} = \frac{\partial \phi}{\partial x} + \frac{\partial \phi}{\partial y}$$

and

$$\vec{V} = \text{grad } \phi .$$

Since $\nabla\vec{V} = 0$, the continuity equation becomes

$$\nabla^2\phi = 0$$

This is also known as Laplace's equation.

Eulers equations for two-dimensional fluid motion are

$$X - \frac{1}{\rho}\frac{\partial P}{\partial x} = a_x = \frac{Du}{Dt} \tag{1}$$

and

$$Y - \frac{1}{\rho}\frac{\partial P}{\partial y} = a_y = \frac{Dv}{Dt} \quad . \tag{2}$$

Where X and Y are the body forces. Since gravity is the only body force acting, the addition of equations (1) and (2) produces

$$\frac{D\vec{V}}{Dt} = Y - \frac{1}{\rho}\left(\frac{\partial P}{\partial x} + \frac{\partial P}{\partial y}\right) .$$

Since

$$Y = \text{Force}/\text{Mass}$$

then,

$$Y = \frac{-\gamma\, \delta_x\, \delta_y}{\rho\, \delta x\, \delta_y}$$

and

$$Y = -g$$

Therefore,

$$\frac{D\vec{V}}{Dt} = -g - \frac{1}{\rho} \text{grad } P \ .$$

The above equation may be written as

$$\rho \frac{D\vec{V}}{Dt} = -\nabla (g\rho Y + P) \ .$$

A solution based on this equation is applicable when the amount of motion is very small, that is, waves of small steepness in deep water.

The velocity potential ϕ must satisfy the continuity equation, Eulers equation, and the following boundary conditions.

(1) At the free surface

$$P = 0$$

(2) At the bed

$$v = \frac{\partial \phi}{\partial Y} = 0$$

Euler equation of motion in the y-direction is

$$\rho \frac{Dv}{Dt} = -g\rho - \frac{\partial P}{\partial Y} \ .$$

Since

$$\frac{Dv}{Dt} = u\frac{\partial v}{\partial x} + v\frac{\partial v}{\partial y} + \frac{\partial v}{\partial t}$$

and by neglecting the two non-linear terms, which tend to zero, on the right side of the equation, Euler's equation for motion in the y-direction is

$$\rho\frac{\partial v}{\partial t} = -\rho g - \frac{\partial p}{\partial y} \quad .$$

This may be rewritten as

$$\rho\frac{\partial}{\partial t}\left(\frac{\partial \phi}{\partial y}\right) = -\rho g - \frac{\partial p}{\partial y} \quad .$$

After integration this equation becomes

$$\rho\frac{\partial \phi}{\partial t} = -\rho g y - p + f_{(t)} \quad .$$

Setting $p + f_{(t)}$ equal to a constant and differentiating

$$\frac{\partial^2 \phi}{\partial t^2} + g\frac{\partial y}{\partial t} = 0 \quad .$$

Since

$$v = \frac{\partial y}{\partial t} = \frac{\partial \phi}{\partial y}$$

then

$$\frac{\partial^2 \phi}{\partial t^2} + g \frac{\partial \phi}{\partial y} = 0.$$

For simple harmonic progressive waves in water of uniform depth the velocity potential as given by Stoker[15] is

$$\phi = A \cosh m(y+d) \cos (mx \pm \sigma t)$$

with m and σ satisfying

$$\sigma^2 = g m \operatorname{Tanh} md$$

Where $\sigma = 2\pi/T$, T = wave period, g = acceleration due to gravity, $m = 2\pi/L$, L = wave length, and d = stillwater depth. The wave celerity is given by

$$c = \frac{\sigma}{m}$$

which in terms of the wave length, L, is expressed as

$$c = \sqrt{\frac{gL}{2\pi} \operatorname{Tanh} \frac{2\pi d}{L}}$$

By expanding the function Tanh = md in a power series Stoker obtained

$$\sigma^2 = \frac{2\pi g}{L} \left[\frac{2\pi d}{L} - \frac{1}{3} \left(\frac{2\pi d}{L} \right)^3 + \cdots \right]$$

As $\frac{d}{L} \to 0$

$$\sigma^2 \to \left(\frac{2\pi}{L} \right)^2 g d = m^2 g d$$

and therefore, if $\frac{d}{L}$ is small

$$c \simeq \sqrt{gd} \quad .$$

This expression states that the wave celerity becomes independent of the wave length when the depth is small compared with the wave length, but varies as the square root of the depth (Shallow Water Theory).

For deep water waves, $d > 0.5L$, $\tanh \frac{2\pi d}{L} \simeq 1$

therefore, the wave celerity, c, is expressed as

$$C = \sqrt{\frac{gL}{2\pi}}$$

When waves encounter an obstacle the waves may be partially or completely reflected. Any remaining energy is transmitted beyond the obstacle and/or dissipated at the obstacle in the form of turbulence and friction. When waves are totally reflected without loss of energy a standing wave occurs. This is referred to as total clapotis. This standing wave is the result of the superposition of an incident wave and a reflected wave of the same period and amplitude but traveling in opposite direction. When the height of the reflected wave is smaller than the height of the incident wave, a partial clapotis is formed. The formation of clapotis, total and partial, occurs seaward of the reflecting structure.

The potential function must satisfy the stated boundary condition which at the free surface is

$$Y = \frac{1}{g} \frac{\partial \phi}{\partial t}$$

therefore,

$$Y(x,t) = \frac{cmA}{g} \cosh m(y+d) \sin m(x \pm ct)$$

Since y = 0 at the free surface then

$$Y(x,t) = \frac{cmA}{g} \cosh (md) \sin m(x \pm ct) .$$

By designating the wave amplitude as

$$a = \frac{cmA}{g} \cosh (md)$$

the expression for the free surface becomes

$$Y(x,t) = a \sin m(x \pm ct) .$$

The simple harmonic incident wave is

$$Y_i = a_i \sin m(x - ct) .$$

The reflected wave is

$$Y_r = a_r \sin m(x + ct)$$

Total clapotis is given by

$$Y_i + Y_r = 2a_i \sin(mx) \cos(mct) .$$

Partial clapotis is given by

$$Y_i + Y_r = (a_i + a_r) \sin(mx) \cos(mct) + (a_r - a_i) \cos(mx) \sin(mct).$$

For cos mx = ± 1, (sin mx = 0)

$$Y_{MAX.} = a_r - a_i$$

and

$$Y_{MIN.} = -(a_r - a_i) .$$

Similarly, for sin mx = ± 1, (cos mx = 0)

$$Y_{MAX} = a_i + a_r$$

and

$$Y_{MIN.} = -(a_i + a_r) .$$

The expression cos mx will equal unity at

$$x = n \frac{L}{2}$$

where n is an integer.

The expression sin mx will equal unity at

$$x = (2n-1) \frac{L}{4}$$

$$x = n \frac{L}{2} - \frac{L}{4}$$

where n is an integer.

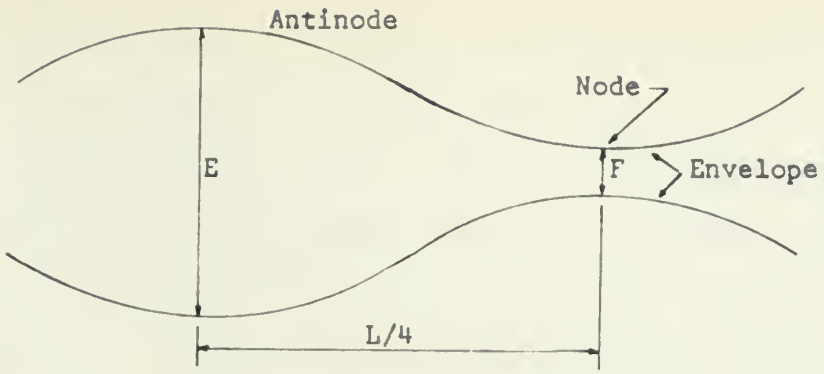

FIGURE 8

VARIATION IN AMPLITUDE FOR PARTIAL CLAPOTIS

As indicated in Figure 8 the maximum amplitude at E and the minimum amplitude at F are located a quarter wave length apart.

$$a_i + a_r = E$$

$$a_i - a_r = F$$

Solving for amplitudes of the incident and reflected waves

$$a_i = \frac{E+F}{2}$$

and

$$a_r = \frac{E-F}{2} \quad .$$

If the reflection coefficient is defined as the ratio of the height of the reflected wave to the incident wave then

$$R_c = \frac{a_r}{a_i} = \frac{E-F}{E+F}$$

In this investigation the reflected wave could not be measured directly but only the magnitude of its superposition with the

incident wave. The reflection coefficient was defined as the ratio of the maximum height of the superimposed reflected and incident waves to the height of the incident wave.

The above analysis for the reflection coefficient applies only for the case where the reflected wave and the incident wave are of the same wave length. Since the reflected wave may be of a different wave length as well as different amplitude than the incident wave the resulting wave pattern for partial clapotis would not be as indicated in Figure 8.

The motion of water particles under the wave is theoretically circular with zero net transport. However, in practice, the particle paths resemble more of an ellipse with some net flow at the surface and return flow at a greater depth. The orbital path is largest at the surface and decreases as the depth increases. The cone of influence of wave motion is theoretically equal to one-half the wave length. Figure 9 illustrates this cone of influence.

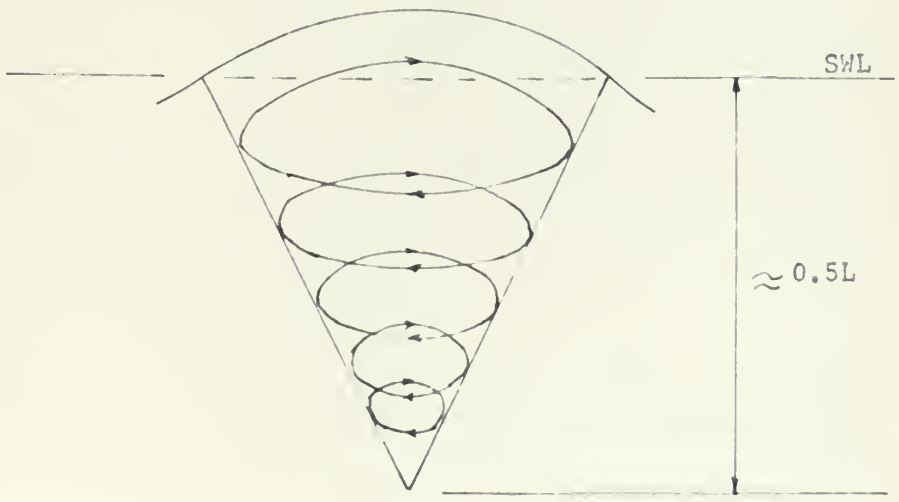

FIGURE 9

CONE OF INFLUENCE OF WAVE MOTION

CHAPTER IV

EXPERIMENTAL APPARATUS

WAVE TANK AND GENERATOR

The wave tank used in the experiments is located in the Hydraulics Laboratory of the University of Colorado (Figure 10). It is a rectangular concrete channel 52 feet long, three feet wide and three feet deep. The channel walls have a plaster finish. The downstream end of the channel is sealed with a steel plate and a rubber gasket. Ten feet upstream from this end a four-foot long section of the channel wall had been removed and replaced with one-fourth inch thick plexiglass for visual observations.

A filter (Figure 11) was installed about six feet downstream from the upstream end of the tank in an effort to absorb and thereby minimize objectionable oblique wave components. The filter consisted of fourteen four-feet long by two-feet high expanded metal sheets spaced about two inches apart and attached to two steel angles across the channel. These metal sheets hung vertically parallel to the longitudinal axis of the channel.

A beach, with a slope of 15 degrees and covered with approximately two inches of loose one-inch nominal size aggregate, was installed at the extreme downstream end to dissipate the waves and minimize reflections.

At the upstream end of the tank a V-shaped plunger-type wave

generator (Figure 12) was installed. The plunger extended across the full width of the channel with minimum side clearances. The plunger was driven by a 5 HP, 1750 RPM A.C. motor through a variable speed Graham transmission. The characteristics of the wave generated could be varied by changing the angle of the plunger, the speed of the transmission or by using different sized eccentrics attached to the plunger. The last method was not used in this investigation. Vertical oscillations of the plunger created the various wave formations. The desired orbital movement of the water particles is obtained after four to six wave lengths.

RECORDING APPARATUS

Waves were recorded by means of two variable resistance probes. The probes were mounted on a carriage which could be moved along the top of the wave tank on rails (Figure 13). The downstream probe was mounted on a vertical gage staff which could be read to the nearest 0.001 feet. The upstream probe was mounted on a similar, but horizontal, gage. These two probes were installed along the center line of the wave tank and spaced exactly 12 inches apart.

The resistance across each probe was proportional to the depth of immersion. Each probe consisted of two six-inch galvanized stainless steel electrodes spaced three-fourths of an inch apart. A change in resistance of the probe caused a change of current in the circuit. This change in current was measured and recorded on a Heiland Visicorder oscillograph recorder, Model 1406 (Figure 14). The recorder produced a trace on special photographic paper. The image of the trace was obtainable by subjecting the paper to

ordinary room illumination. Only two of the available six galvanometers were used in this experiment. The sensitivity of the galvanometers was 520 millivolts per inch deflection, with a frequency response of 220 cycles per second. Since the resistance of the galvanometers was of the order of 800 ohms, a shunt resistance of 60 ohms was included in the circuit to reduce the total resistance. The resistance of each probe was of the order of 20,000 ohms, therefore, the current in the circuit was essentially linearly proportional to any change in the probe resistance. This permitted calibration of the equipment by relating the depth of immersion to the magnitude of the deflection of the trace.

BREAKWATER

The submerged breakwater used in the experiments consisted of quarter-cylinder sections with a radius of 12 inches (Figure 15). They were constructed of three-eighths inch exterior grade plywood and covered with 26 gage galvanized iron. The plywood was treated and varnished. Each section was adequately braced and weighted to prevent movement during passage of the waves. All quarter-cylinder sections were wide enough to fill the channel with small clearances at the walls. To insure rigidity of the test section small wedges were placed between the tank walls and the structure. The degree of submergence of the breakwater was varied by raising each quarter-cylinder section in three-inch increments. The upstream faces of the blocks used to vary the submergence were covered with 26 gage galvanized iron. Successive rows of the breakwater sections were used to determine the effect of increased breakwater width on transmission and reflection.

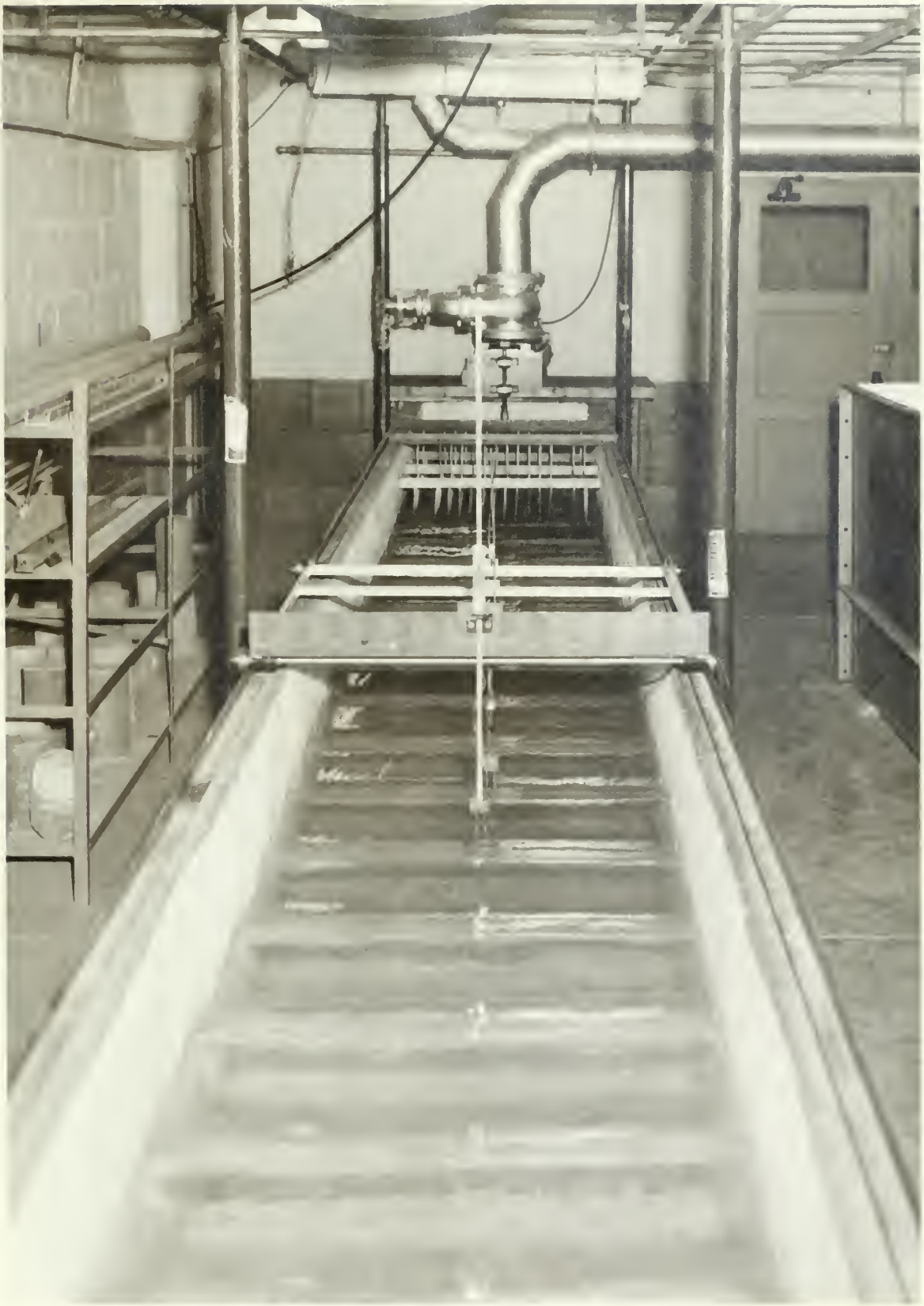

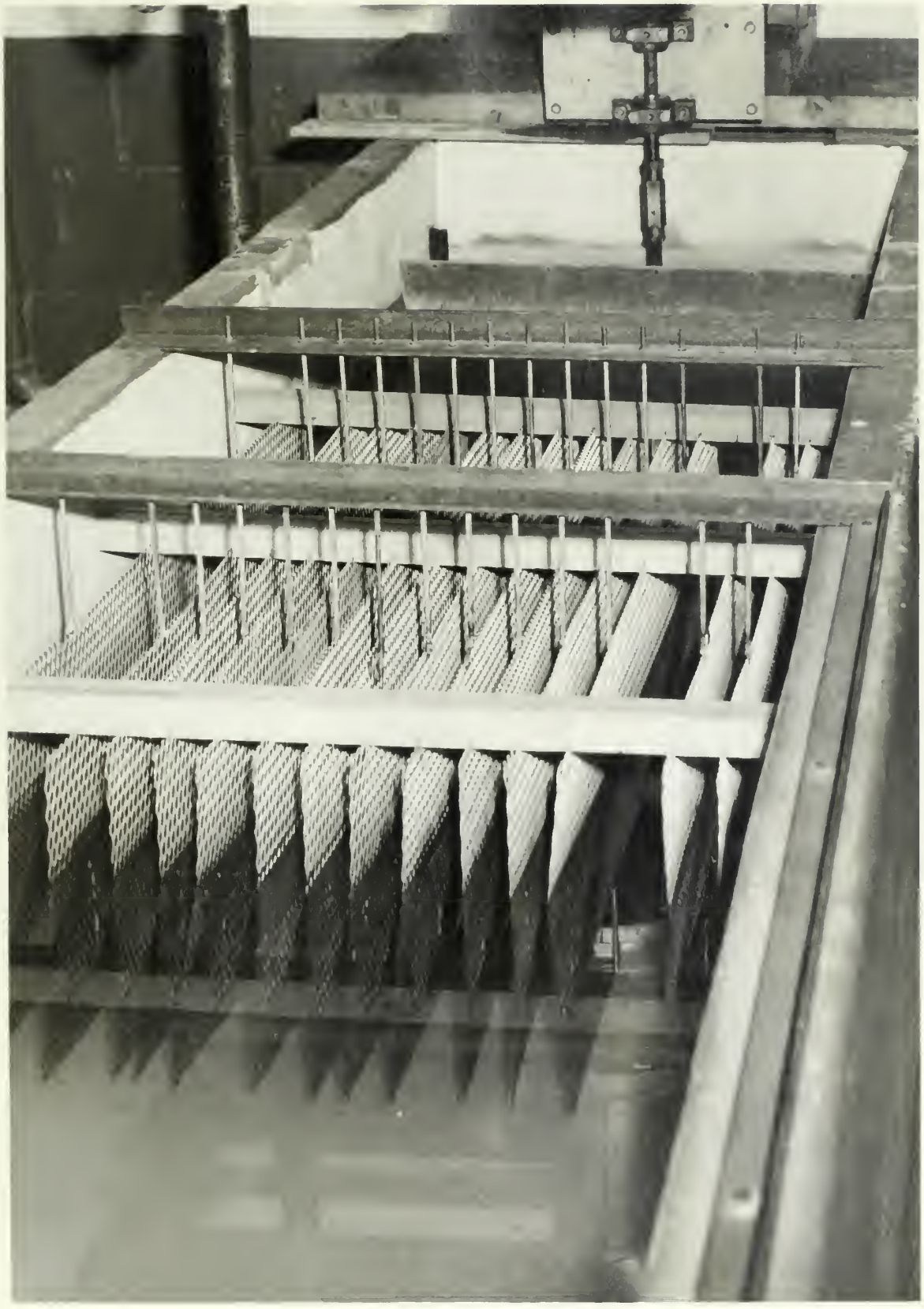

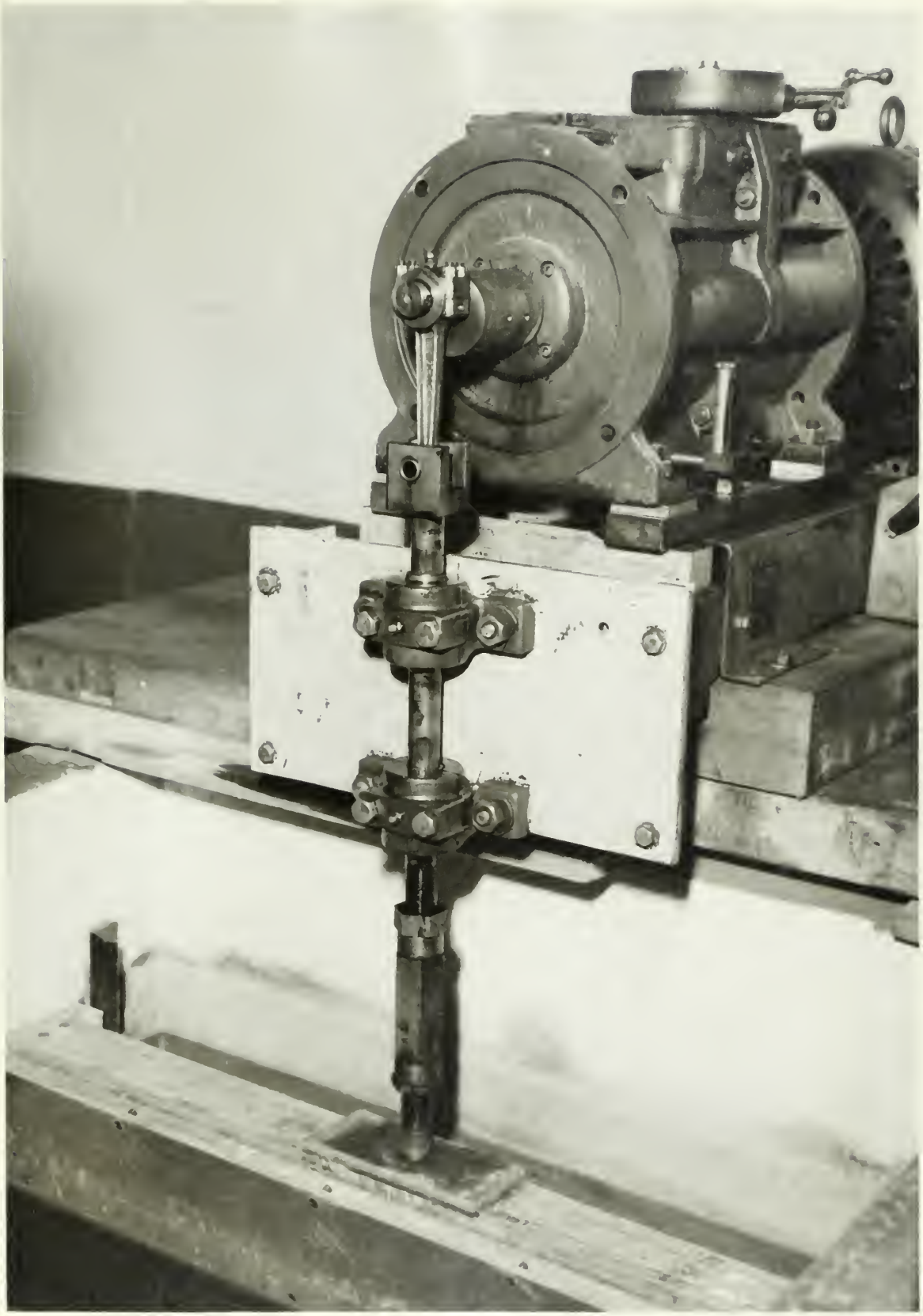

FIGURE 13 VARIABLE RESISTANCE PROBE AND CARRIAGE

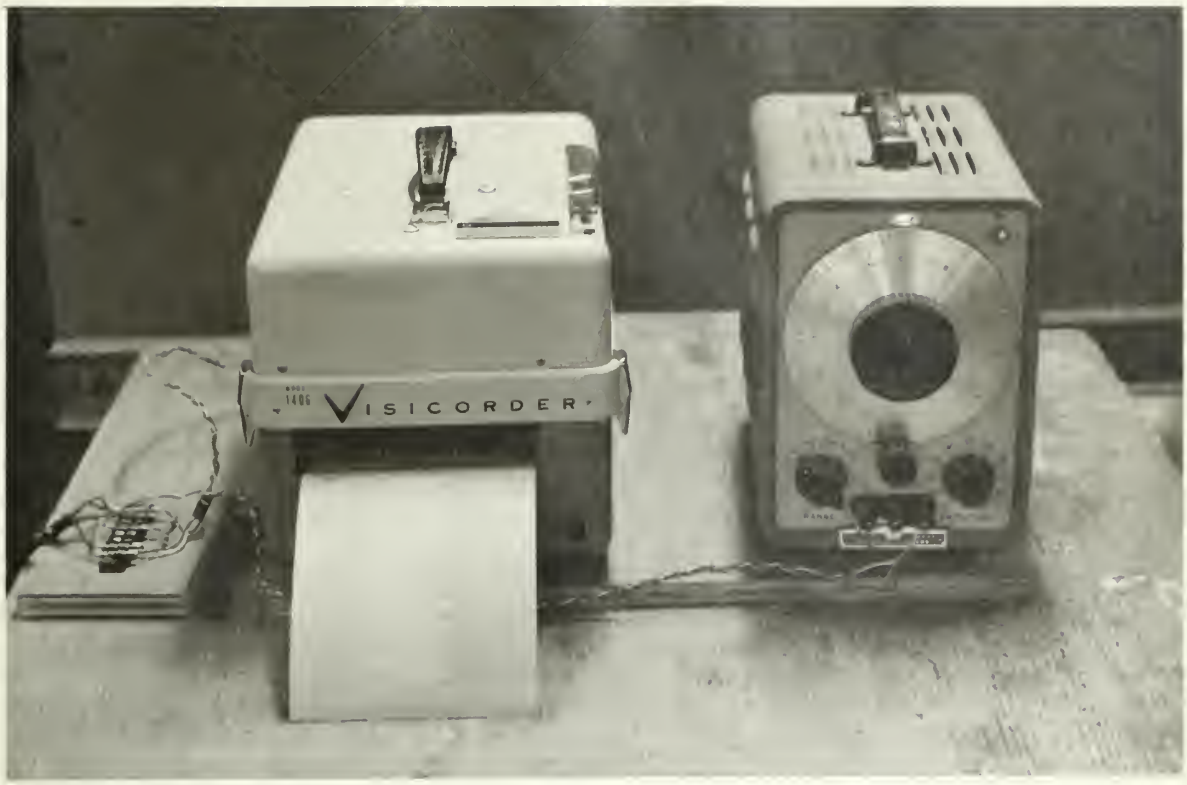

FIGURE 14 VISICORDER OSCILLOGRAPH RECORDER

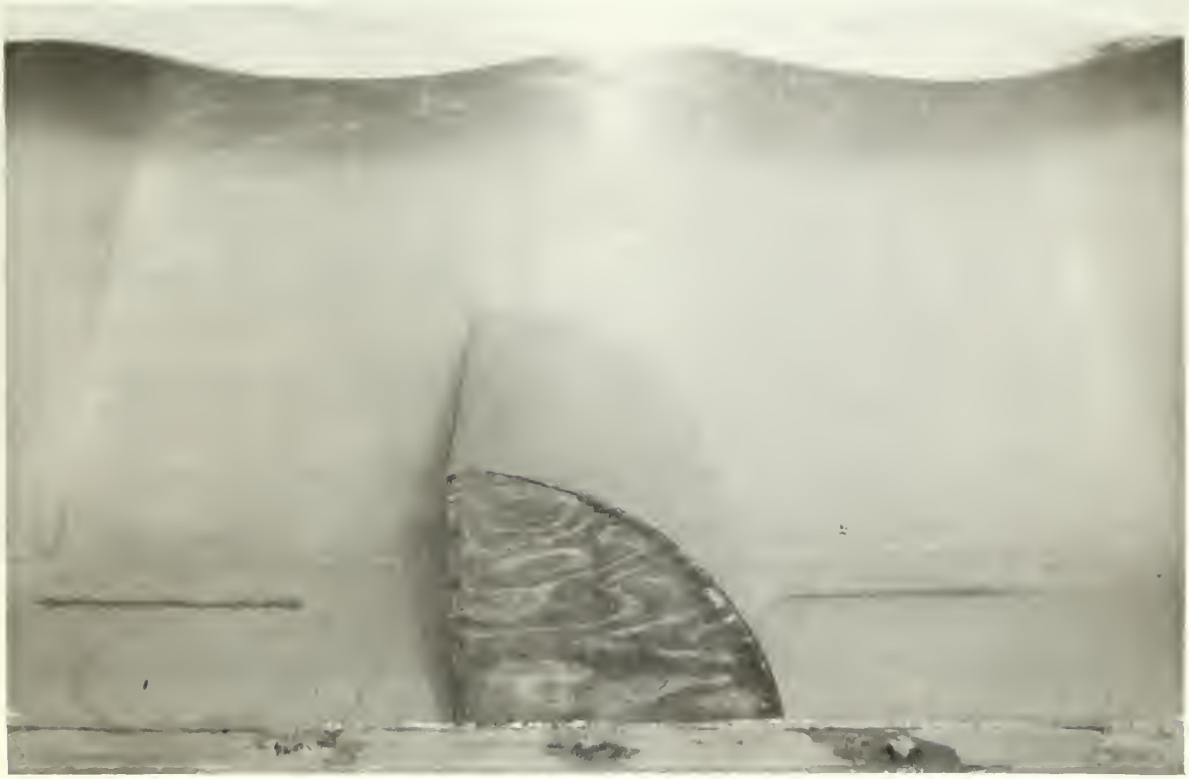

FIGURE 15 WAVE ACTION OVER THE SUBMERGED BREAKWATER

CHAPTER V

EXPERIMENTAL PROCEDURE

A complete series of experiments consisting of 16 runs at four different wave steepnesses were conducted on the four breakwater configurations shown in Figure 16. The configurations were designated A, B, C, and D. Reference to a particular breakwater in the subsequent sections of this study will be by letter designation. Six breakwater heights were utilized.

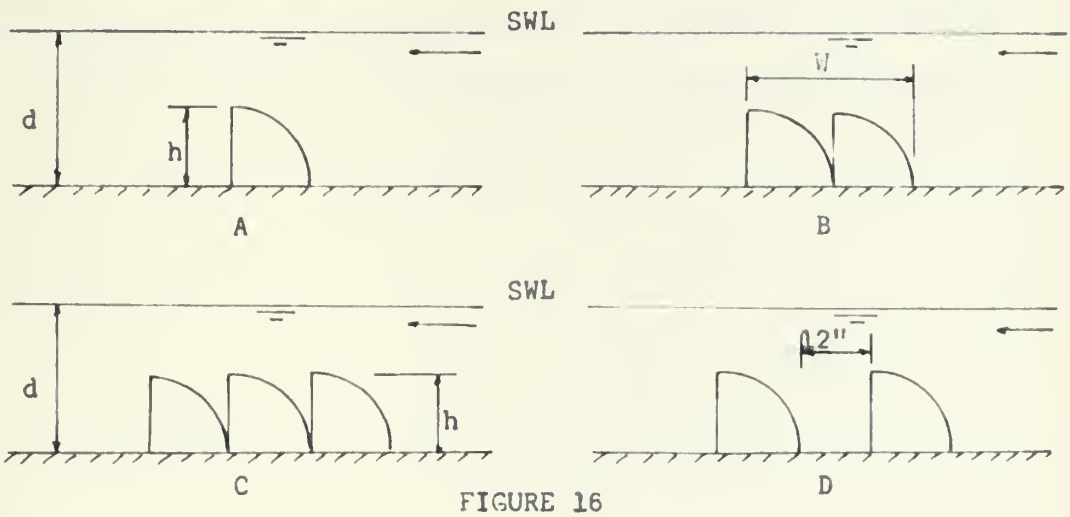

FIGURE 16

BREAKWATER CONFIGURATIONS

The stillwater level was maintained at 27 inches throughout the experiment. The different degrees of submergence were obtained by raising the height of the breakwater in three-inch increments. To provide the desired wave steepnesses the speed of the hydraulic transmission and the angle of the plunger were properly adjusted. Initially, it was planned to keep the height of the sill constant

and vary the stillwater depth, however, this approach did not prove satisfactory. At shallow depths the disturbance produced by the plunger resulted in waves with numerous irregularities. The close proximity of the plunger to the end wall produced violent turbulence in the immediate vicinity which affected the profile of the generated waves. With deep water and relatively slow speeds this turbulence was minimized.

The general procedure in making an experimental run was as follows:

(1) The wave recorder was calibrated. This was accomplished by turning on the recorder and lowering the resistance probe into the stillwater by increments. The resulting stepped trace on the photographic paper was then measured to determine the factor relating the depth of probe immersion to the trace deflection.

FIGURE 17

EXAMPLE OF CALIBRATION TRACE

The calibration factor was computed as follows (see Figure 17):

$$CF = \frac{\text{Magnitude of trace deflection}}{\text{Depth of probe immersion}}$$

$$CF = \frac{a}{0.6} \quad \left(\frac{CM.}{INCH.}\right)$$

The increment of probe immersion was kept constant at 0.05 feet. The value of "a" became constant after the probe immersion reached 0.25 feet. For all runs the probe immersion in still water was set at 0.30 feet. The calibration factor was used to determine the actual height of the water waves in the tank.

(2) Prior to installing the test structure the desired angle of the plunger and speed of the transmission were set. The wave generator was turned on and the incident wave train was recorded utilizing both probes. Since the first few generated waves were irregular in height the recorder was not turned on until after the tenth wave had passed. The incident wave was measured five feet upstream and downstream from the centerline of the structure location. The final values for the incident waves were the averages of ten runs for each setting.

(3) The generator was turned off and the test structure was installed. After steady state conditions were reached the wave generator was again turned on. The probe carriage was so located that the transmitted wave was measured first. The center of the test structure was located 17.5 feet upstream from the leading edge of the sloping beach. After the first 10 to 12 waves passed over the structure the recorder was turned on and the transmitted wave train was recorded. A maximum of ten waves were recorded to insure that any reflection from the sloping beach would not affect the transmitted recordings. The probe carriage was then moved upstream

of the test structure. By observing the trace deflections for various upstream carriage locations the point of maximum deflection was determined. The recorder was then turned on and the wave train was recorded. This maximum was the height of the incident wave reinforced by the reflected wave.

Figure 18 shows an example of the wave recordings.

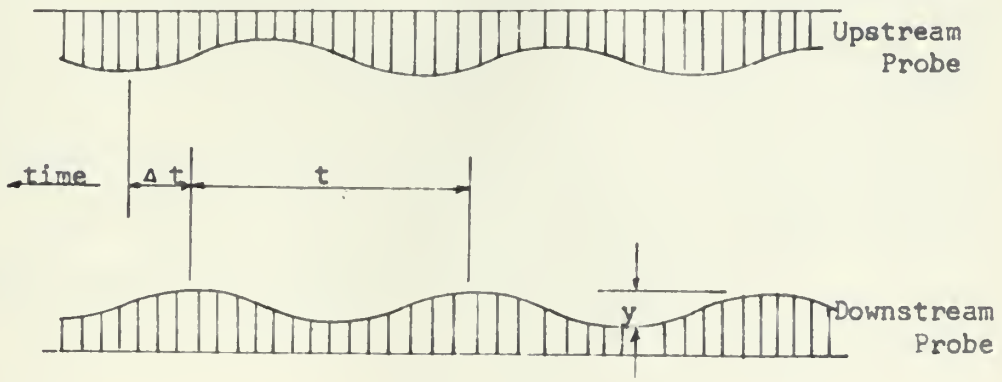

FIGURE 18

SAMPLE OF WAVE RECORD TRACE

The downstream and upstream probes were spaced exactly 12 inches apart. Since time was the horizontal axis the celerity of the wave could be determined by measuring Δt. Knowing the celerity of the wave and measuring the period, t, the wave length could be computed. The wave height was calculated by measuring the amplitude y and applying the calibration factor. From this information the wave steepness (H/L) was easily calculated. The height of the transmitted wave was determined by measuring the amplitude, y, on the transmitted wave-train recordings. Similarly, the magnitude of the superimposed reflected and incident waves was determined by measuring the amplitude, y, on the reflected wave-train recordings. The actual height of the waves was calculated by applying the calibration

factor to the measured amplitude y. This concluded one run.

Having recorded the incident wave length, height and steepness, and both transmitted and reflected wave patterns for one breakwater configuration the process was repeated for three other wave steepnesses. Then a different breakwater configuration was installed and the above process was repeated. This procedure involved 16 experimental runs. The height of the structure was then changed and the entire process was again repeated. When the submergence ratio was equal to 1.0 only the reflection was measured. A total of ninety-six experimental runs were utilized in this investigation.

The calibration was checked periodically to insure that the proper factor was applied in all calculations.

CHAPTER VI

EXPERIMENTAL RESULTS

In an effort to determine the effect of specific factors on the transmission and reflection of the incident waves over a submerged breakwater, the height of the breakwater, wave steepness, and breakwater widths were varied in this investigation. The four wave steepnesses used were essentially of two different wave lengths. Six submergence depths and four breakwater configurations provided a reasonable range over which the effect of the variables could be analyzed. All the data for the experimental curves are shown in Tables I to X inclusive. The definitions of the symbols used in this study are contained in Table XI.

Figures 19 through 34 show the effect of relative depth, d/L, relative width, W/L, and submergence ratio, h/d, on the reflection and transmission coefficients. Figures 35 through 38 provide a graphical comparison of the reflection and transmission coefficients for breakwater configurations C and D, as shown in Figure 16, for equal wave steepnesses. Figures 39 through 42 provide a graphical comparison of the transmission coefficients of breakwater C and the trapezoidal and triangular shaped breakwaters studied by the Beach Erosion Board and analyzed by Johnson, Fuchs and Morison.[16] Figures 43 through 50 graphically illustrate the effect of the depth of wave motion on the reflection and transmission coefficients for

the four wave steepnesses used in this investigation.

For a zero submergence ratio the height of the transmitted wave equalled the height of the incident wave, i.e. $H_t/H_i = 1.0$. On all figures illustrating the variation of the transmission coefficient with different submergence ratios, a dashed line was constructed from the point of maximum transmission to the value of the transmission coefficient obtained for the minimum submergence ratio of 0.445. All curves on the same figure were constructed to show the same general trend.

The height of the breakwater proved to be the factor having the greatest effect on the transmission and reflection of the incident waves. All curves, except Figures 43 through 50, are graphical plots of the reflection and transmission coefficients versus the submergence ratio. Figures 43 through 50 show the relation between the transmission and reflection coefficients and the effective wave motion ratio, $\frac{d-h}{0.5L}$, for different wave steepnesses for all breakwater configurations.

The stillwater depth was maintained at 27 inches throughout all experimental runs. This depth was measured at the upstream face of the breakwater. The bottom of the channel was not truly horizontal as a very small slope had been provided for drainage. However, the depth of stillwater was essentially the same at the upstream and downstream faces of the breakwater for all breakwater configurations.

Four incident waves, with four values of wave steepness of approximately two different wave lengths, were used in all runs. Steepness values were 0.0222, 0.0383, 0.0455 and 0.0675. The corresponding wave lengths were 31.9, 31.6, 18.9 and 19.4 inches

respectively. Although the wave steepness values did not vary appreciably, the average values for ten runs for each setting were used in the computations.

Figures 19 through 22 show that the reflection coefficient, for approximately equal relative depth values, varied over a small range for the higher wave steepnesses and that the individual coefficient values for the same depth of submergence were larger for lower wave steepnesses. The transmission coefficients, Figures 23 through 26, show the opposite trend for approximately equal relative depths.

Figures 27 through 34 graphically show the variation of reflection and transmission coefficients with breakwater width for equal relative depths and wave steepnesses. For increasing breakwater widths there was a decrease in wave transmission and an increase in wave reflection. However, the magnitude of the range of this decrease in transmission was small, particularly for low wave steepnesses. Conversely, the magnitude of the range of the increase in reflection was small for high wave steepnesses.

For the maximum wave steepness used in this investigation, 0.0675, the value of the reflection coefficient for the greatest submergence depth is approximately the same for all breakwater configurations. Similarly, for increasing submergence depths less wave transmission is obtained but the magnitude of the transmission coefficients does not vary to any great extent for the different breakwater configurations. For example, for wave steepness 0.0222, the range of the transmission coefficients for submergence ratios of 0.445 to 0.889 for all designated breakwaters are as follows:

A - 0.864 to 0.949, B - 0.916 to 0.958, C - 0.854 to 0.944, and D - 0.919 to 0.973.

Since breakwater configuration D was simply breakwater C with the center section removed, Figures 35 through 38 were constructed to show the effect of this breakwater configuration change. At the higher wave steepnesses the variation of the reflection and transmission coefficients for the two breakwater configurations was relatively small. The variation at the lower wave steepnesses was slightly larger. Breakwater C produced less transmission and greater reflection than breakwater D for the submergence ratio used in this investigation.

At a submergence ratio of 0.889 and for breakwaters B, C, and D it was observed that the transmitted wave had a tendency to become distorted and in some instances split into multiple waves. At a submergence ratio of 1.0 and for all four breakwater configurations the incident wave broke at the upstream face and only multiple ripples of reduced wave length moved shoreward. The breaking of the incident wave substantially reduced the amount of reflection from the breakwater. This reduction in the reflection coefficients is tabulated in Table V. For this maximum submergence ratio the reflection coefficient, for equal wave steepnesses, varied over a small range for increasing breakwater widths. The minimum width, breakwater configuration A, produced the largest reflection.

Figures 43 through 46 show that the incident wave having the shortest wave length was reflected to a small degree even when the depth of water over the top of the breakwater exceeded the theoretical depth of wave motion, i.e. $\frac{d-h}{0.5L} > 1.0$. Figures 47 through

50 show the reduction in height of the incident wave beyond the test structure when the effective wave motion ratio was greater than 1.0.

CHAPTER VII

CONCLUSIONS

The effects of three variables on the reflection and transmission of waves over a submerged breakwater were investigated. These variables were the height of the breakwater, wave steepness, and width of the breakwater.

The reflection coefficient was defined as the ratio of the maximum height of the superimposed incident and reflected waves to the height of the incident wave. The transmission coefficient was defined as the ratio of the height of the transmitted wave to the height of the incident wave.

A comparison of the basic geometric shape used in this investigation and the trapezoidal and triangular shapes analyzed by Johnson, Fuchs, and Morison show that at approximately the same high wave steepness the shape did not substantially affect the magnitude of the transmission coefficients. However, at approximately the same low wave steepness the values and range of the transmission coefficients for each of the geometric shapes were considerably different. This comparison was limited to the range of submergence ratios used in this investigation. It is interesting to note that for the trapezoidal and triangular breakwaters the lower wave steepness produced less transmission than the steeper waves, whereas, for the basic cyclindrical shape used in this

investigation the high wave steepnesses produced less transmission than the lower values of wave steepness. Breakwater configuration C was used for the comparison.

The height of the breakwater had the greatest affect on the reflection and transmission of the incident waves. Small changes in the submergence ratio, defined as the ratio of the height of the breakwater to the stillwater depth, other things being equal, resulted in large changes in the magnitude of the reflection and transmission coefficients. For the range of submergence ratios tabulated in Tables I to IV an increased submergence ratio resulted in increased wave reflection and decreased wave transmission. When the submergence ratio was equal to 1.0 a considerable portion of the incident wave energy was dissipated when breaking occurred. This resulted in increased turbulence over the structure and reduced the energy available for reflection. At maximum submergence ratio the transmitted wave consisted of multiple waves of small amplitude and small wave lengths.

Varying wave steepnesses did not affect the reflection and transmission coefficients to the same degree as did varying submergence ratios. In general, the high wave steepnesses produced only a relatively small change in the magnitude of the reflection coefficients over the range of submergence ratios, for example, for wave steepness of 0.0675 and breakwater A, the reflection coefficient varied from 1.083 at submergence ratio of 0.445 to 1.157 for submergence ratio of 0.889. The lowest wave steepness produced the greatest reflection whereas the highest wave steepness resulted in the smallest transmission of the incident wave. For breakwater B

and wave steepness 0.0222, the maximum reflection coefficient obtained was 1.380, whereas, for wave steepness 0.0675 the maximum was only 1.179. Similarly, for breakwater B and wave steepness 0.0222 the minimum transmission coefficient obtained was 0.916, whereas, for wave steepness 0.0675 the minimum was 0.727. For approximately equal relative depths, the two higher wave steepnesses did not appreciably affect the value of the coefficients. However, at the lower wave steepness the affect of wave steepness on the magnitude of these coefficients was of significance.

Increasing the width of the breakwater had very little effect on the reflection and transmission coefficients. Increases in width did slightly reduce transmission and increase reflection.

Since the cone of influence of wave motion theoretically extends down from the stillwater level approximately one-half a wave length, a submerged obstacle below this cone of influence should not affect the passing incident wave. However, an incident wave with a wave length of 19.4 inches and a theoretical effective wave motion depth of 9.7 inches, as used in this investigation, was affected by the submerged breakwater when the depth of water over the top of the breakwater was 15.0 inches. Therefore, the cone of influence of wave motion extends below the stillwater level more than the theoretical value of one-half a wave length.

The range of transmission coefficients for wave lengths 31.9 and 31.6 inches was approximately the same for the two lower wave steepnesses. The range of reflection coefficients for wave lengths 19.4 and 18.9 inches did not vary significantly for the two highest wave steepness used in this study. The incident waves of shorter

wave lengths were reflected less over the full range of breakwater heights than the longer incident waves.

The overall results of this study indicate that high breakwater heights should be used for a submerged breakwater if effective reduction of the incident wave is to be obtained. To prevent subjecting the breakwater to the force of breaking waves the top of the breakwater should be below the stillwater level. For this condition, the tidal range in the localities in which submerged breakwaters are contemplated must be considered. Since the top of the submerged breakwater should always be below the stillwater depth, a submerged breakwater in areas having large tidal ranges would have to be of minimum height for the lowest tide. At the maximum tide the breakwater effectiveness would be reduced due to the high degree of submergence. Therefore, in areas where large tidal ranges exist the construction of a submerged breakwater would be unjustified because of its reduced effectiveness. For high breakwater heights and a constant stillwater depth, the submerged breakwaters tested in this experiment provided high reflection and low transmission.

As in all engineering problems, an effective design must always consider economics. Therefore, the design and construction of a submerged breakwater must be a balance between the cost, which is a function of the height, shape, and width of the structure, and the benefits of the engineering performance required. These benefits are susceptible to evaluation as reductions in damage to water front structures, harbor facilities and recreational beaches and erosion of the coastline.

Since varying the breakwater width did not substantially affect the results it is suggested that further research be concentrated on geometric shapes and types of breakwaters. Consideration should be given to the study of permeable breakwaters, and breakwaters of various roughnesses using breaking waves as well as smooth waves. Possibly the use of floating breakwaters should be investigated. The top of such a breakwater could be at or slightly below the still-water level with the bottom extending down various depths. For all investigations, the length of the wave channel used in laboratory experiments should be sufficient to prevent the beach reflections from interfering with the measured transmitted waves. Also, the distance from the wave generator to the reflecting structure should be such that reflections from the plunger could be prevented or at least minimized and thereby not affect the characteristics of the incident wave. Since it had not been originally intended to utilize the effective wave motion ratio as a parameter, only two wave lengths were studied. Further study using this parameter may provide the necessary data for determining the actual effective depth of wave motion. In this investigation it was observed that the roughness of the tank walls did induce small secondary waves. Although this effect was not measurable with the equipment utilized it could adversely affect the wave height measurements under other conditions.

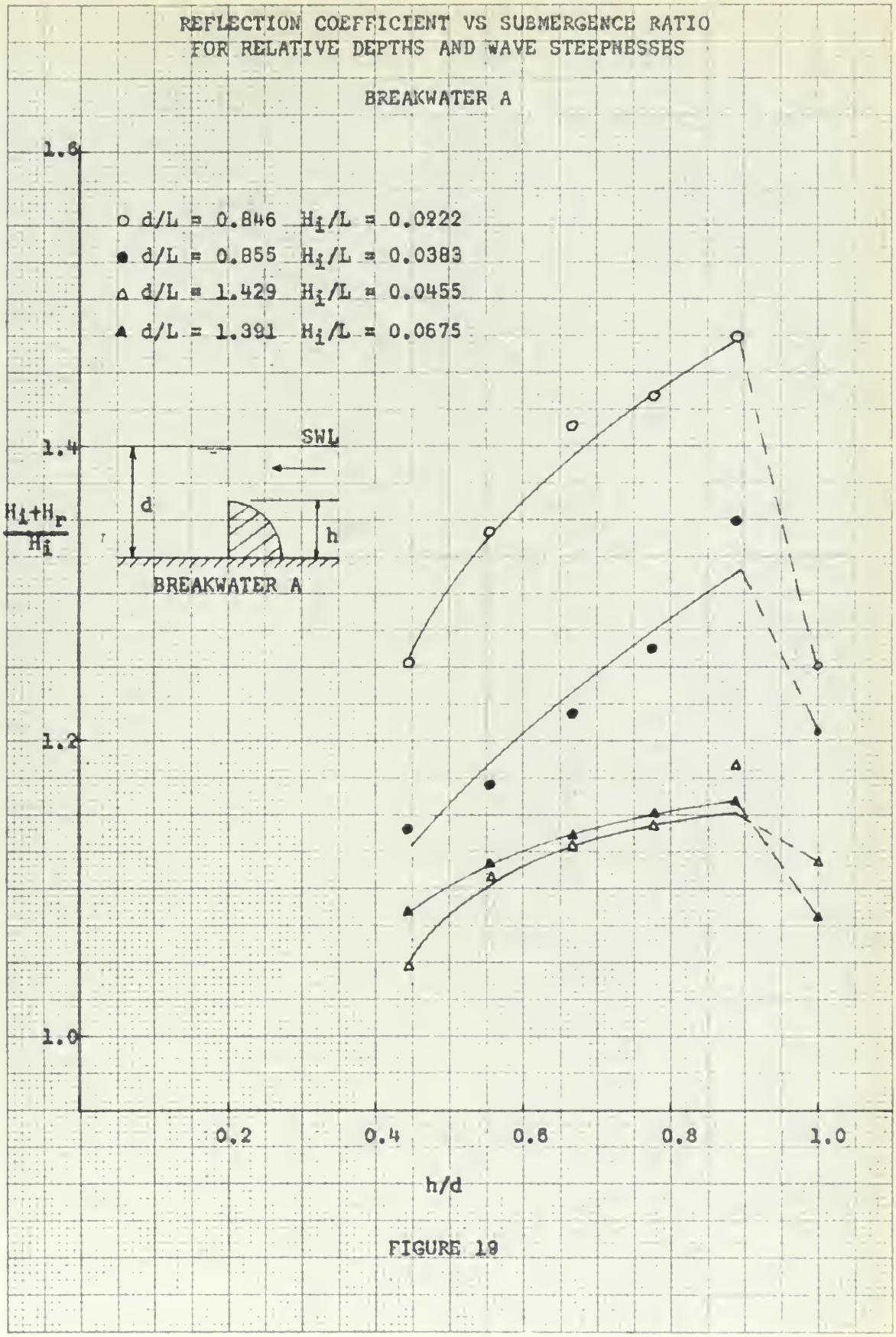
REFLECTION COEFFICIENT VS SUBMERGENCE RATIO
FOR RELATIVE DEPTHS AND WAVE STEEPNESSES
BREAKWATER A
○ d/L = 0.846 Hi/L = 0.0222
● d/L = 0.855 Hi/L = 0.0383
△ d/L = 1.429 Hi/L = 0.0455
▲ d/L = 1.391 Hi/L = 0.0675
SWL
d
h
BREAKWATER A
(Hi+Hr)/Hi
1.6
1.4
1.2
1.0
0.2
0.4
0.6
0.8
1.0
h/d

FIGURE 19

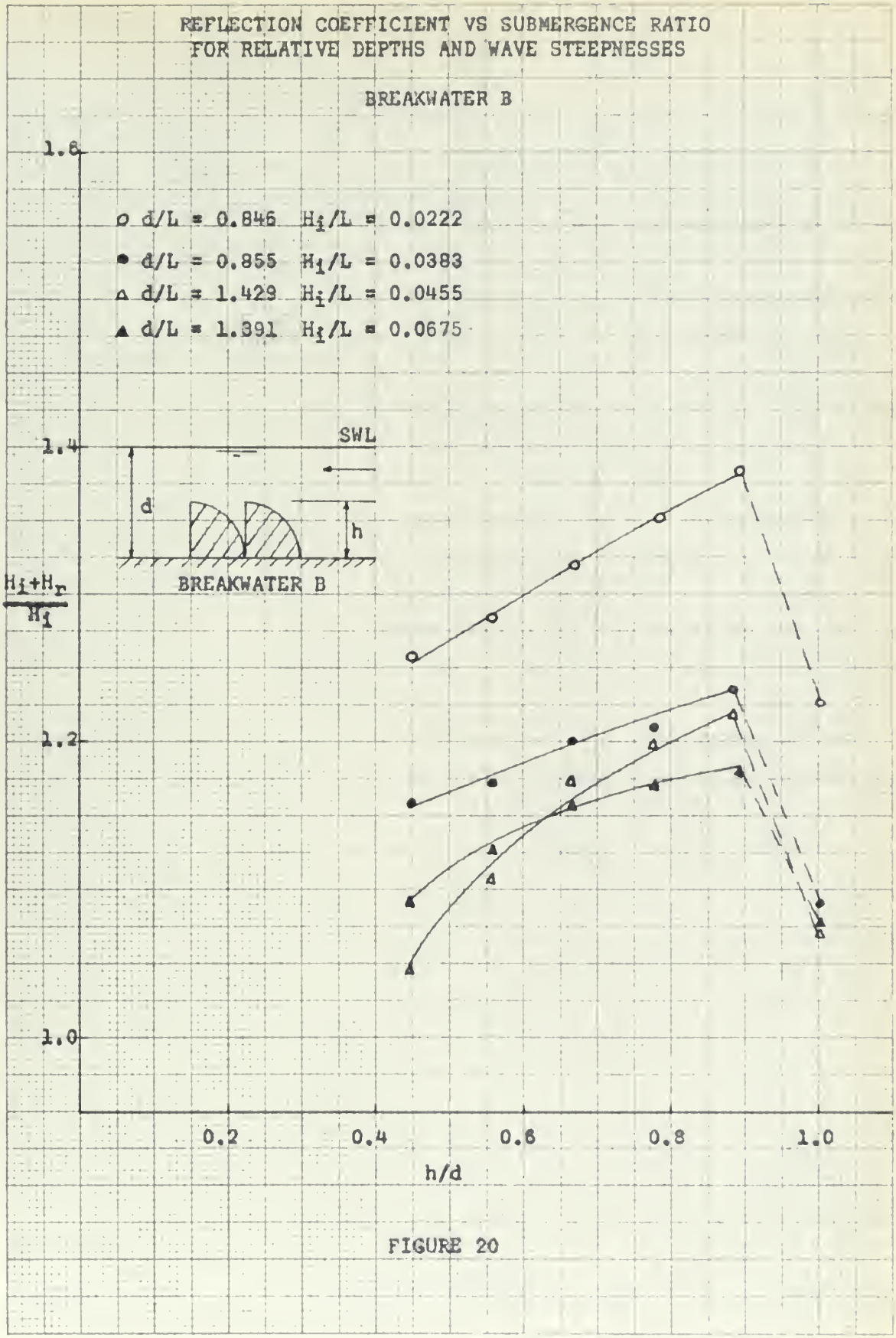
REFLECTION COEFFICIENT VS SUBMERGENCE RATIO
FOR RELATIVE DEPTHS AND WAVE STEEPNESSES
BREAKWATER B
o d/L = 0.846 Hi/L = 0.0222
• d/L = 0.855 Hi/L = 0.0383
Δ d/L = 1.429 Hi/L = 0.0455
▲ d/L = 1.391 Hi/L = 0.0675
SWL
d
h
BREAKWATER B
Hi+Hr / Hi
1.6
1.4
1.2
1.0
0.2
0.4
0.6
0.8
1.0
h/d

FIGURE 20

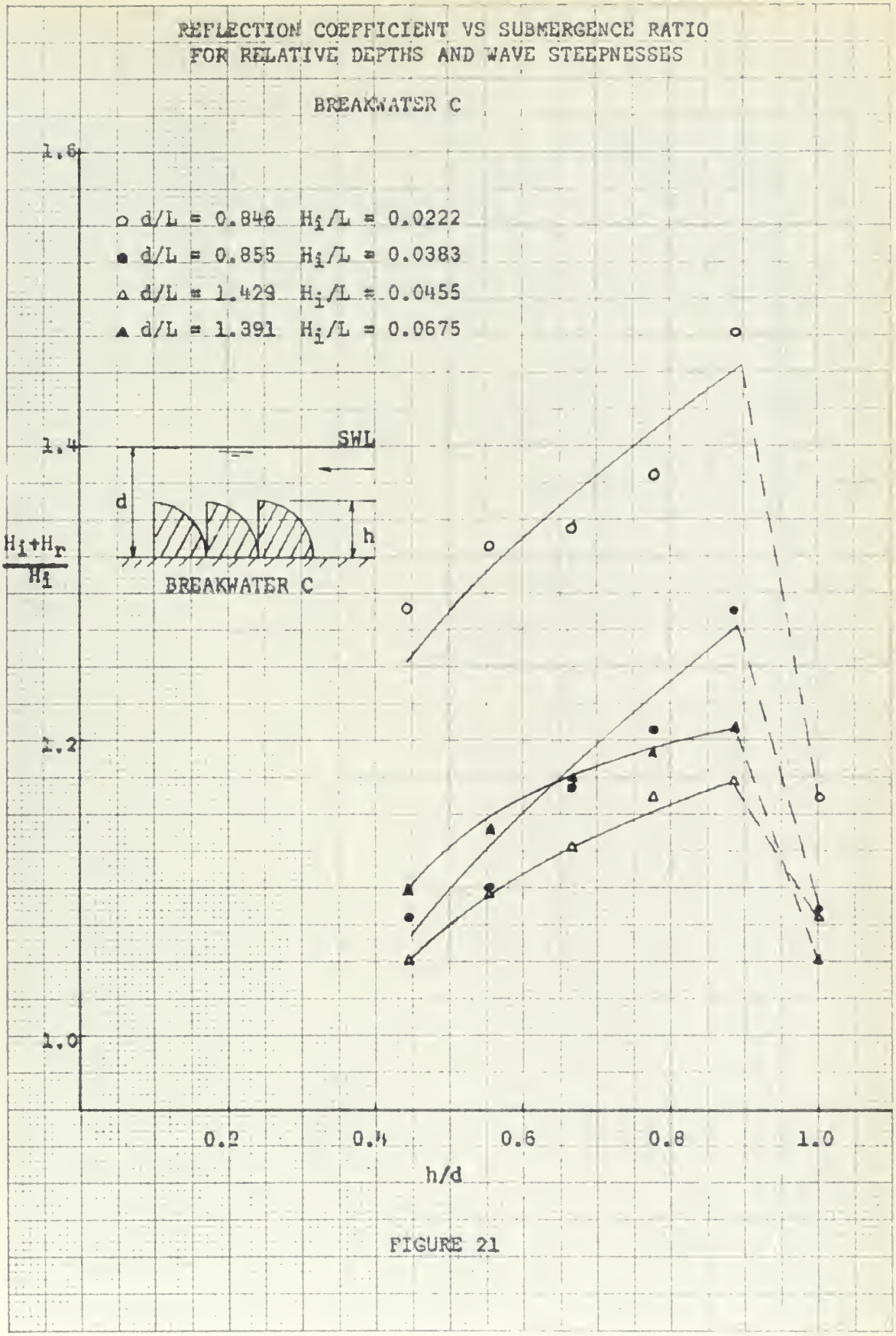
REFLECTION COEFFICIENT VS SUBMERGENCE RATIO
FOR RELATIVE DEPTHS AND WAVE STEEPNESSES
BREAKWATER C
○ d/L = 0.846 Hi/L = 0.0222
● d/L = 0.855 Hi/L = 0.0383
△ d/L = 1.429 Hi/L = 0.0455
▲ d/L = 1.391 Hi/L = 0.0675
SWL
d
h
BREAKWATER C
Hi+Hr / Hi
1.6
1.4
1.2
1.0
0.2
0.4
0.6
0.8
1.0
h/d

FIGURE 21

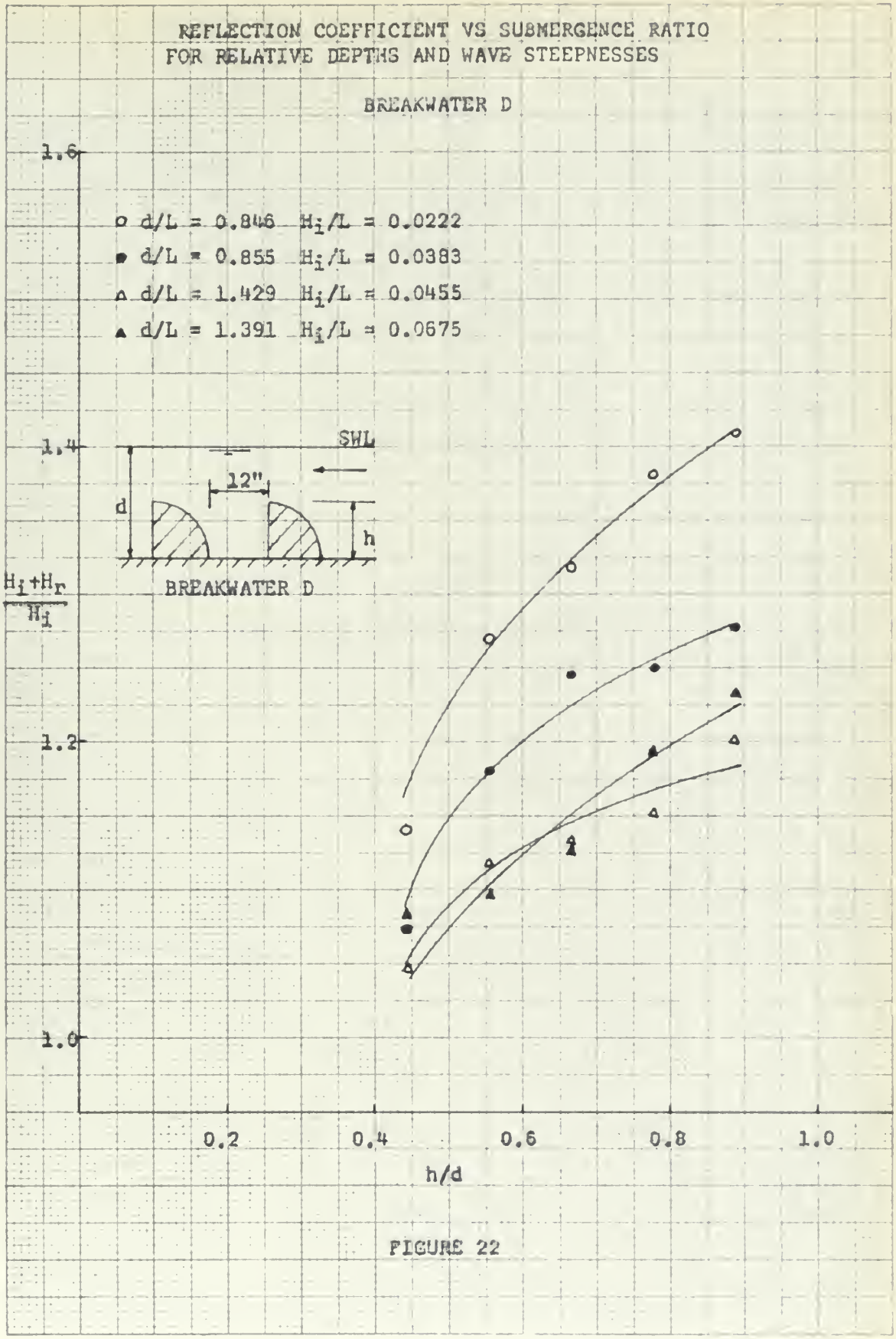
REFLECTION COEFFICIENT VS SUBMERGENCE RATIO
FOR RELATIVE DEPTHS AND WAVE STEEPNESSES
BREAKWATER D
o d/L = 0.846 Hi/L = 0.0222
• d/L = 0.855 Hi/L = 0.0383
Δ d/L = 1.429 Hi/L = 0.0455
▲ d/L = 1.391 Hi/L = 0.0675
SWL
12"
d
h
BREAKWATER D
Hi+Hr / Hi
1.6
1.4
1.2
1.0
0.2
0.4
0.6
0.8
1.0
h/d

FIGURE 22

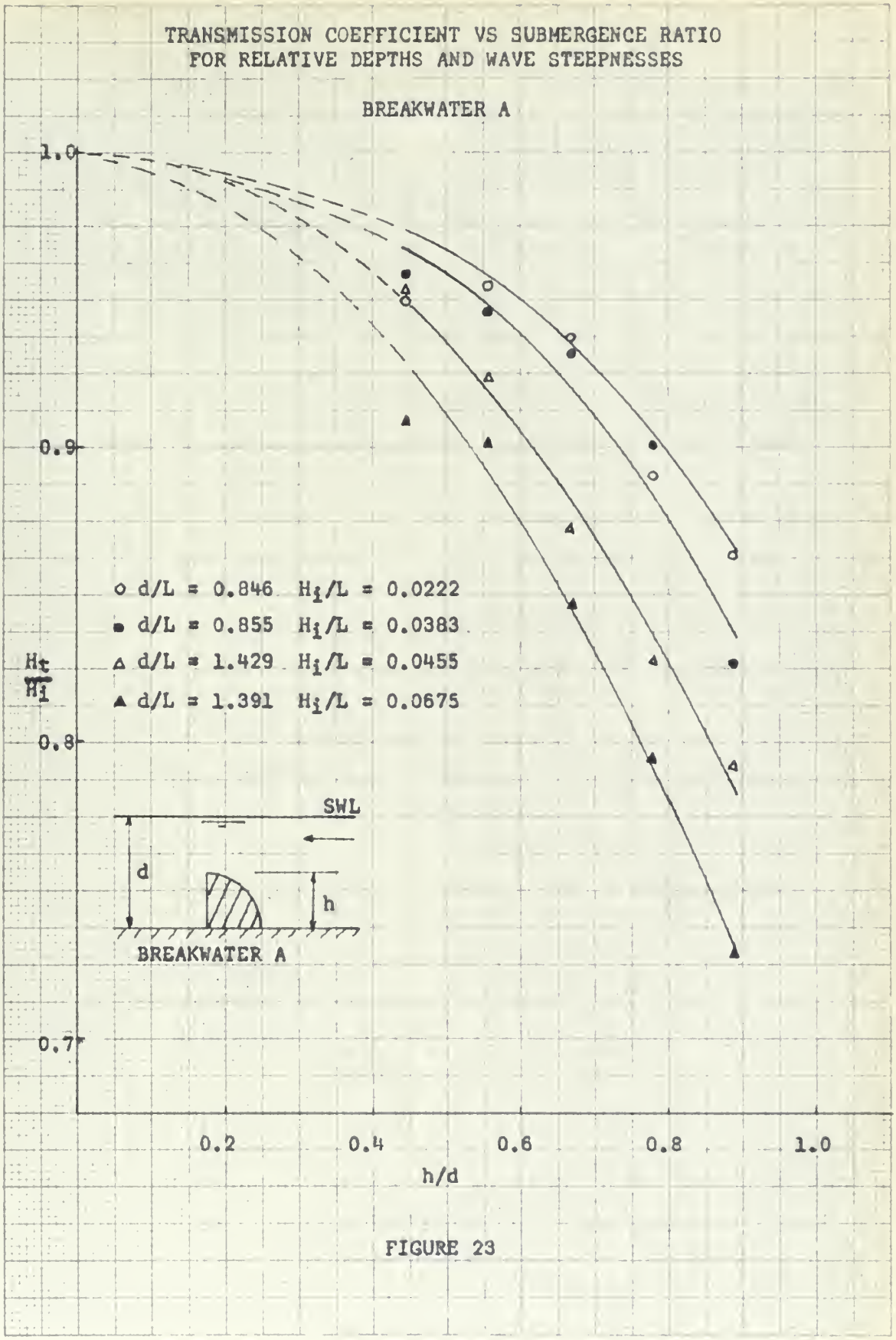
TRANSMISSION COEFFICIENT VS SUBMERGENCE RATIO
FOR RELATIVE DEPTHS AND WAVE STEEPNESSES
BREAKWATER A
1.0
0.9
0.8
0.7
$\frac{H_t}{H_i}$
○ d/L = 0.846 H_i/L = 0.0222
● d/L = 0.855 H_i/L = 0.0383
△ d/L = 1.429 H_i/L = 0.0455
▲ d/L = 1.391 H_i/L = 0.0675
SWL
d
h
BREAKWATER A
0.2
0.4
0.6
0.8
1.0
h/d

FIGURE 23

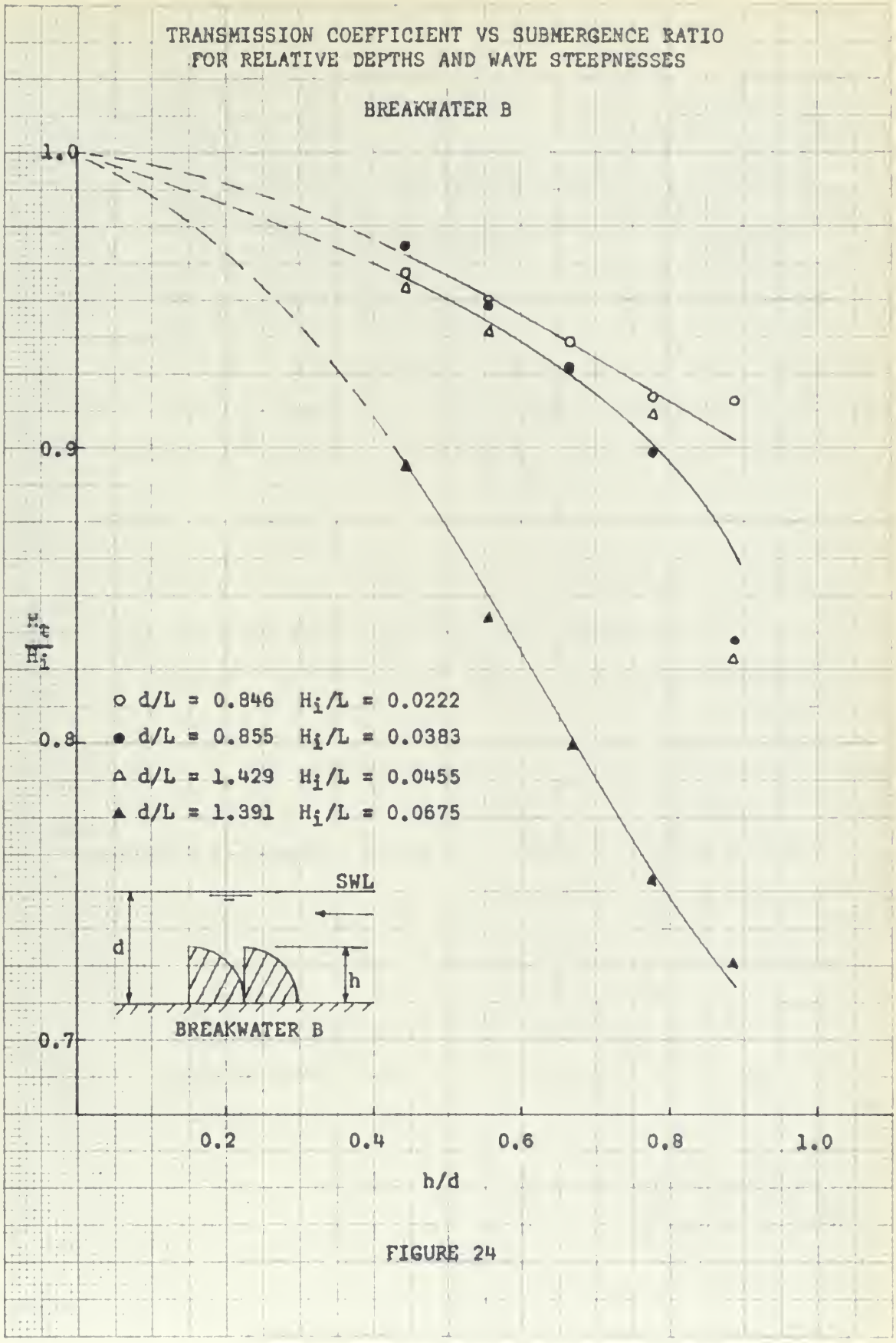
TRANSMISSION COEFFICIENT VS SUBMERGENCE RATIO
FOR RELATIVE DEPTHS AND WAVE STEEPNESSES
BREAKWATER B
1.0
0.9
0.8
0.7
$\frac{H_t}{H_i}$
○ d/L = 0.846 H_i/L = 0.0222
● d/L = 0.855 H_i/L = 0.0383
△ d/L = 1.429 H_i/L = 0.0455
▲ d/L = 1.391 H_i/L = 0.0675
SWL
d
h
BREAKWATER B
0.2
0.4
0.6
0.8
1.0
h/d

FIGURE 24

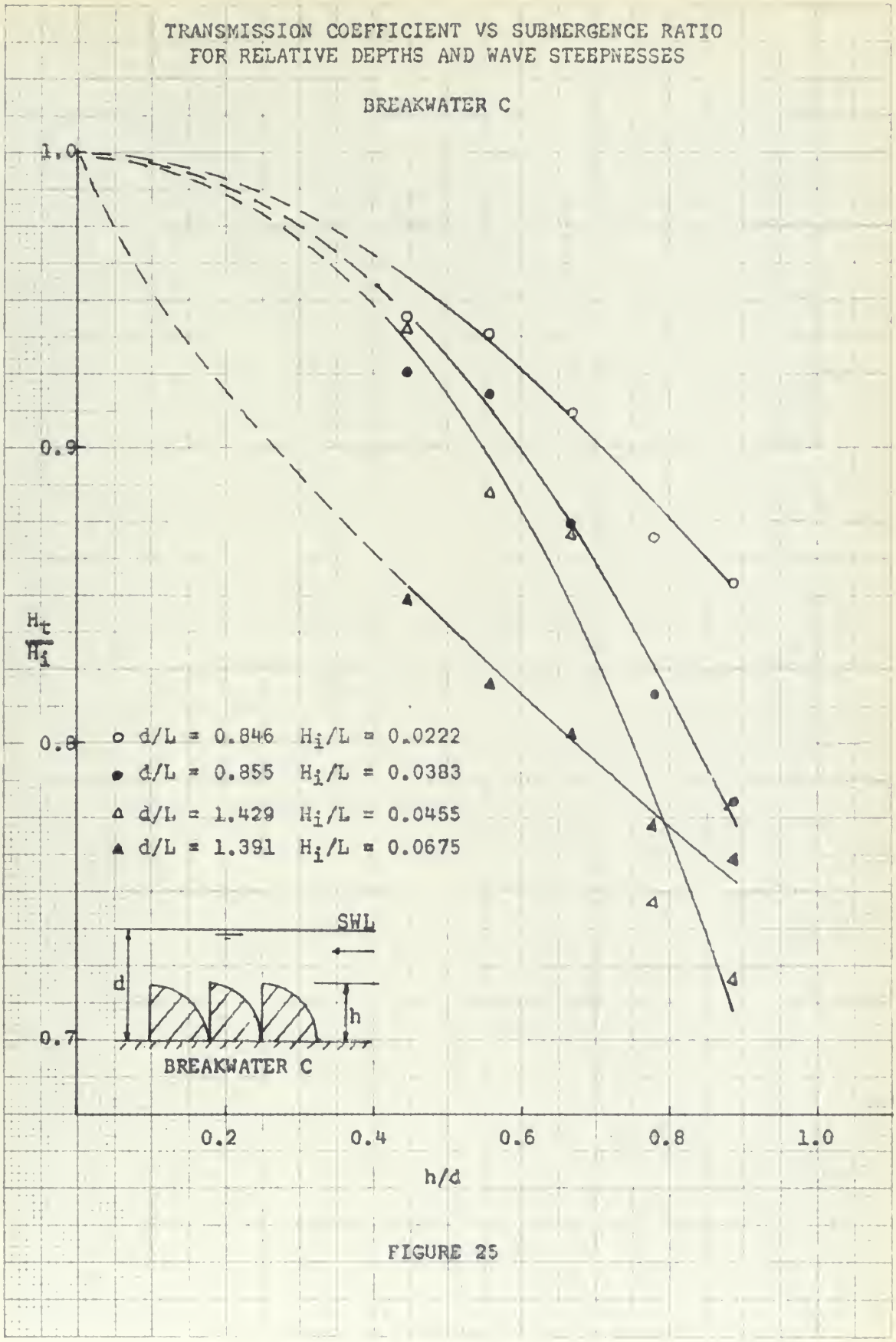
TRANSMISSION COEFFICIENT VS SUBMERGENCE RATIO
FOR RELATIVE DEPTHS AND WAVE STEEPNESSES
BREAKWATER C
1.0
0.9
0.8
0.7
$\frac{H_t}{H_i}$
○ d/L = 0.846 H_i/L = 0.0222
● d/L = 0.855 H_i/L = 0.0383
△ d/L = 1.429 H_i/L = 0.0455
▲ d/L = 1.391 H_i/L = 0.0675
SWL
d
h
BREAKWATER C
0.2
0.4
0.6
0.8
1.0
h/d

FIGURE 25

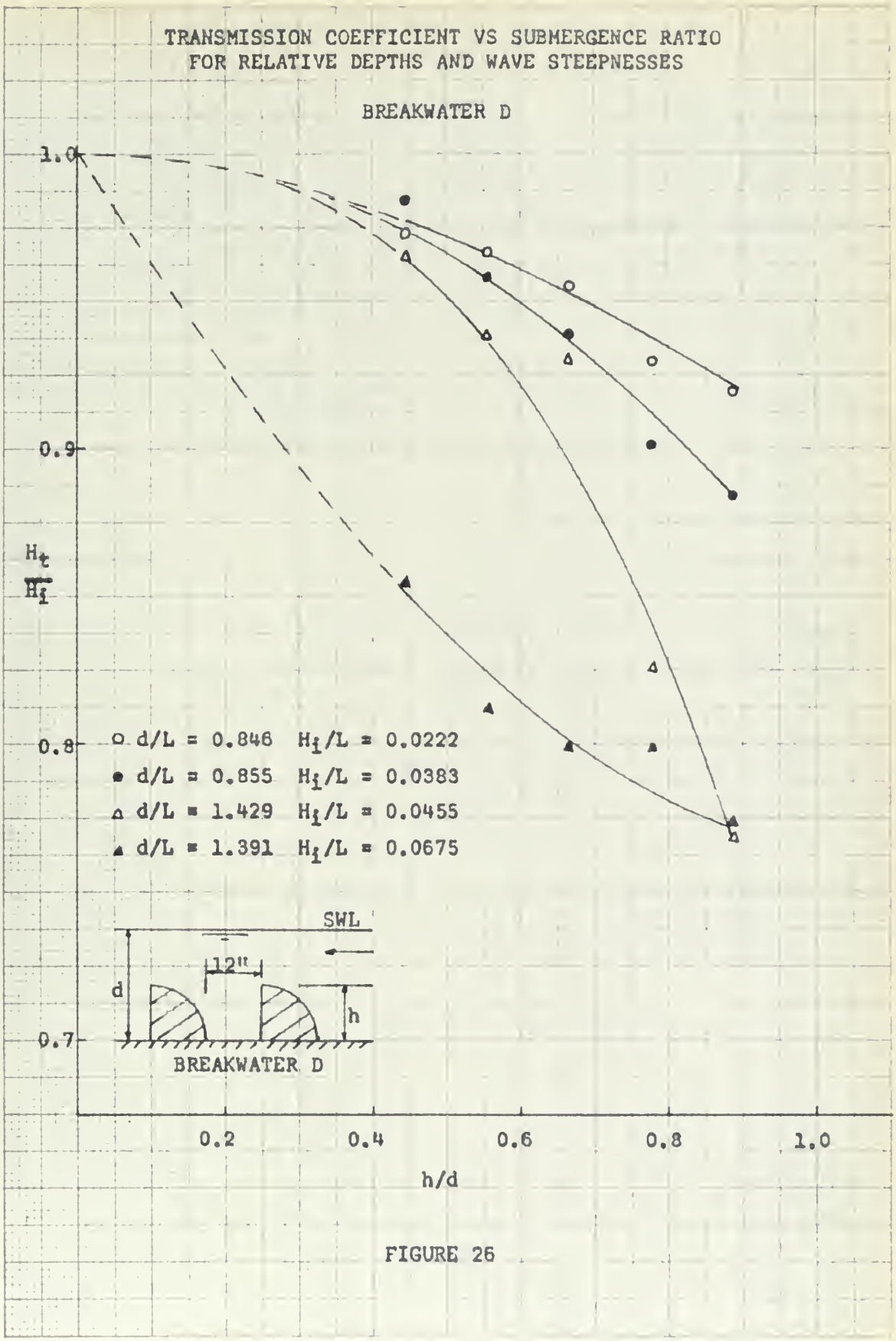
TRANSMISSION COEFFICIENT VS SUBMERGENCE RATIO
FOR RELATIVE DEPTHS AND WAVE STEEPNESSES
BREAKWATER D
1.0
0.9
0.8
0.7
$\frac{H_t}{H_i}$
○ d/L = 0.846 H_i/L = 0.0222
● d/L = 0.855 H_i/L = 0.0383
△ d/L = 1.429 H_i/L = 0.0455
▲ d/L = 1.391 H_i/L = 0.0675
SWL
12"
d
h
BREAKWATER D
0.2
0.4
0.6
0.8
1.0
h/d

FIGURE 26

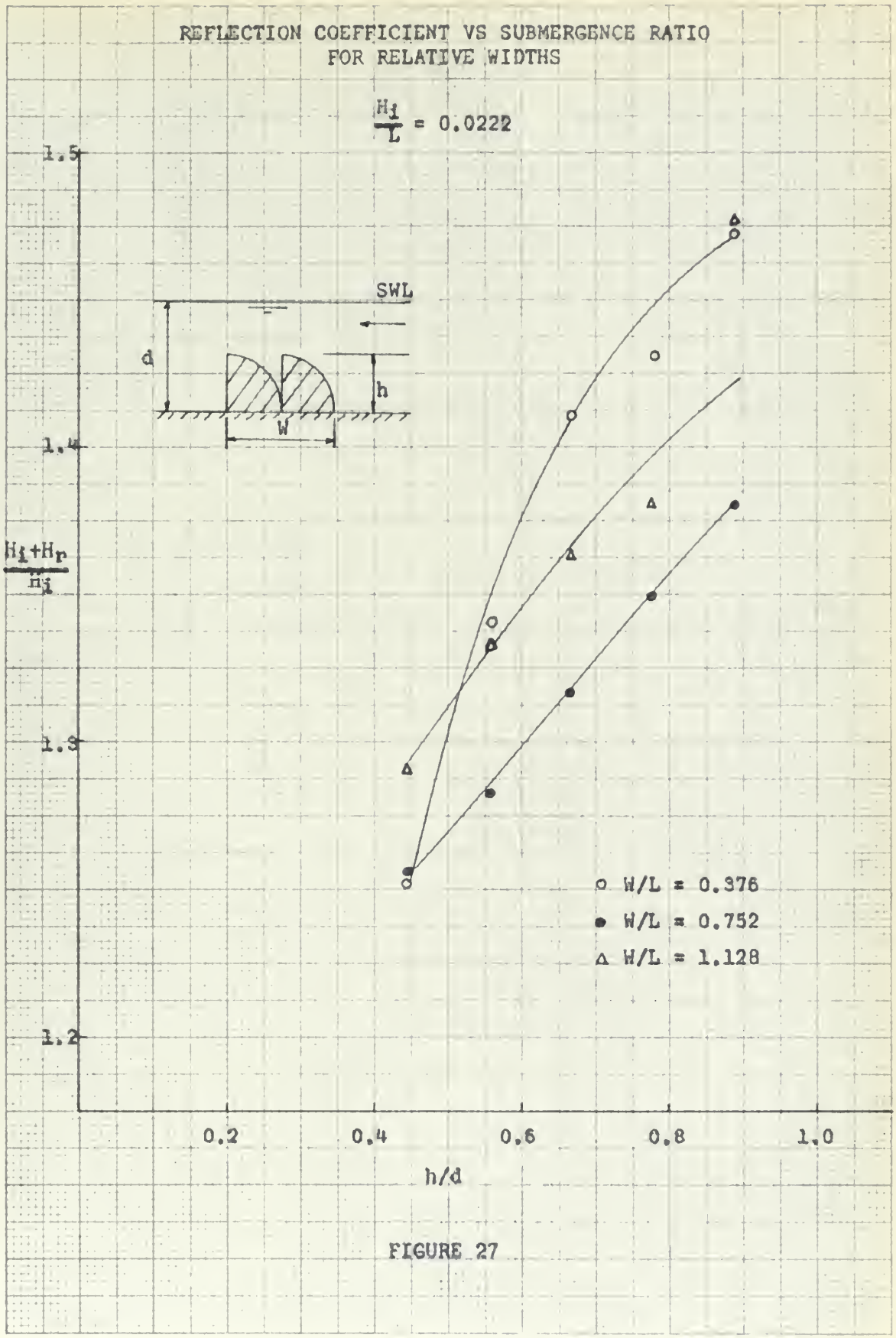
REFLECTION COEFFICIENT VS SUBMERGENCE RATIO
FOR RELATIVE WIDTHS
$\frac{H_i}{L}$ = 0.0222
SWL
d
h
W
1.5
1.4
1.3
1.2
$\frac{H_i+H_r}{H_i}$
0.2
0.4
0.6
0.8
1.0
h/d
o W/L = 0.376
• W/L = 0.752
Δ W/L = 1.128

FIGURE 27

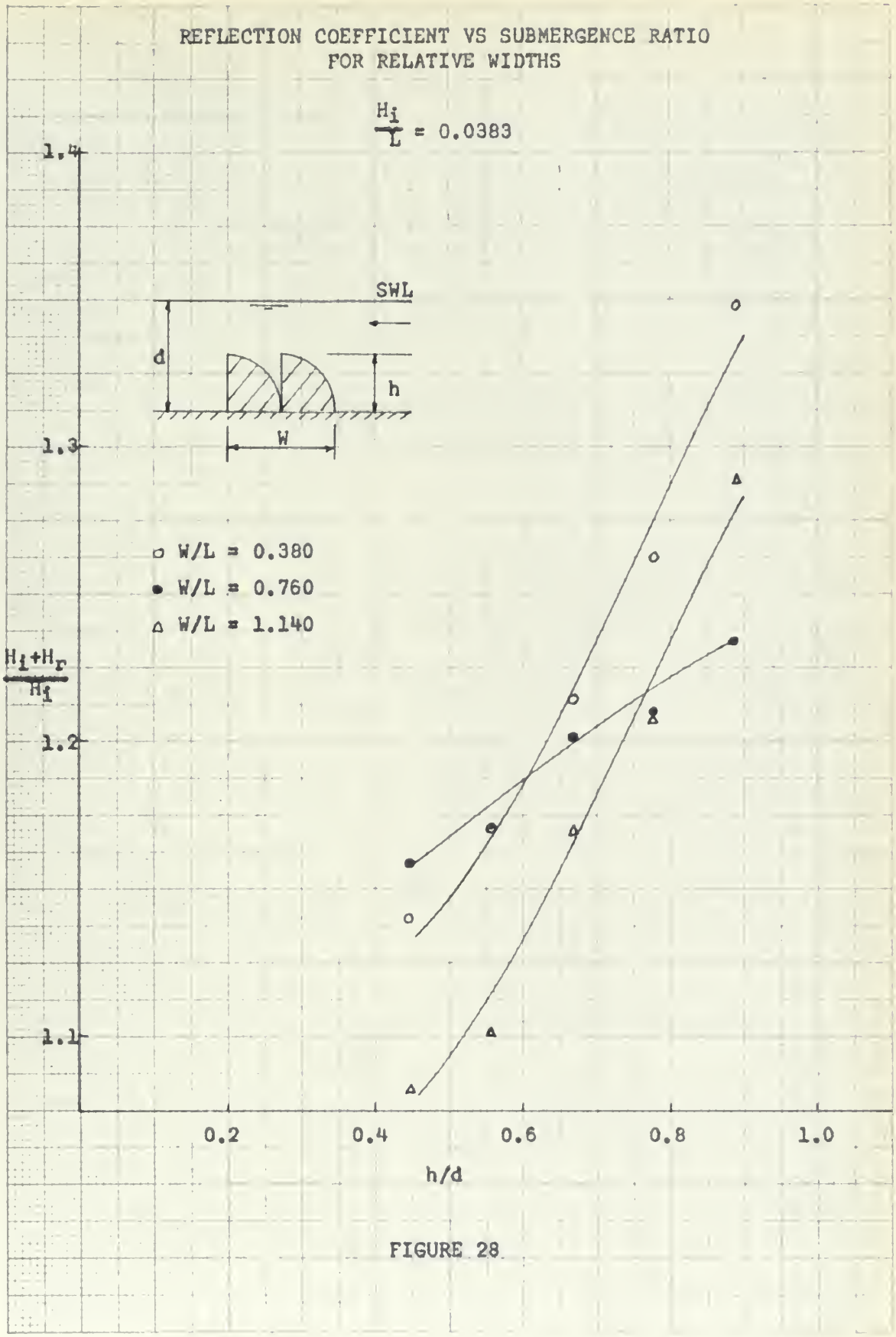
REFLECTION COEFFICIENT VS SUBMERGENCE RATIO
FOR RELATIVE WIDTHS
$\frac{H_i}{L}$ = 0.0383
SWL
d
h
W
o W/L = 0.380
• W/L = 0.760
Δ W/L = 1.140
$\frac{H_i+H_r}{H_i}$
1.4
1.3
1.2
1.1
0.2
0.4
0.6
0.8
1.0
h/d

FIGURE 28

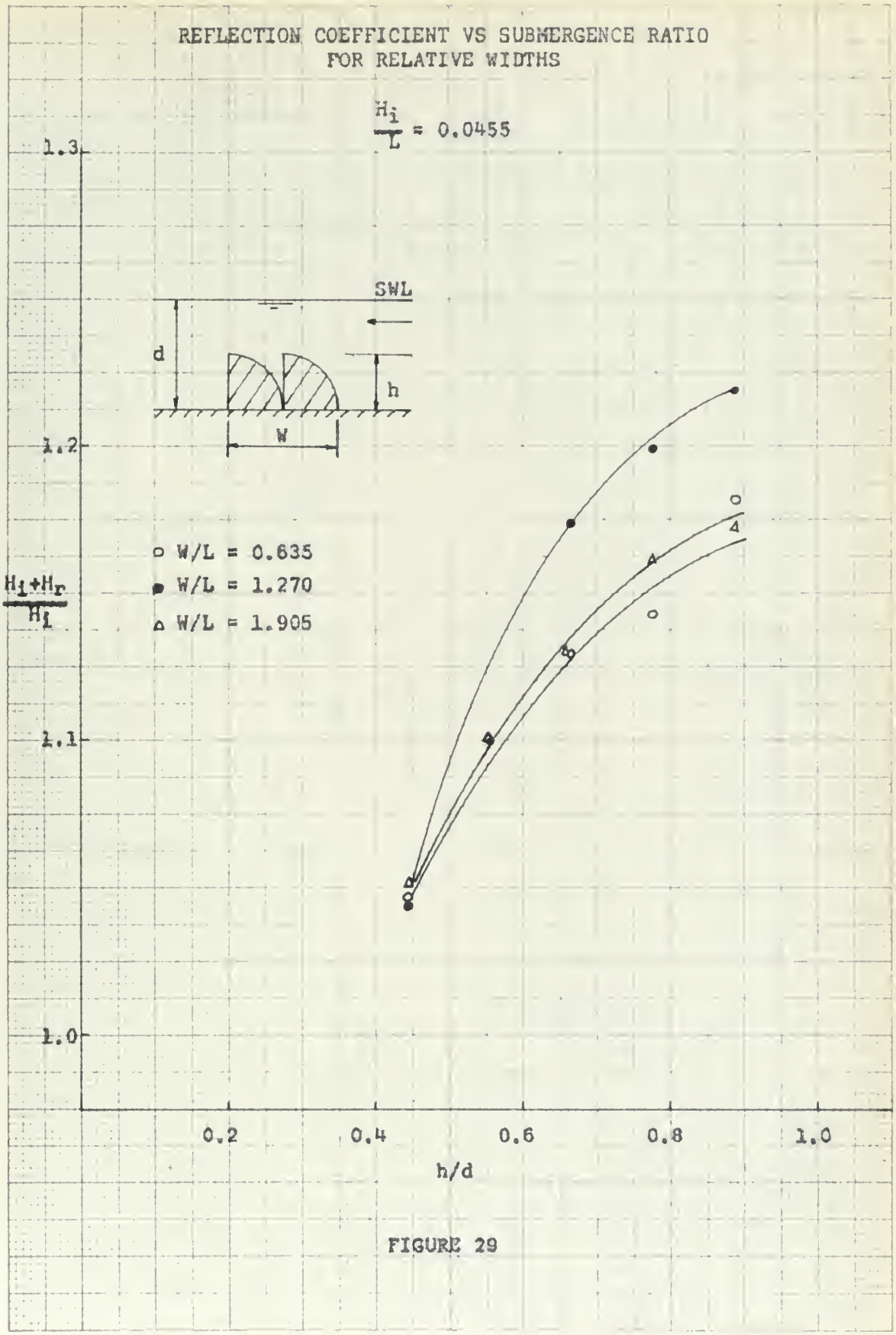
REFLECTION COEFFICIENT VS SUBMERGENCE RATIO
FOR RELATIVE WIDTHS
$\frac{H_i}{L}$ = 0.0455
SWL
d
h
W
o W/L = 0.635
• W/L = 1.270
Δ W/L = 1.905
$\frac{H_i+H_r}{H_i}$
1.3
1.2
1.1
1.0
0.2
0.4
0.6
0.8
1.0
h/d

FIGURE 29

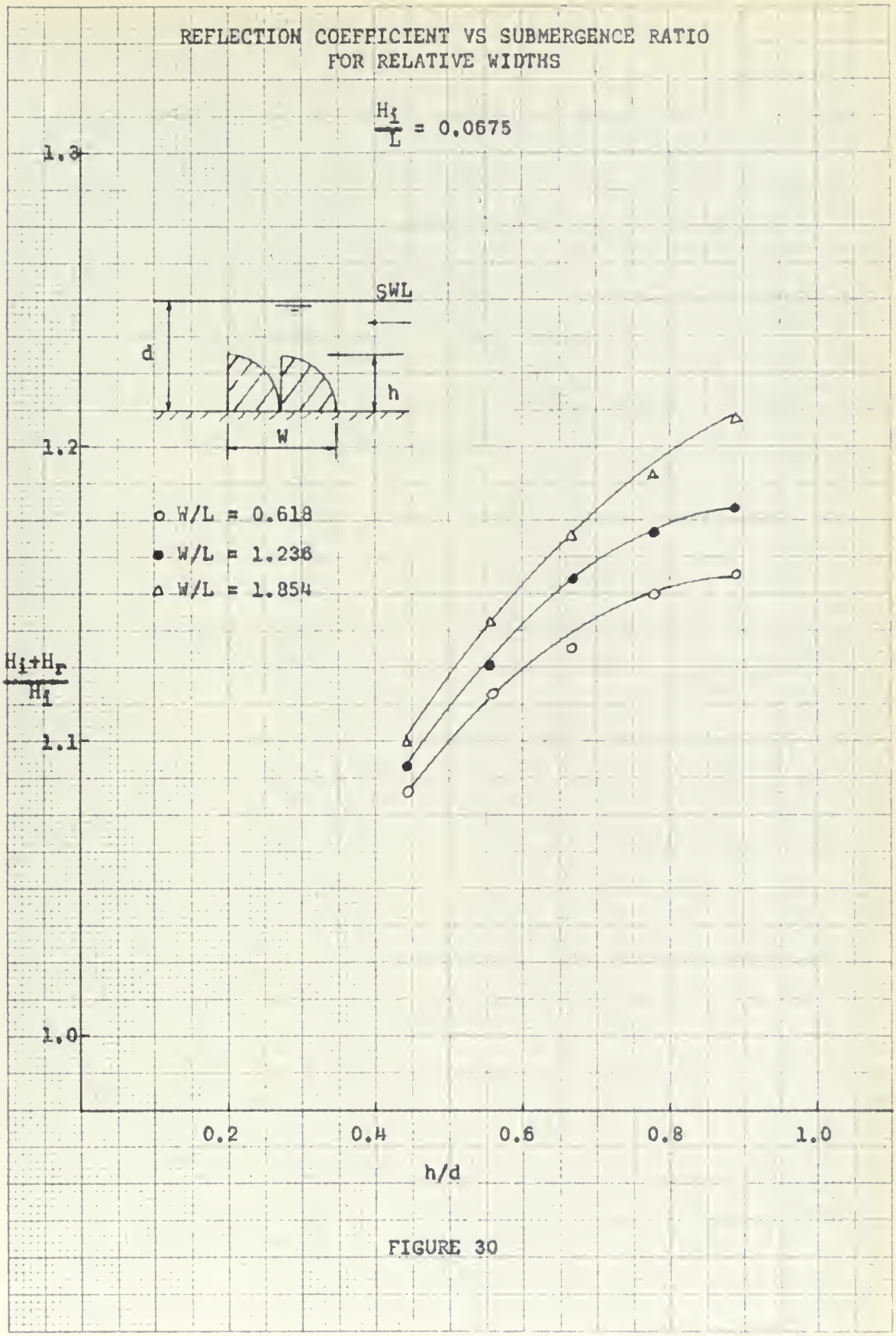
REFLECTION COEFFICIENT VS SUBMERGENCE RATIO
FOR RELATIVE WIDTHS
$\frac{H_i}{L}$ = 0.0675
SWL
d
h
W
o W/L = 0.618
• W/L = 1.236
Δ W/L = 1.854
$\frac{H_i+H_r}{H_i}$
1.3
1.2
1.1
1.0
0.2
0.4
0.6
0.8
1.0
h/d

FIGURE 30

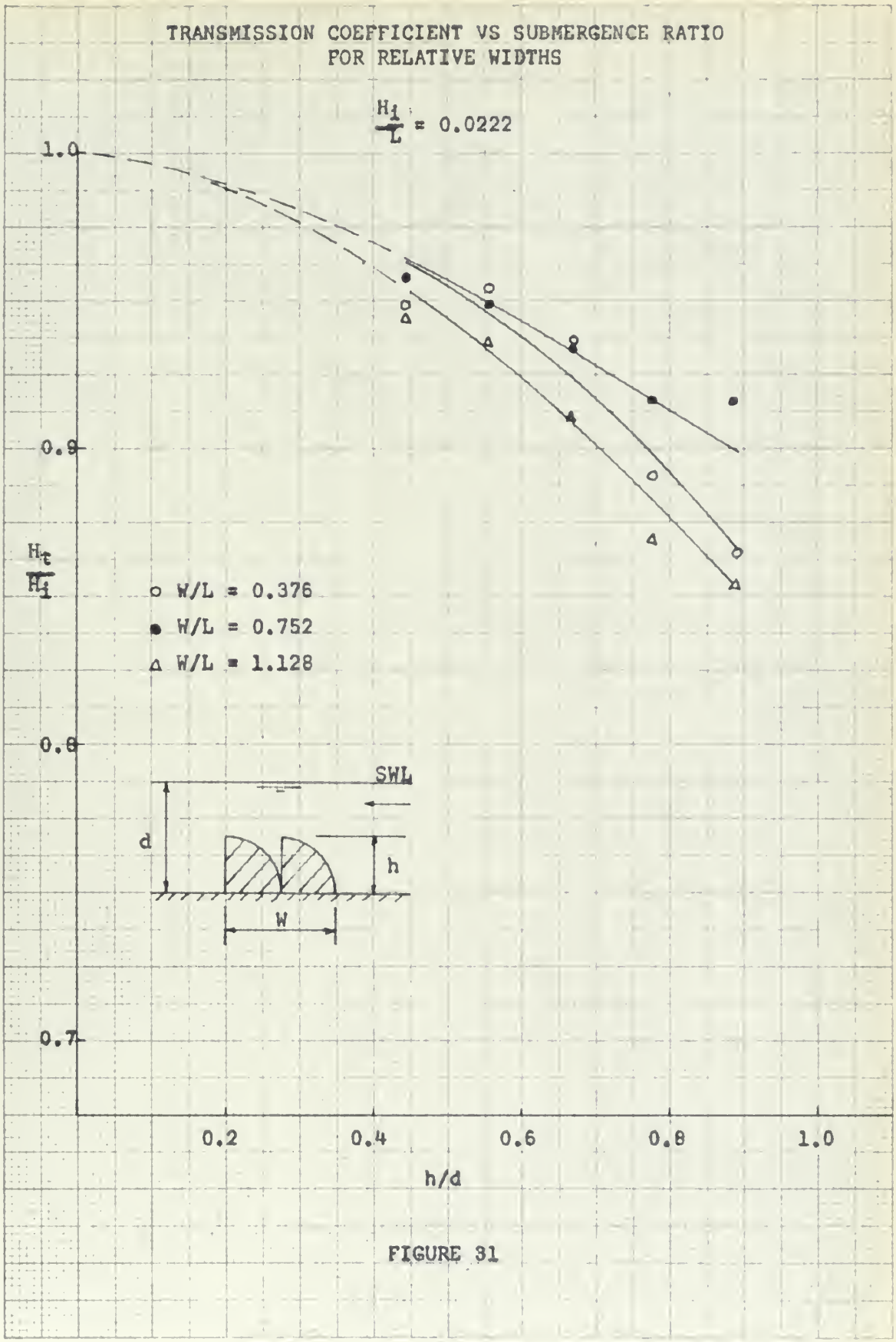
TRANSMISSION COEFFICIENT VS SUBMERGENCE RATIO
FOR RELATIVE WIDTHS
$\frac{H_i}{L}$ = 0.0222
1.0
0.9
0.8
0.7
$\frac{H_t}{H_i}$
○ W/L = 0.376
● W/L = 0.752
△ W/L = 1.128
SWL
d
h
W
0.2
0.4
0.6
0.8
1.0
h/d

FIGURE 31

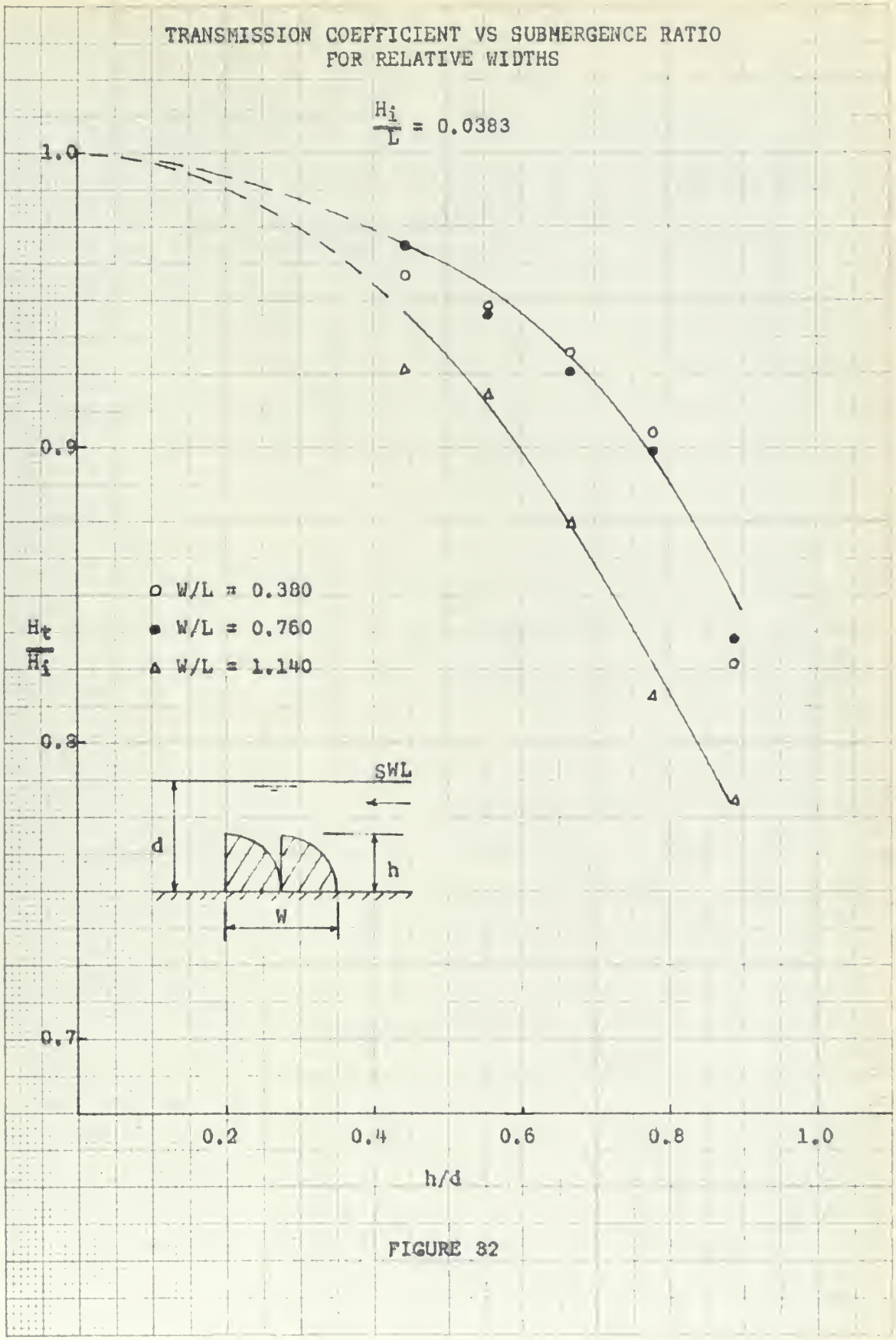
TRANSMISSION COEFFICIENT VS SUBMERGENCE RATIO
FOR RELATIVE WIDTHS
$\frac{H_i}{L}$ = 0.0383
1.0
0.9
0.8
0.7
$\frac{H_t}{H_i}$
o W/L = 0.380
• W/L = 0.760
Δ W/L = 1.140
SWL
d
h
W
0.2
0.4
0.6
0.8
1.0
h/d

FIGURE 32

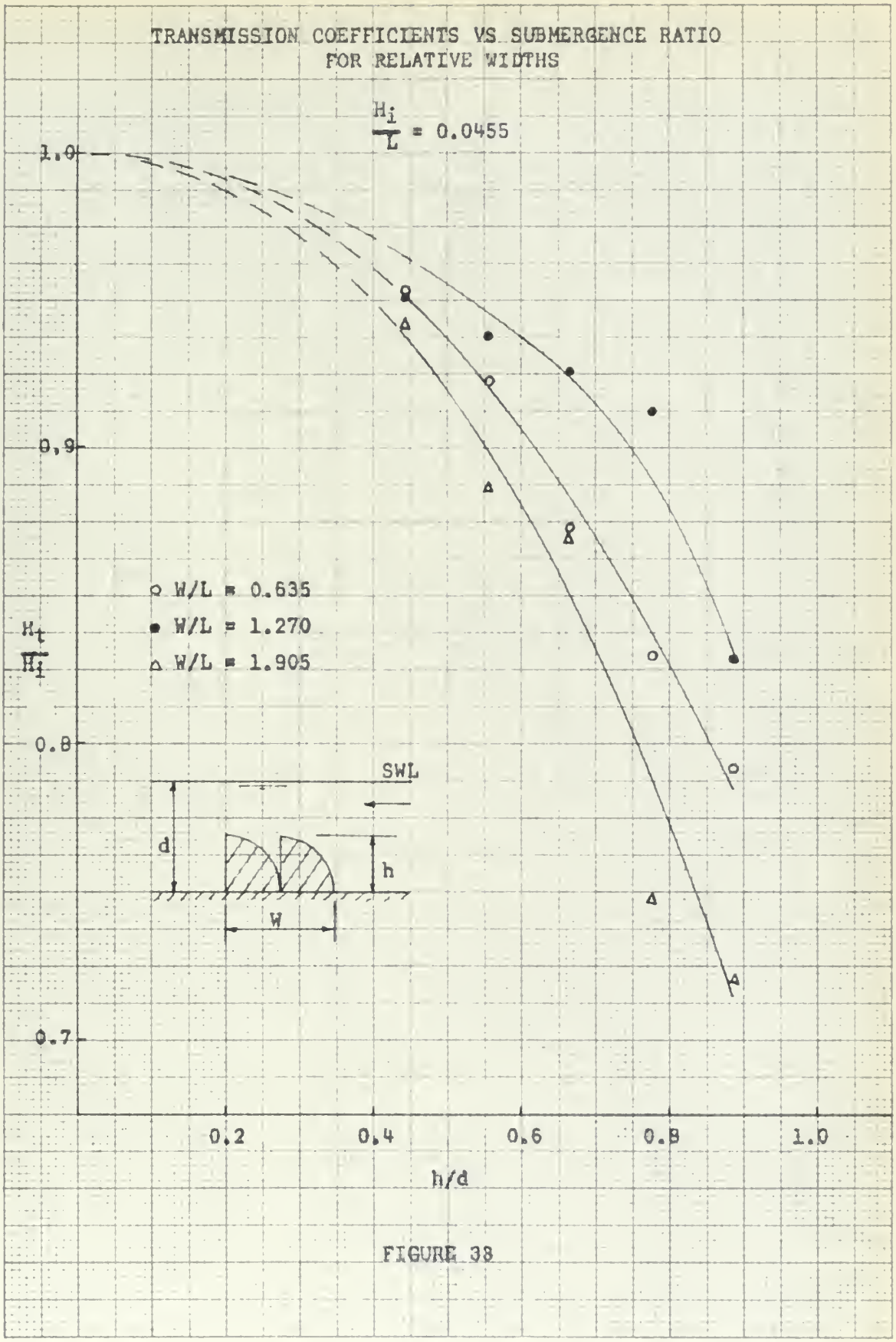
TRANSMISSION COEFFICIENTS VS SUBMERGENCE RATIO
FOR RELATIVE WIDTHS
Hi/L = 0.0455
1.0
0.9
0.8
0.7
Ht/Hi
o W/L = 0.635
• W/L = 1.270
Δ W/L = 1.905
SWL
d
h
W
0.2
0.4
0.6
0.8
1.0
h/d

FIGURE 38

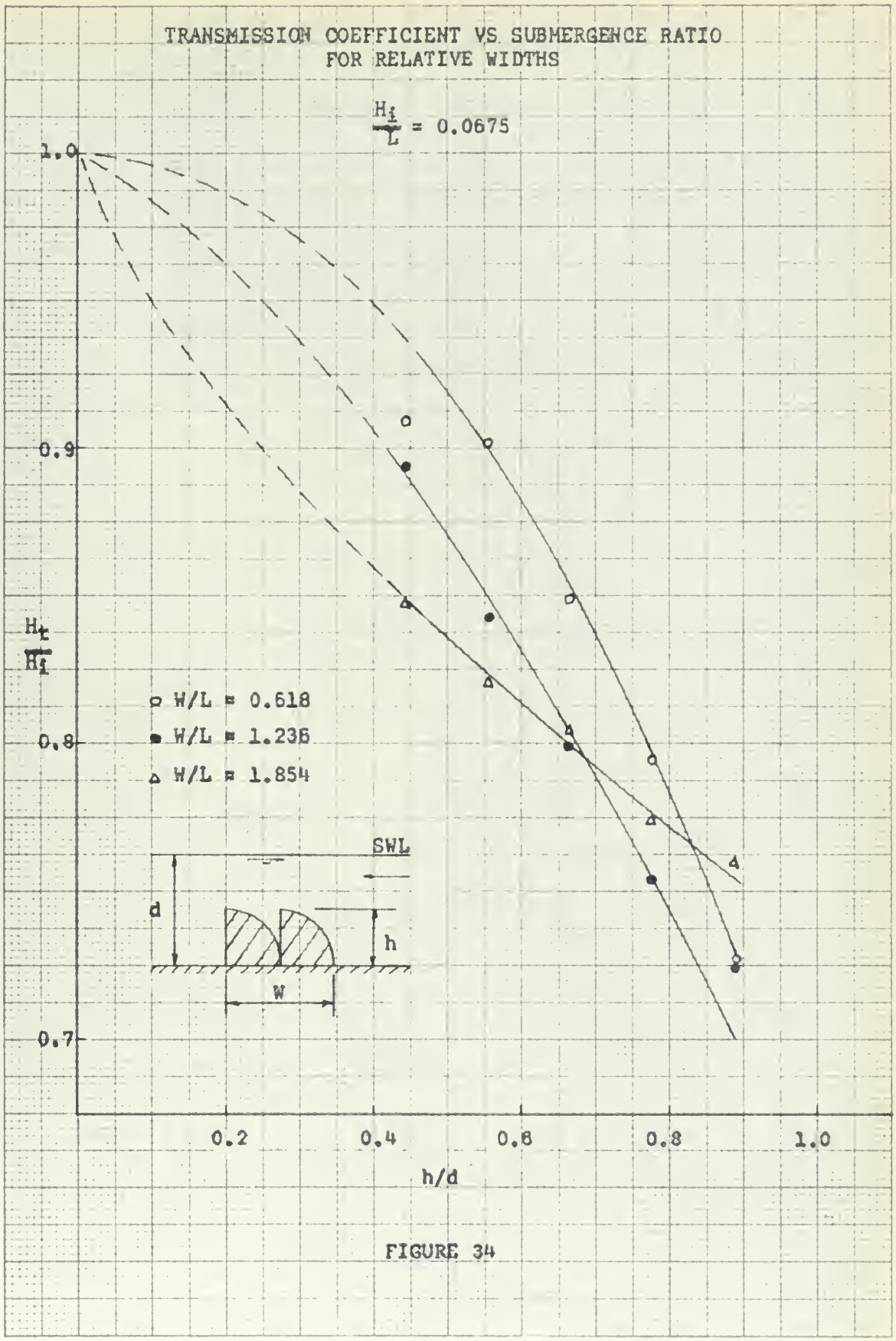
TRANSMISSION COEFFICIENT VS SUBMERGENCE RATIO
FOR RELATIVE WIDTHS
$\frac{H_i}{L}$ = 0.0675
1.0
0.9
0.8
0.7
$\frac{H_t}{H_i}$
o W/L = 0.618
• W/L = 1.236
Δ W/L = 1.854
SWL
d
h
W
0.2
0.4
0.6
0.8
1.0
h/d

FIGURE 34

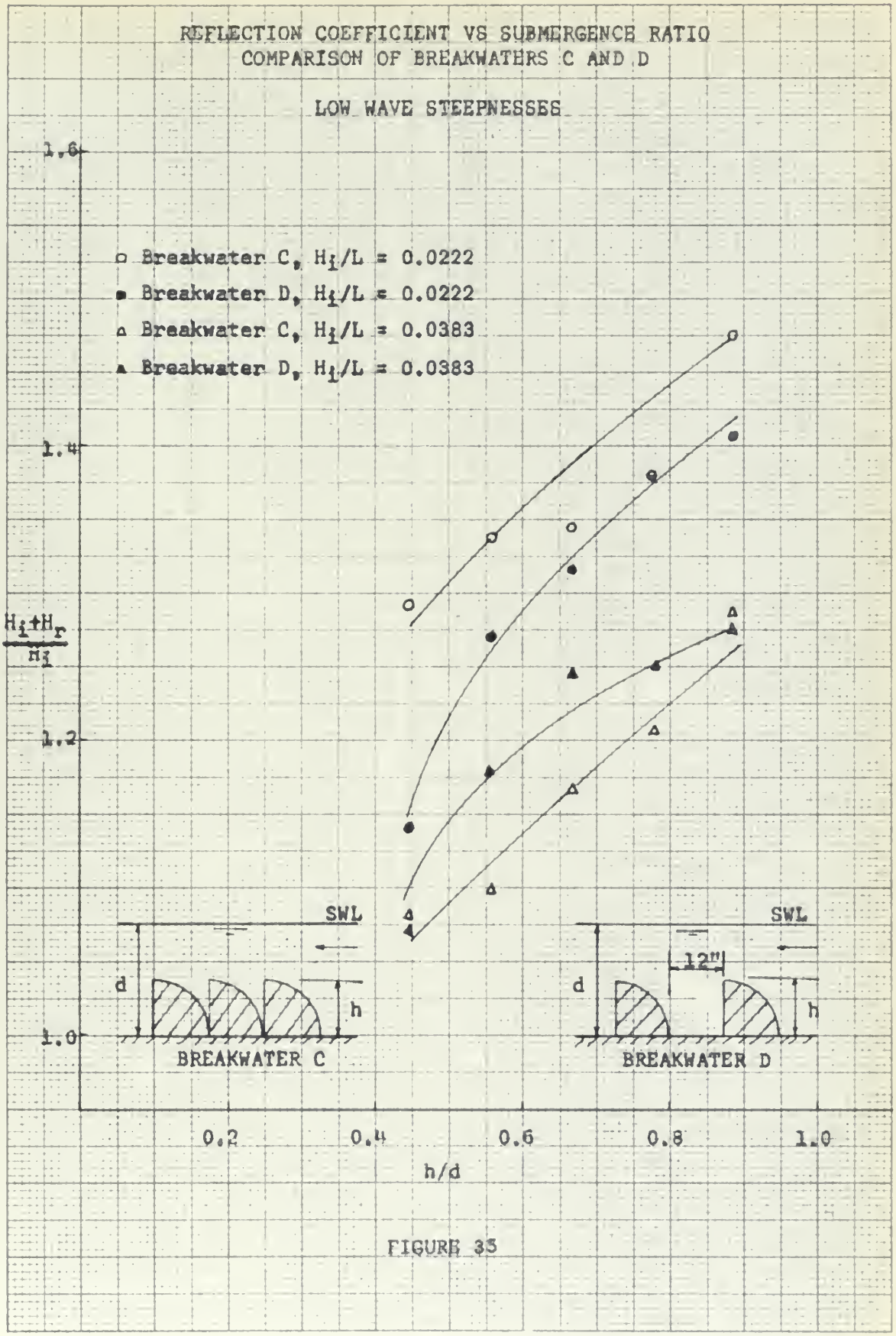
REFLECTION COEFFICIENT VS SUBMERGENCE RATIO
COMPARISON OF BREAKWATERS C AND D
LOW WAVE STEEPNESSES
○ Breakwater C, H_i/L = 0.0222
● Breakwater D, H_i/L = 0.0222
△ Breakwater C, H_i/L = 0.0383
▲ Breakwater D, H_i/L = 0.0383
$\frac{H_i+H_r}{H_i}$
1.6
1.4
1.2
1.0
SWL
d
h
BREAKWATER C
SWL
12"
d
h
BREAKWATER D
0.2
0.4
0.6
0.8
1.0
h/d

FIGURE 35

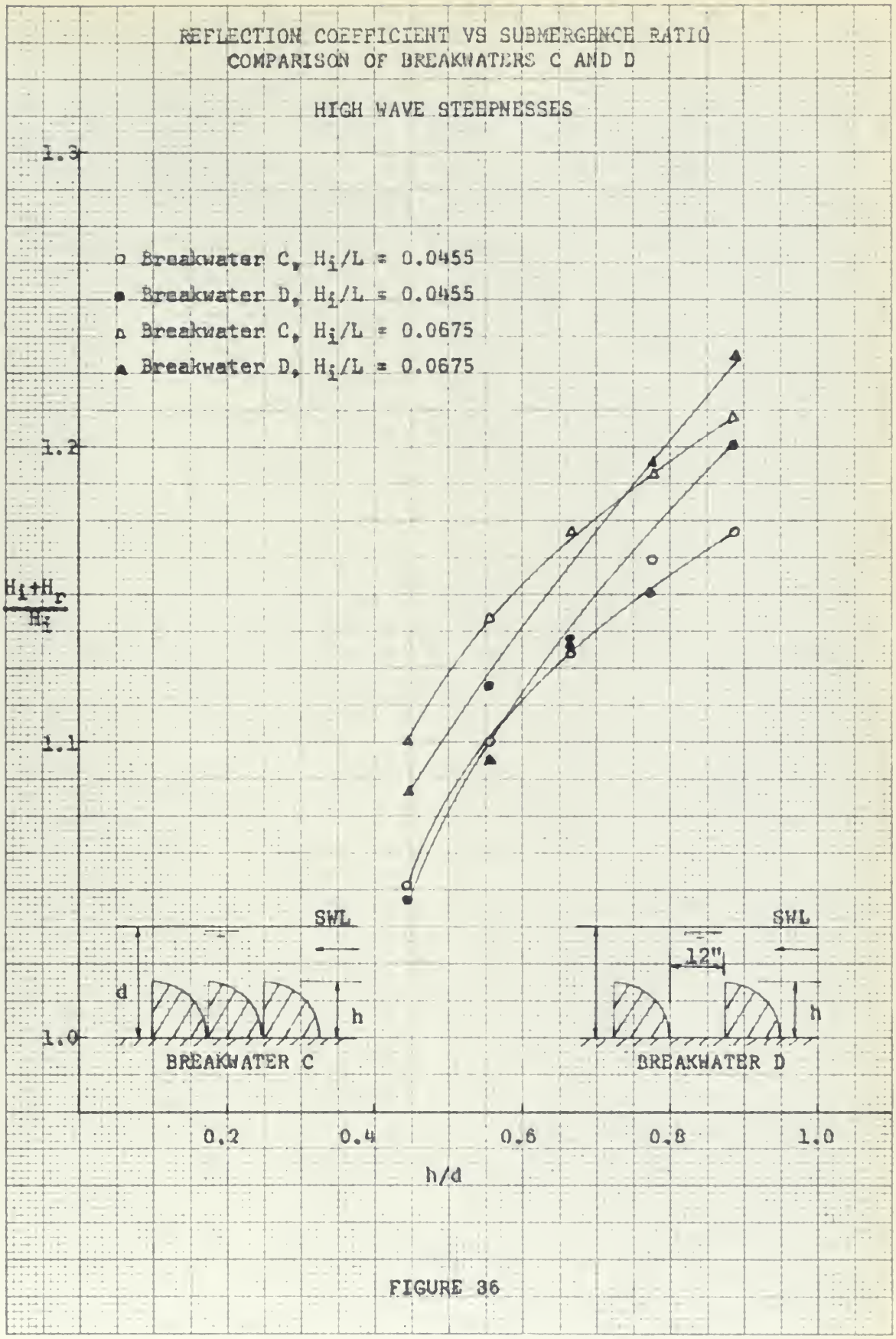
REFLECTION COEFFICIENT VS SUBMERGENCE RATIO
COMPARISON OF BREAKWATERS C AND D
HIGH WAVE STEEPNESSES
Breakwater C, Hi/L = 0.0455
Breakwater D, Hi/L = 0.0455
Breakwater C, Hi/L = 0.0675
Breakwater D, Hi/L = 0.0675
1.3
1.2
1.1
1.0
(Hi+Hr)/Hi
SWL
d
h
BREAKWATER C
SWL
12"
h
BREAKWATER D
0.2
0.4
0.6
0.8
1.0
h/d

FIGURE 36

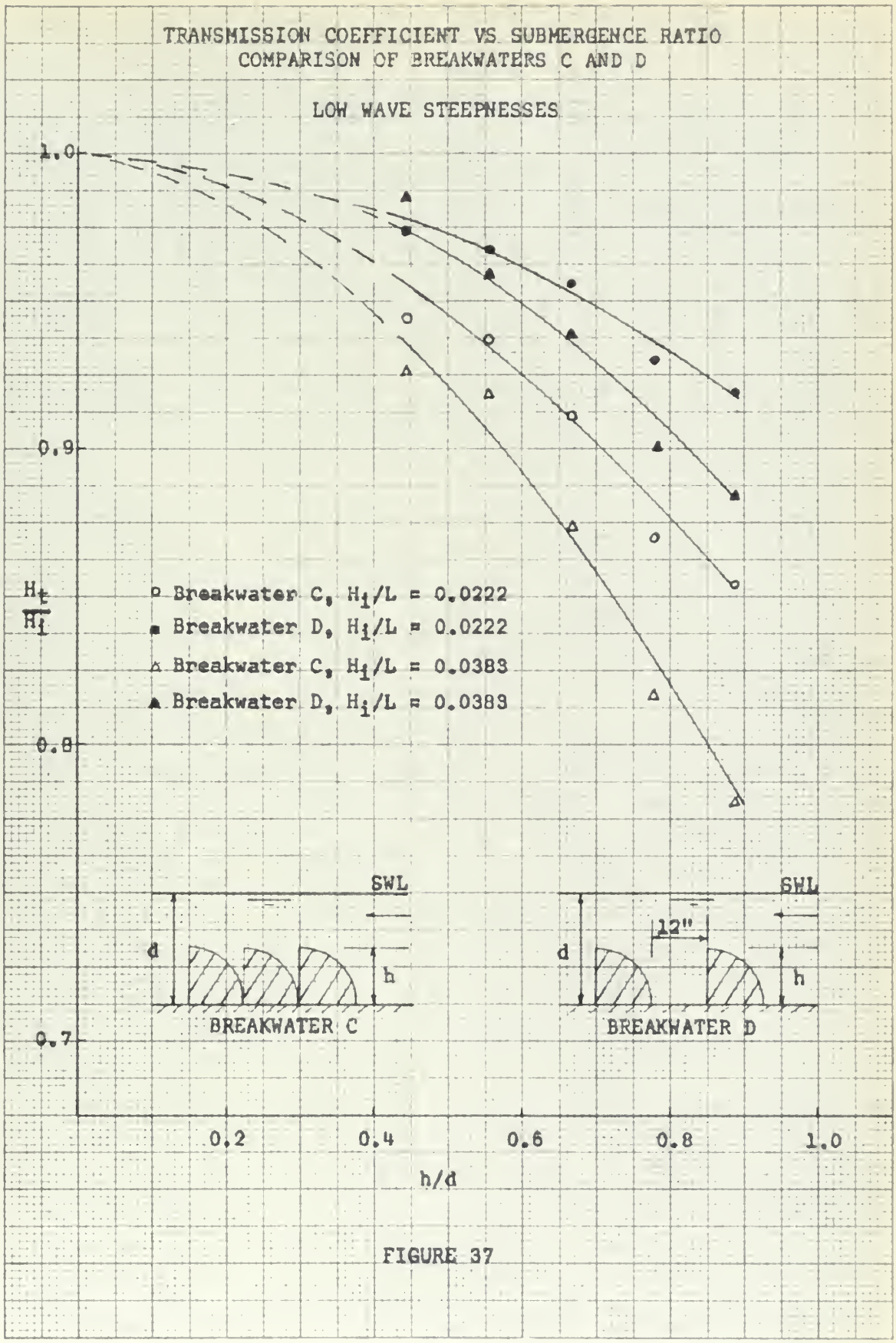
TRANSMISSION COEFFICIENT VS SUBMERGENCE RATIO
COMPARISON OF BREAKWATERS C AND D
LOW WAVE STEEPNESSES
1.0
0.9
0.8
0.7
$\frac{H_t}{H_i}$
Breakwater C, H_i/L = 0.0222
Breakwater D, H_i/L = 0.0222
Breakwater C, H_i/L = 0.0383
Breakwater D, H_i/L = 0.0383
SWL
d
h
BREAKWATER C
SWL
12"
d
h
BREAKWATER D
0.2
0.4
0.6
0.8
1.0
h/d

FIGURE 37

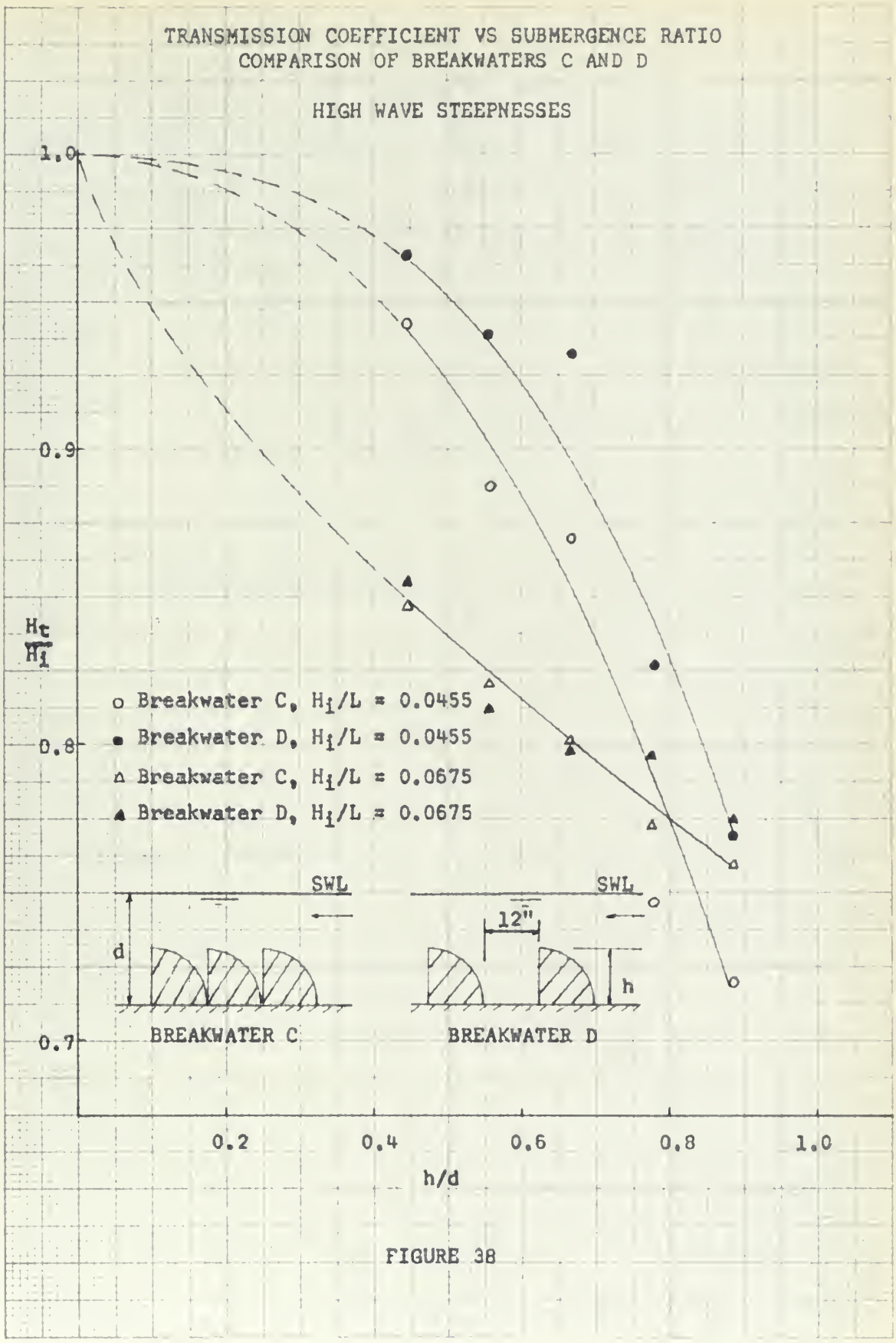
TRANSMISSION COEFFICIENT VS SUBMERGENCE RATIO
COMPARISON OF BREAKWATERS C AND D
HIGH WAVE STEEPNESSES
1.0
0.9
0.8
0.7
Ht/Hi
o Breakwater C, Hi/L = 0.0455
• Breakwater D, Hi/L = 0.0455
△ Breakwater C, Hi/L = 0.0675
▲ Breakwater D, Hi/L = 0.0675
SWL
d
BREAKWATER C
SWL
12"
h
BREAKWATER D
0.2
0.4
0.6
0.8
1.0
h/d

FIGURE 38

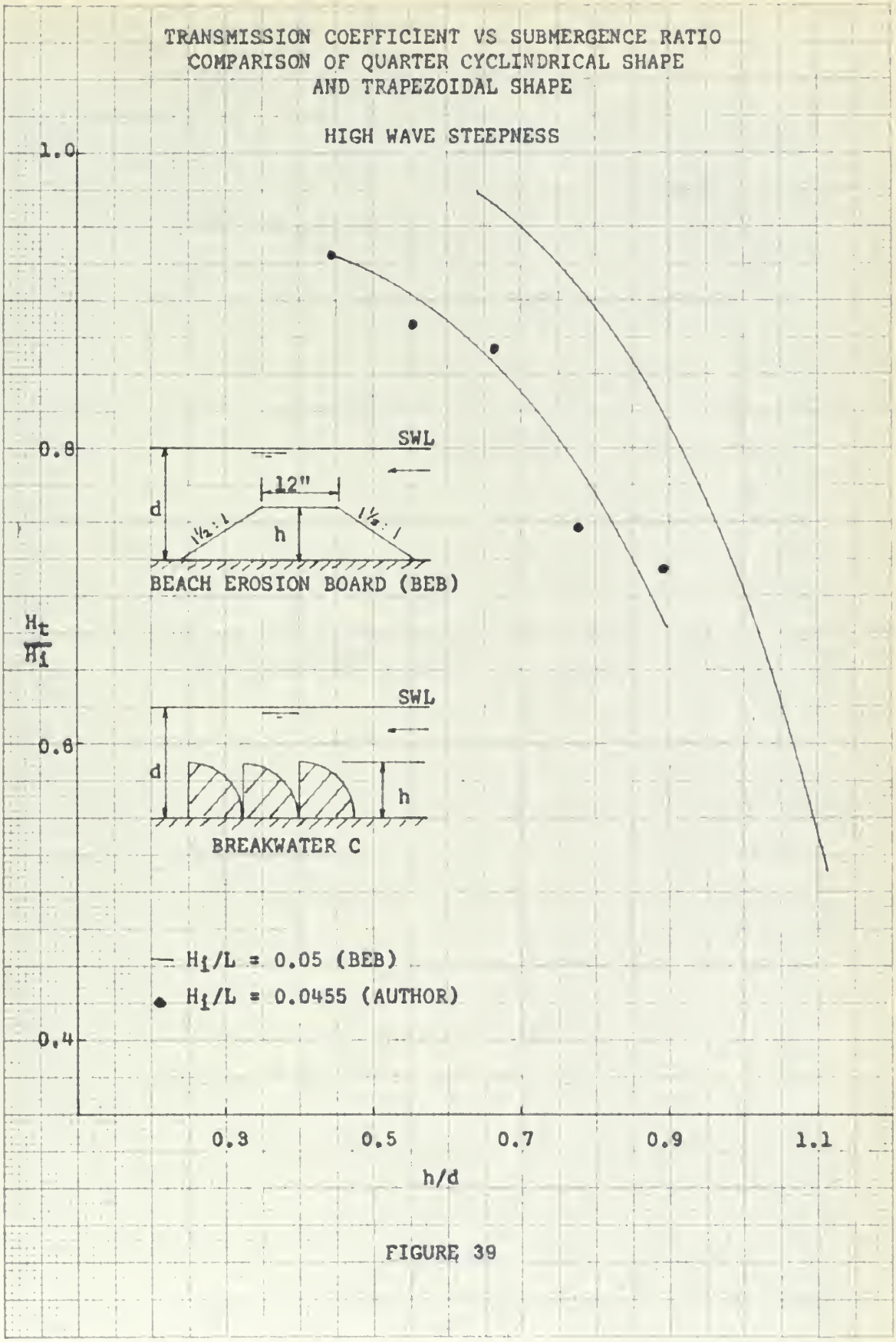
TRANSMISSION COEFFICIENT VS SUBMERGENCE RATIO
COMPARISON OF QUARTER CYCLINDRICAL SHAPE
AND TRAPEZOIDAL SHAPE
HIGH WAVE STEEPNESS
1.0
0.8
0.6
0.4
$\frac{H_t}{H_i}$
SWL
12"
d
h
1½ : 1
1½ : 1
BEACH EROSION BOARD (BEB)
SWL
d
h
BREAKWATER C
— H_i/L = 0.05 (BEB)
● H_i/L = 0.0455 (AUTHOR)
0.3
0.5
0.7
0.9
1.1
h/d

FIGURE 39

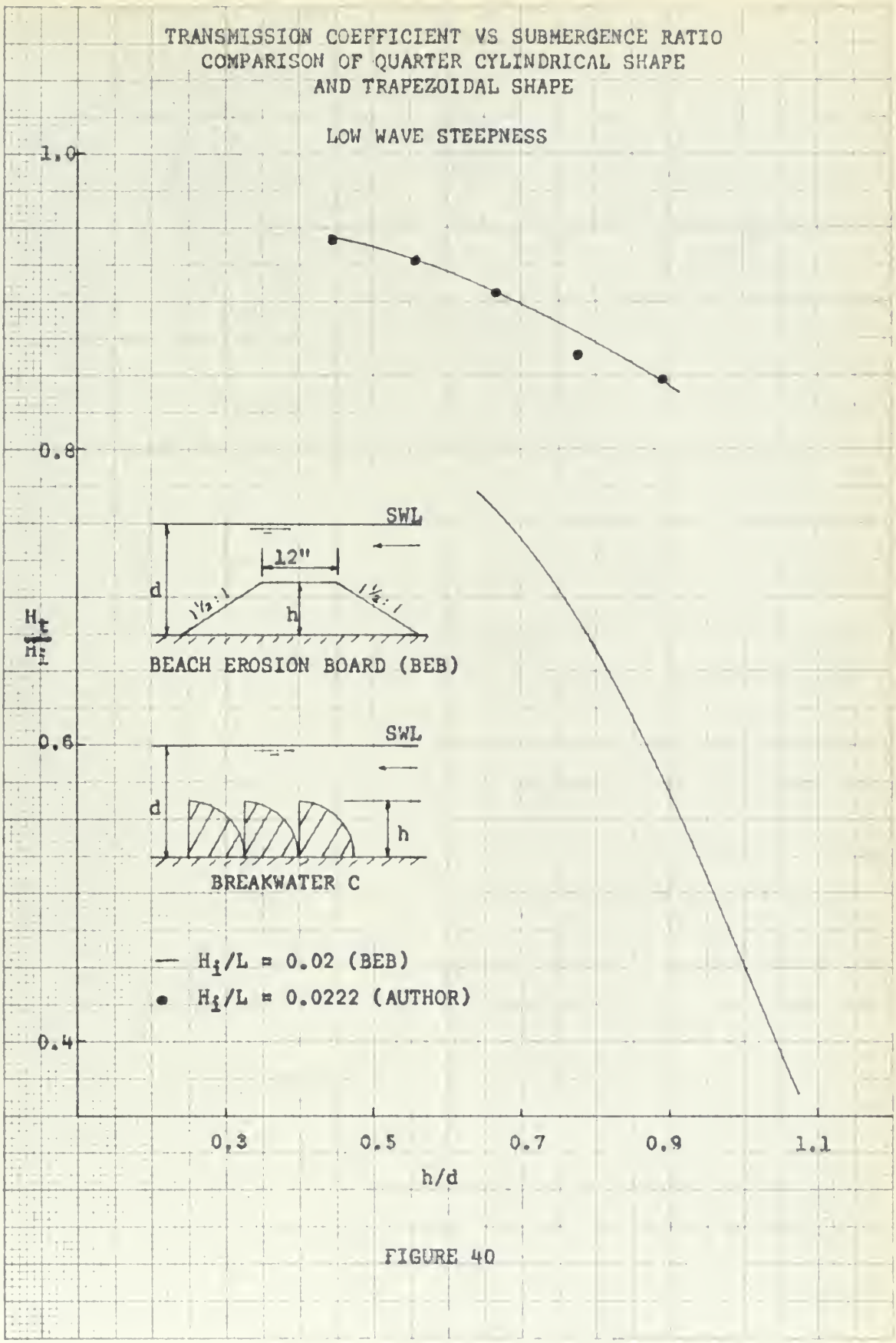
TRANSMISSION COEFFICIENT VS SUBMERGENCE RATIO
COMPARISON OF QUARTER CYLINDRICAL SHAPE
AND TRAPEZOIDAL SHAPE
LOW WAVE STEEPNESS
1.0
0.8
0.6
0.4
$\frac{H_t}{H_i}$
SWL
12"
d
1½:1
h
1½:1
BEACH EROSION BOARD (BEB)
SWL
d
h
BREAKWATER C
— H_i/L = 0.02 (BEB)
• H_i/L = 0.0222 (AUTHOR)
0.3
0.5
0.7
0.9
1.1
h/d

FIGURE 40

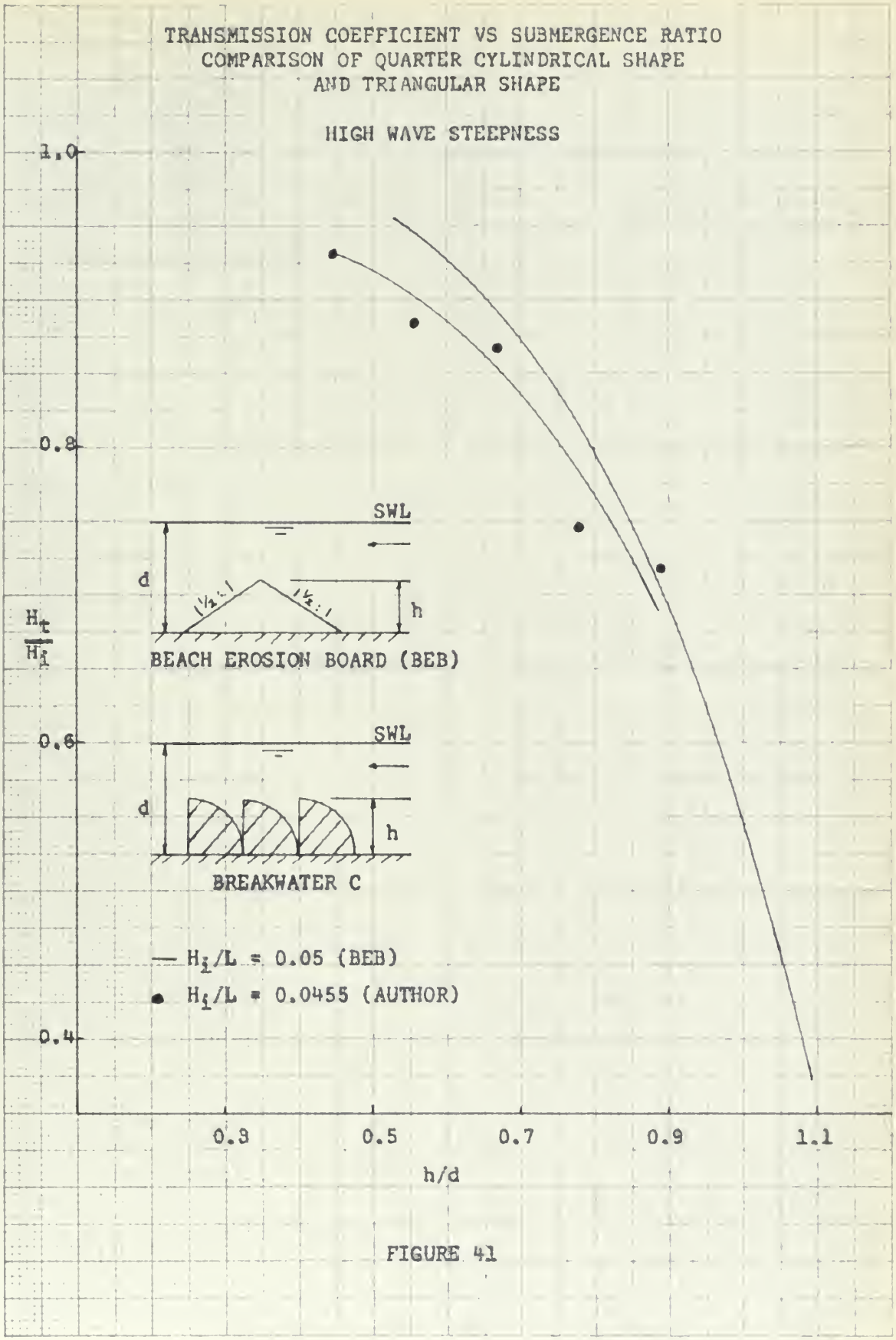
TRANSMISSION COEFFICIENT VS SUBMERGENCE RATIO
COMPARISON OF QUARTER CYLINDRICAL SHAPE
AND TRIANGULAR SHAPE
HIGH WAVE STEEPNESS
1.0
0.8
0.6
0.4
$\frac{H_t}{H_i}$
SWL
d
h
1½:1
1½:1
BEACH EROSION BOARD (BEB)
SWL
d
h
BREAKWATER C
— H_i/L = 0.05 (BEB)
• H_i/L = 0.0455 (AUTHOR)
0.3
0.5
0.7
0.9
1.1
h/d

FIGURE 41

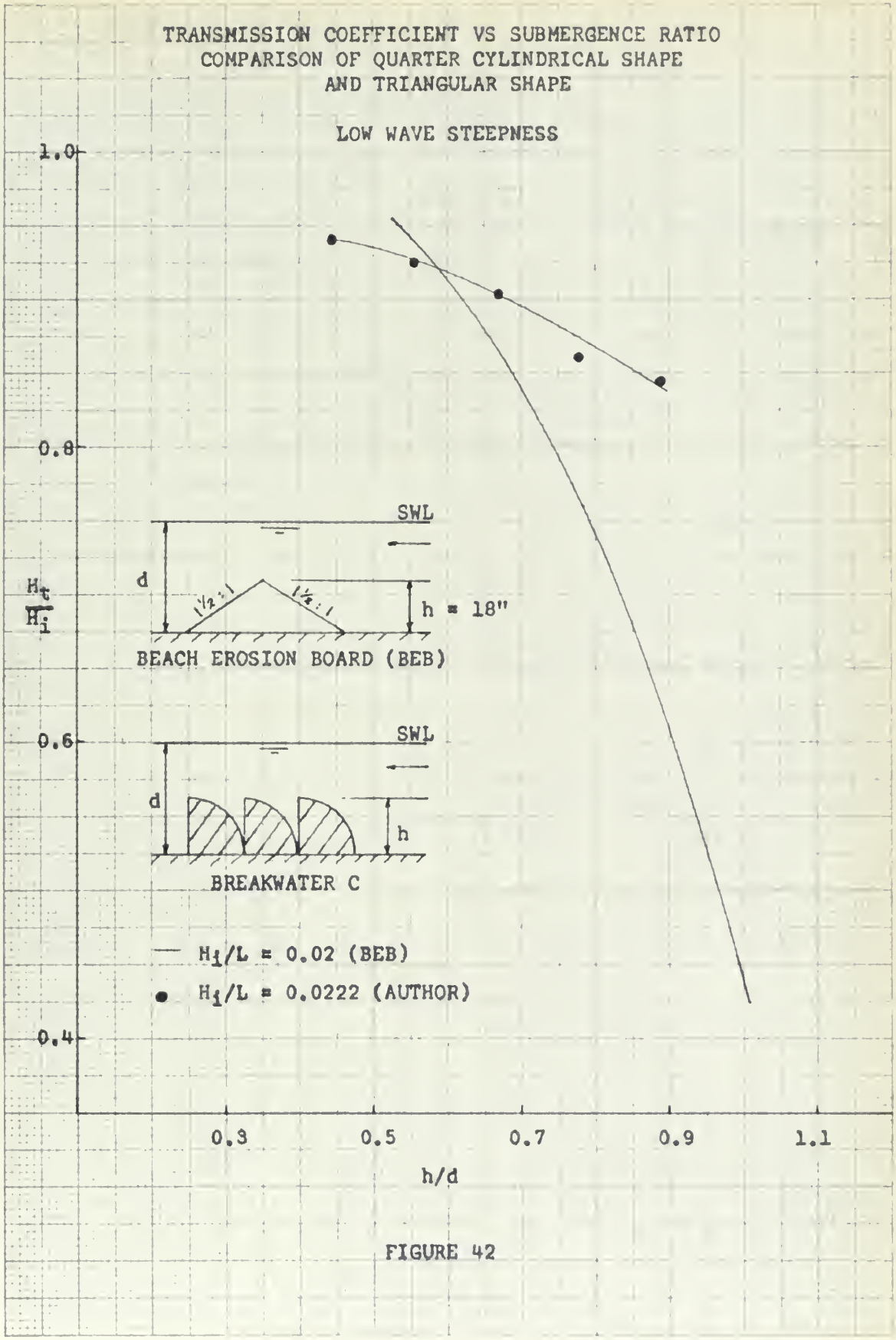
TRANSMISSION COEFFICIENT VS SUBMERGENCE RATIO
COMPARISON OF QUARTER CYLINDRICAL SHAPE
AND TRIANGULAR SHAPE
LOW WAVE STEEPNESS
1.0
0.8
0.6
0.4
$\frac{H_t}{H_i}$
SWL
d
1½:1
1¼:1
h = 18"
BEACH EROSION BOARD (BEB)
SWL
d
h
BREAKWATER C
H_i/L = 0.02 (BEB)
H_i/L = 0.0222 (AUTHOR)
0.3
0.5
0.7
0.9
1.1
h/d

FIGURE 42

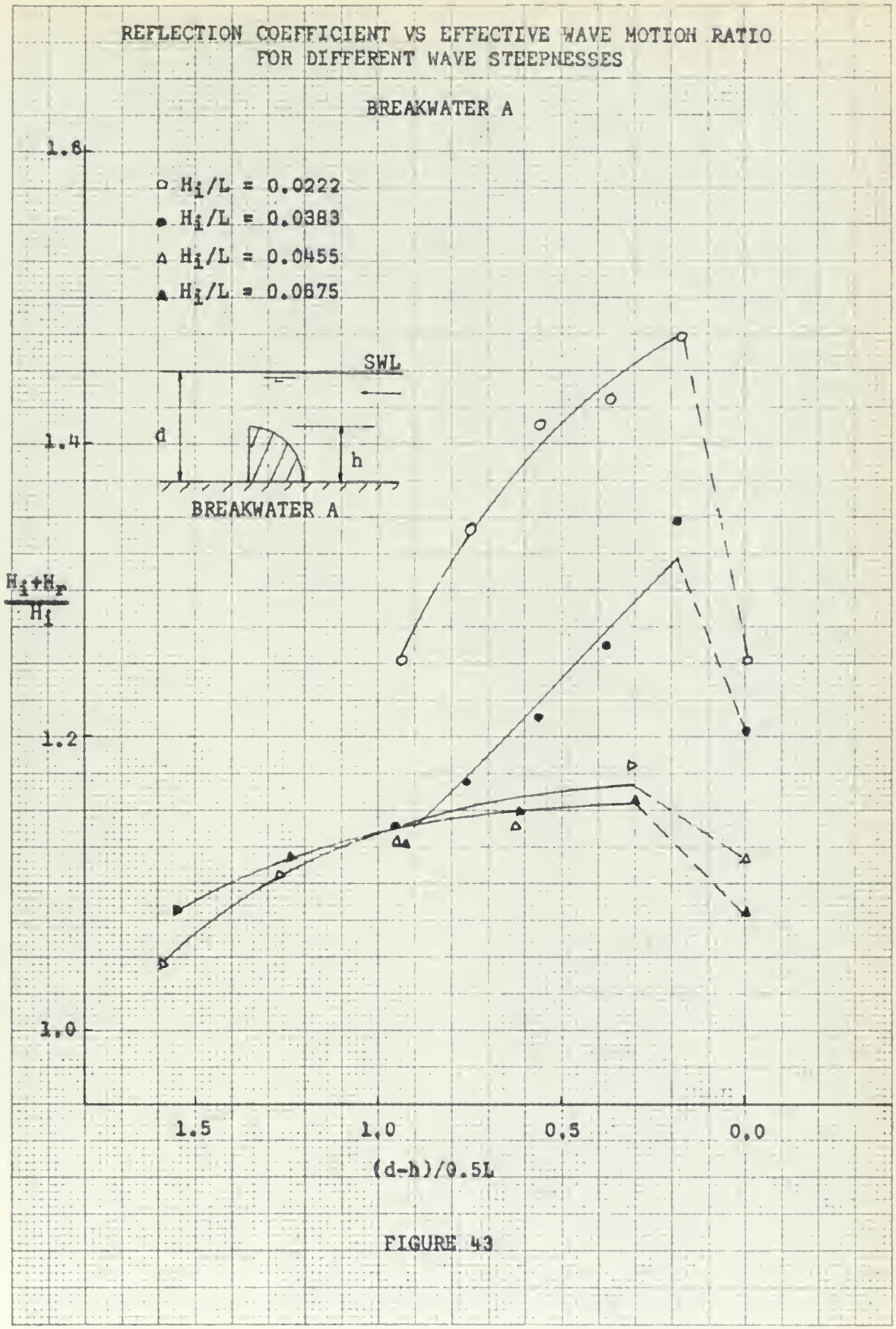
REFLECTION COEFFICIENT VS EFFECTIVE WAVE MOTION RATIO
FOR DIFFERENT WAVE STEEPNESSES
BREAKWATER A
1.6
1.4
1.2
1.0
H_i/L = 0.0222
H_i/L = 0.0383
H_i/L = 0.0455
H_i/L = 0.0875
SWL
d
h
BREAKWATER A
$\frac{H_i+H_r}{H_i}$
1.5
1.0
0.5
0.0
(d-h)/0.5L

FIGURE 43

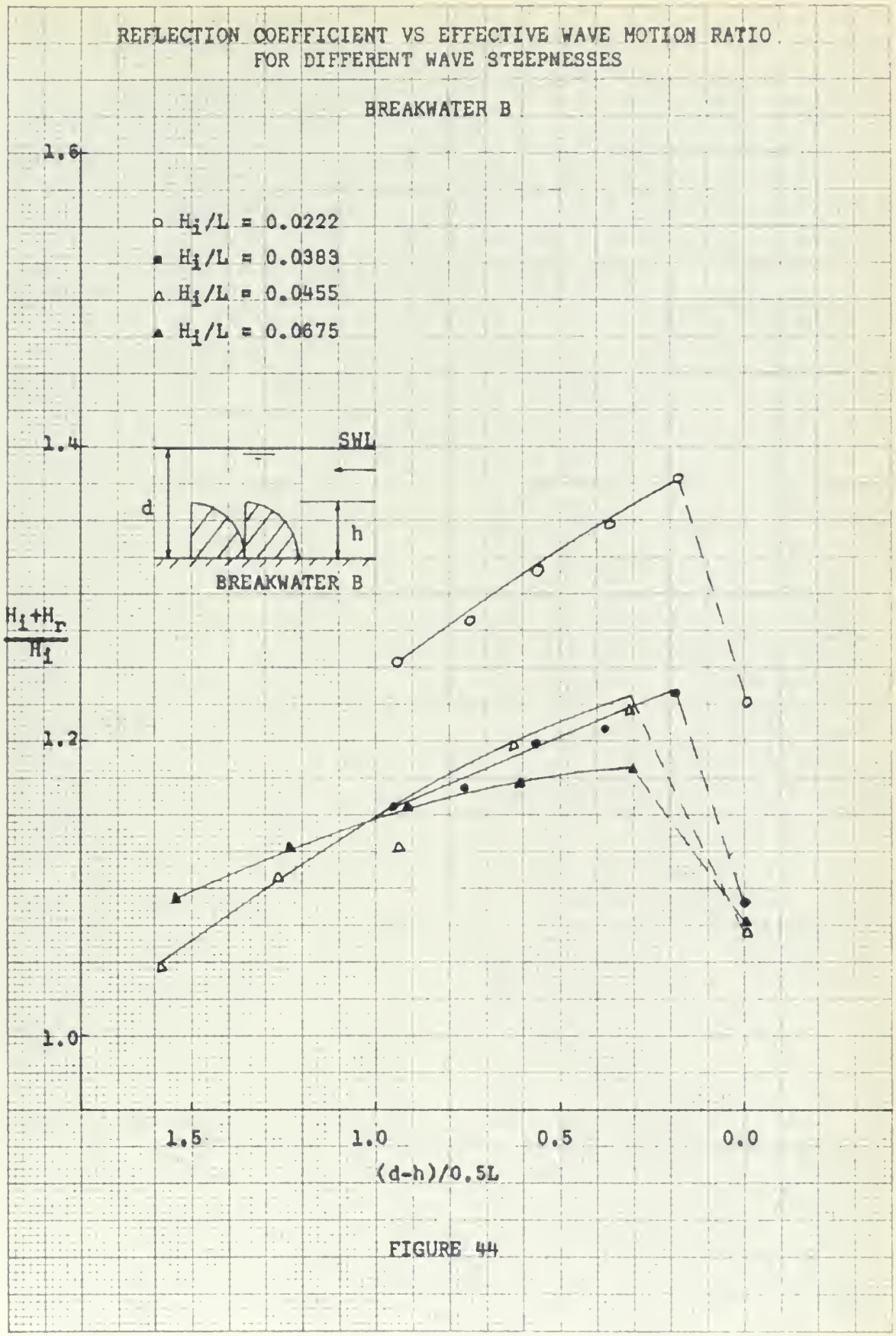
REFLECTION COEFFICIENT VS EFFECTIVE WAVE MOTION RATIO
FOR DIFFERENT WAVE STEEPNESSES
BREAKWATER B
1.6
1.4
1.2
1.0
○ Hi/L = 0.0222
● Hi/L = 0.0383
△ Hi/L = 0.0455
▲ Hi/L = 0.0675
SWL
d
h
BREAKWATER B
Hi+Hr / Hi
1.5
1.0
0.5
0.0
(d-h)/0.5L

FIGURE 44

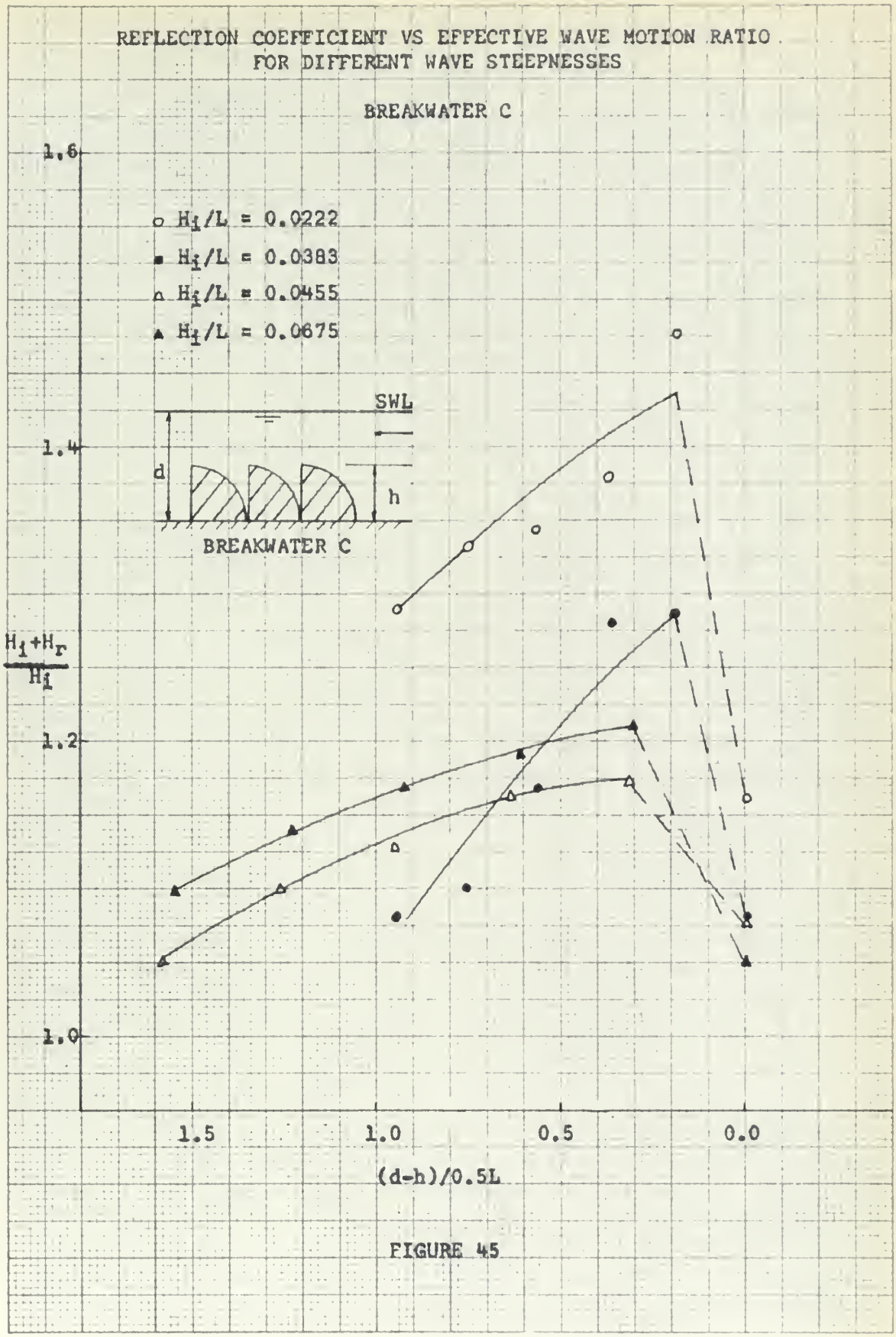
REFLECTION COEFFICIENT VS EFFECTIVE WAVE MOTION RATIO
FOR DIFFERENT WAVE STEEPNESSES
BREAKWATER C
1.6
1.4
1.2
1.0
o Hi/L = 0.0222
■ Hi/L = 0.0383
▵ Hi/L = 0.0455
▲ Hi/L = 0.0675
SWL
d
h
BREAKWATER C
(Hi+Hr)/Hi
1.5
1.0
0.5
0.0
(d-h)/0.5L

FIGURE 45

REFLECTION COEFFICIENT VS EFFECTIVE WAVE MOTION RATIO
FOR DIFFERENT WAVE STEEPNESSES

BREAKWATER D

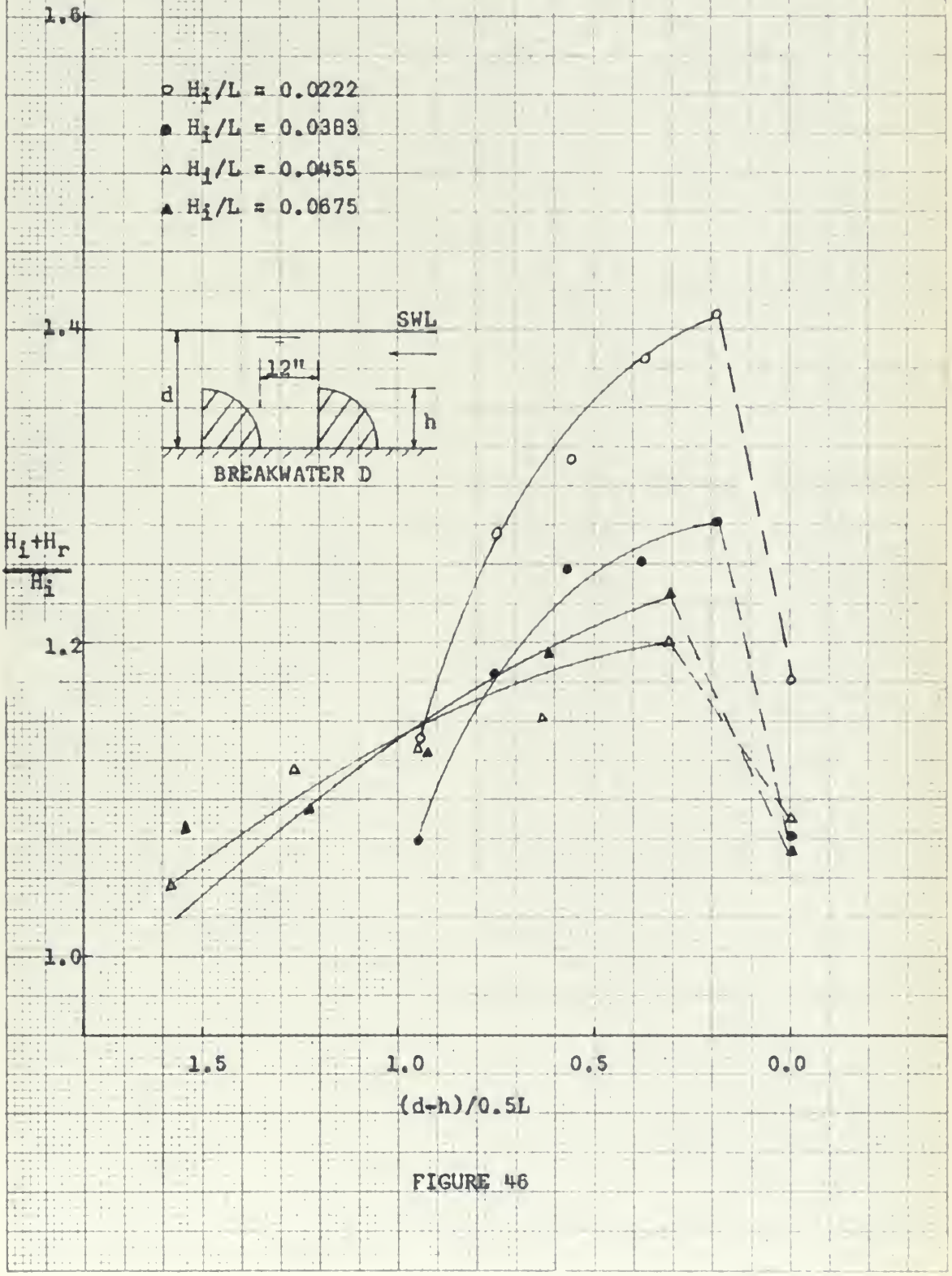

FIGURE 46

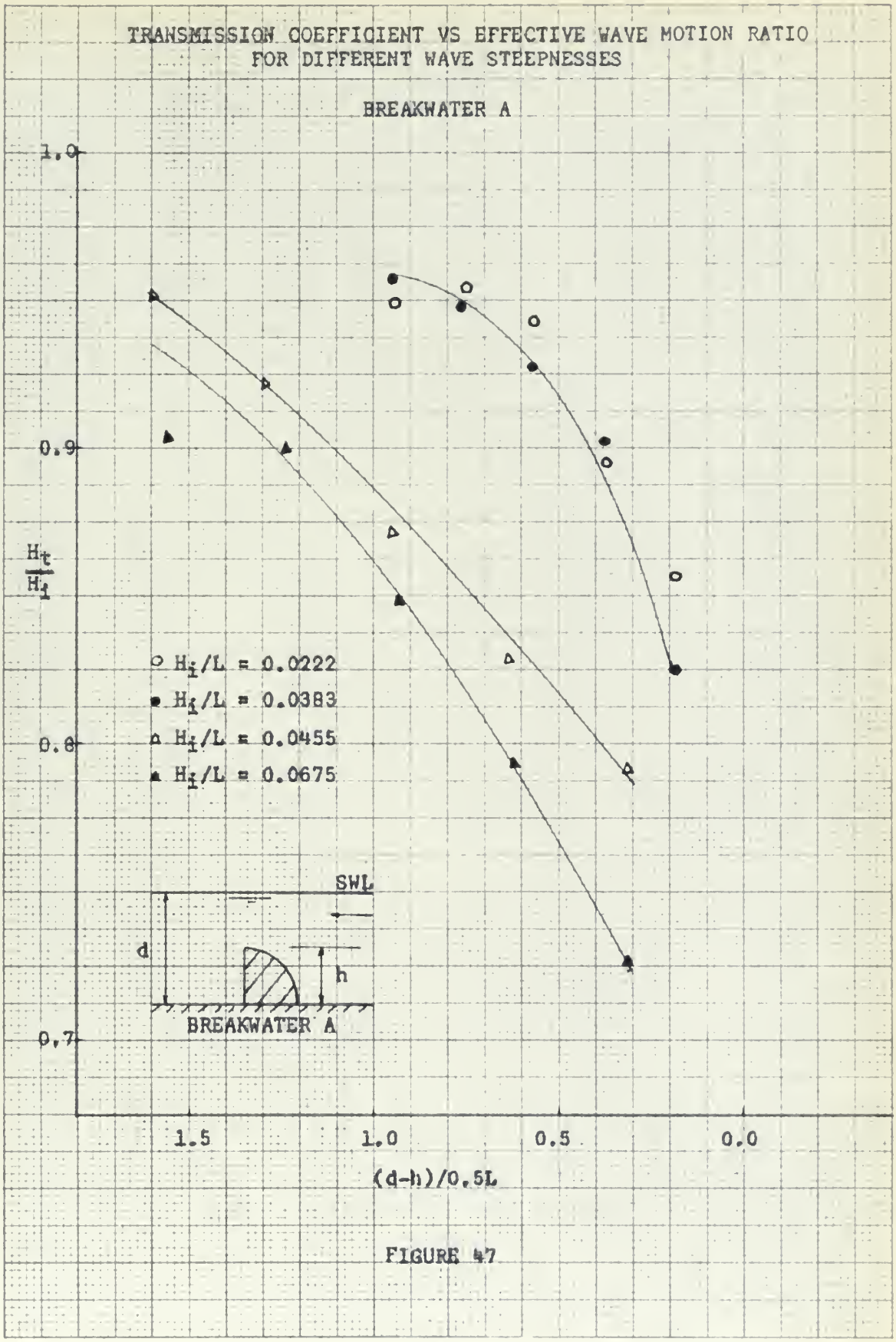
TRANSMISSION COEFFICIENT VS EFFECTIVE WAVE MOTION RATIO
FOR DIFFERENT WAVE STEEPNESSES
BREAKWATER A
1.0
0.9
0.8
0.7
$\frac{H_t}{H_i}$
○ H_i/L = 0.0222
● H_i/L = 0.0383
△ H_i/L = 0.0455
▲ H_i/L = 0.0675
SWL
d
h
BREAKWATER A
1.5
1.0
0.5
0.0
(d-h)/0.5L

FIGURE 47

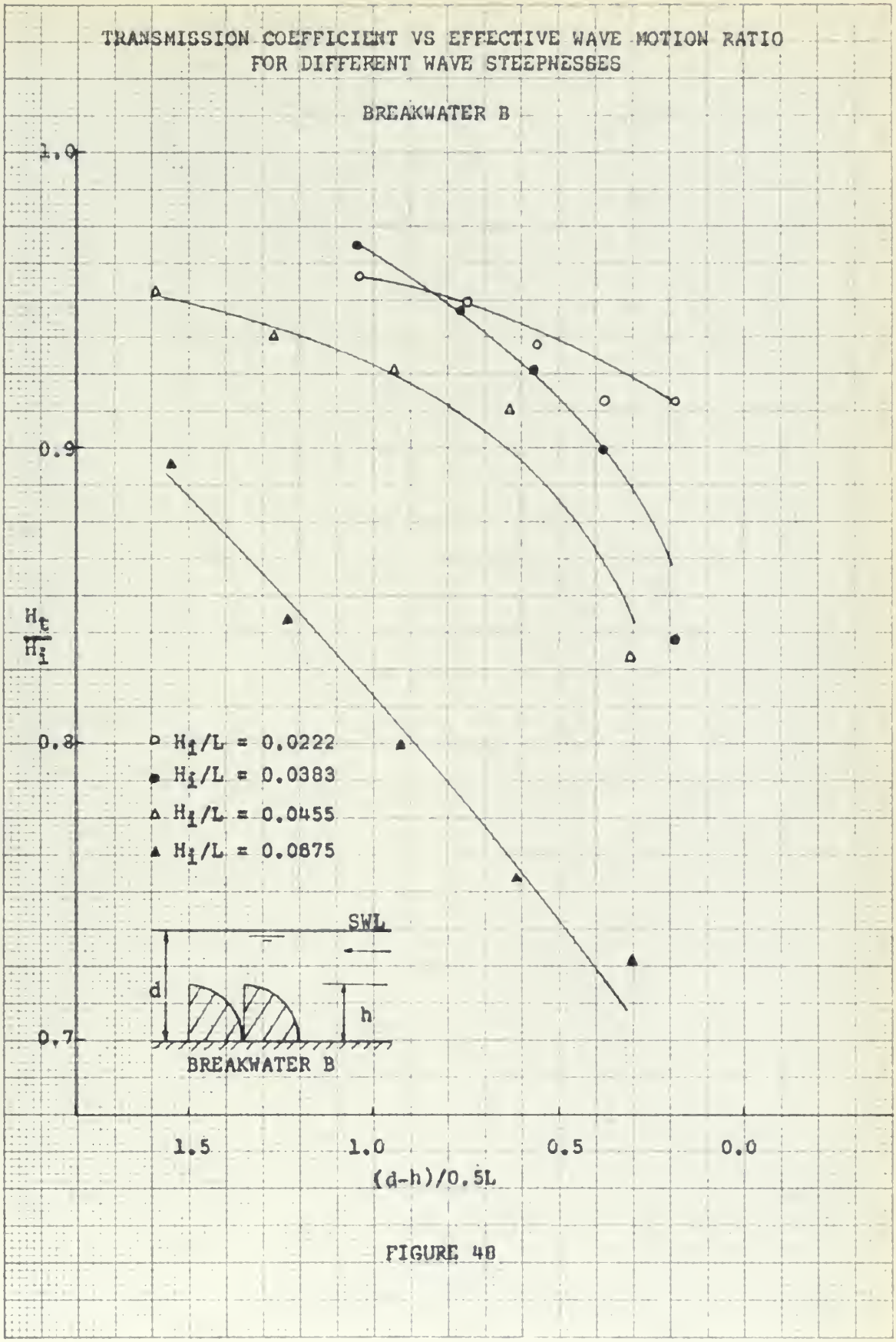
TRANSMISSION COEFFICIENT VS EFFECTIVE WAVE MOTION RATIO
FOR DIFFERENT WAVE STEEPNESSES
BREAKWATER B
1.0
0.9
0.8
0.7
$\frac{H_t}{H_i}$
H_i/L = 0.0222
H_i/L = 0.0383
H_i/L = 0.0455
H_i/L = 0.0875
SWL
d
h
BREAKWATER B
1.5
1.0
0.5
0.0
(d-h)/0.5L

FIGURE 48

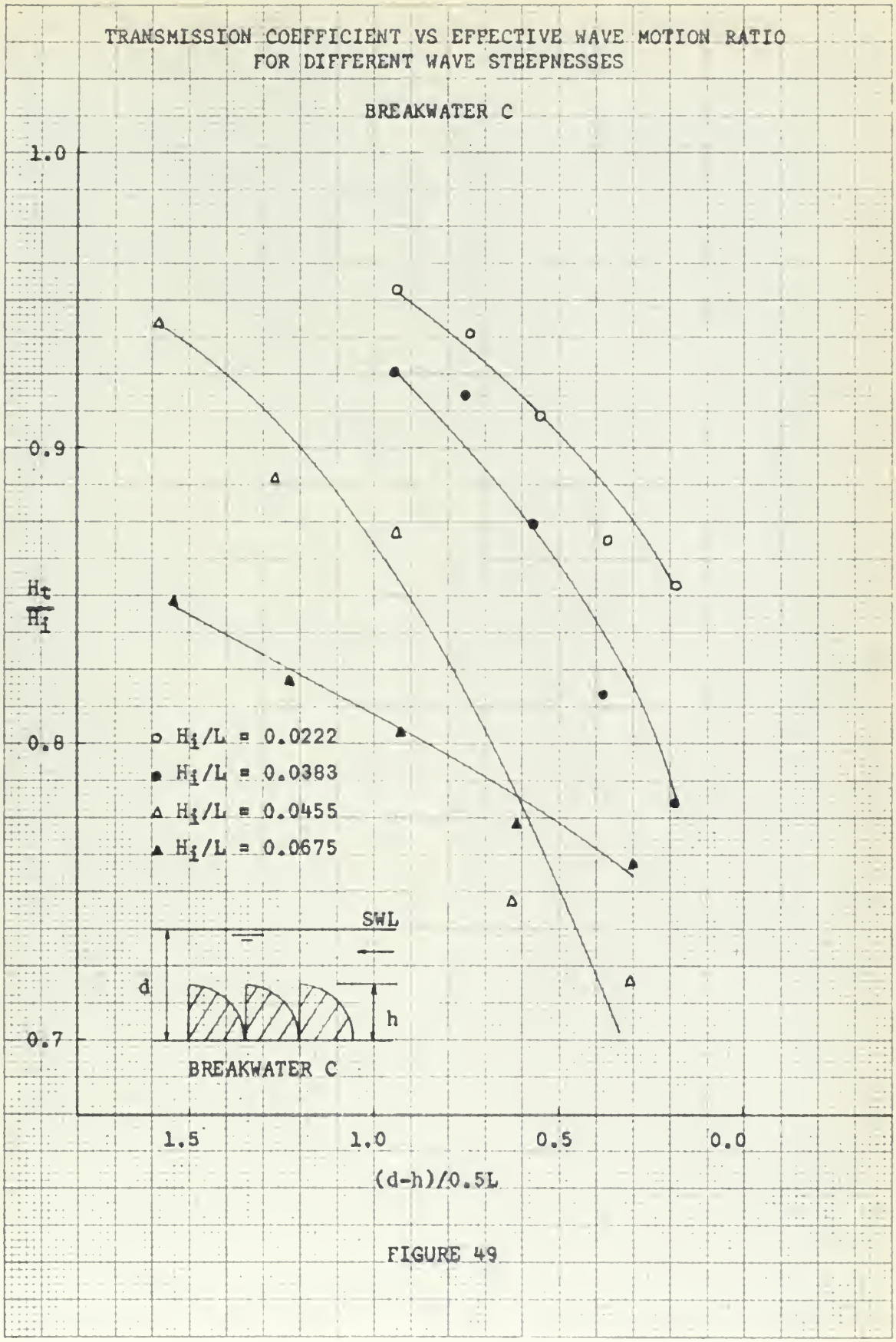
TRANSMISSION COEFFICIENT VS EFFECTIVE WAVE MOTION RATIO
FOR DIFFERENT WAVE STEEPNESSES
BREAKWATER C
1.0
0.9
0.8
0.7
$\frac{H_t}{H_i}$
○ H_i/L = 0.0222
● H_i/L = 0.0383
△ H_i/L = 0.0455
▲ H_i/L = 0.0675
SWL
d
h
BREAKWATER C
1.5
1.0
0.5
0.0
(d-h)/0.5L

FIGURE 49

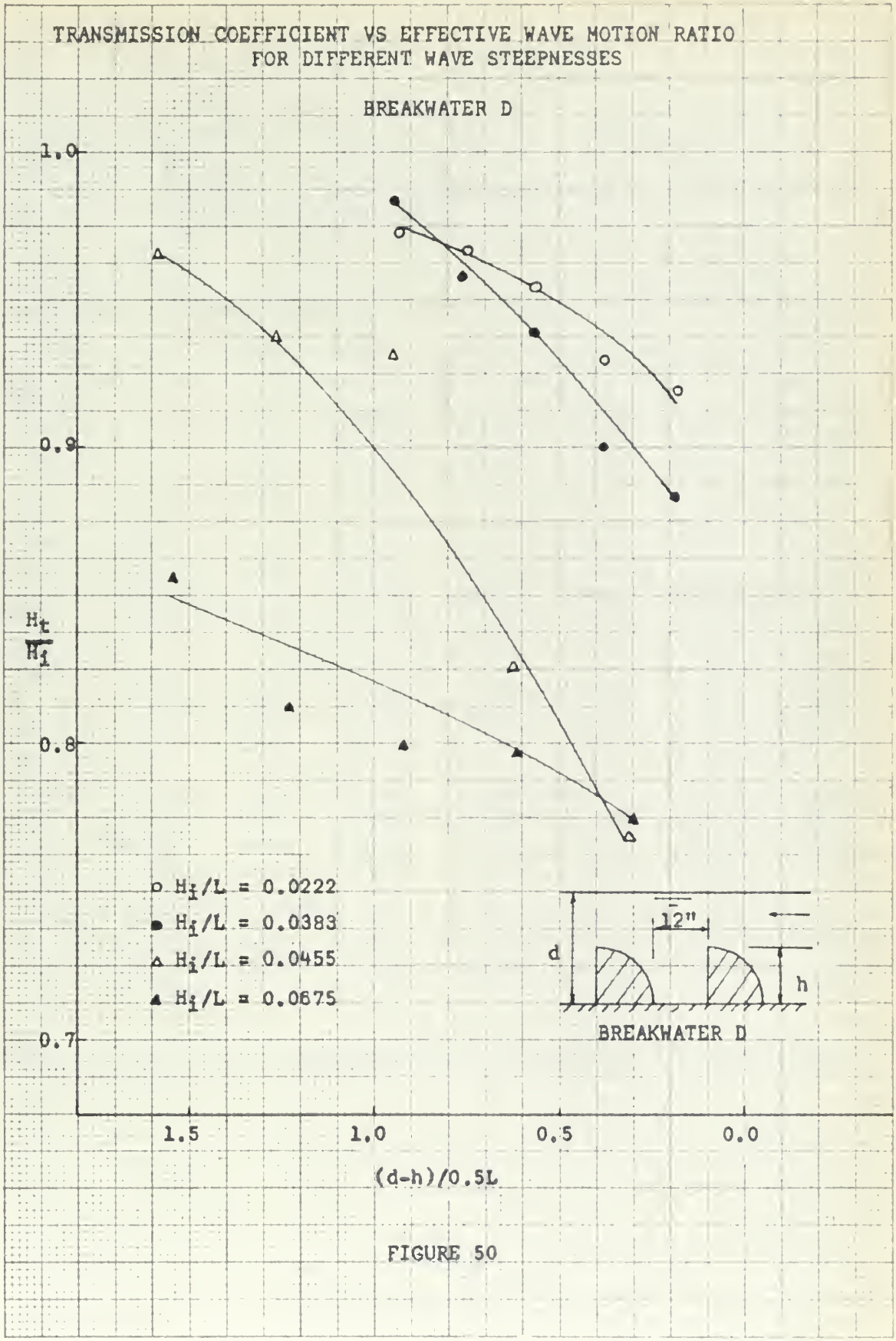
TRANSMISSION COEFFICIENT VS EFFECTIVE WAVE MOTION RATIO
FOR DIFFERENT WAVE STEEPNESSES
BREAKWATER D
1.0
0.9
0.8
0.7
$\frac{H_t}{H_i}$
H_i/L = 0.0222
H_i/L = 0.0383
H_i/L = 0.0455
H_i/L = 0.0675
12"
d
h
BREAKWATER D
1.5
1.0
0.5
0.0
(d-h)/0.5L

FIGURE 50

TABLE I

EXPERIMENTAL DATA - SUBMERGENCE RATIO
BREAKWATER A

h/d	H_i	L	H_i/L	H_i+H_r	$(H_i+H_r)H_i$	H_t	H_t/H_i
0.445	0.710	31.9	0.0222	0.890	1.252	0.674	0.949
	1.210	31.6	0.0383	1.380	1.140	1.160	0.958
	0.860	18.9	0.0455	0.900	1.047	0.820	0.953
	1.310	19.4	0.0675	1.420	1.083	1.190	0.909
0.556	0.710	31.9	0.0222	0.953	1.340	0.679	0.955
	1.210	31.6	0.0383	1.418	1.170	1.145	0.947
	0.860	18.9	0.0455	0.953	1.107	0.794	0.923
	1.310	19.4	0.0675	1.462	1.117	1.181	0.902
0.667	0.710	31.9	0.0222	1.001	1.411	0.665	0.937
	1.210	31.6	0.0383	1.470	1.214	1.128	0.932
	0.860	18.9	0.0455	0.973	1.130	0.750	0.873
	1.310	19.4	0.0675	1.483	1.132	1.110	0.848
0.778	0.710	31.9	0.0222	1.016	1.431	0.643	0.891
	1.210	31.6	0.0383	1.528	1.262	1.098	0.906
	0.860	18.9	0.0455	0.983	1.142	0.713	0.829
	1.310	19.4	0.0675	1.508	1.150	1.040	0.794
0.889	0.710	31.9	0.0222	1.046	1.472	0.614	0.864
	1.210	31.6	0.0383	1.630	1.348	1.000	0.827
	0.860	18.9	0.0455	1.018	1.182	0.681	0.792
	1.310	19.4	0.0675	1.515	1.157	0.953	0.727

TABLE II

EXPERIMENTAL DATA - SUBMERGENCE RATIO
BREAKWATER B

h/d	H_i	L	H_i/L	H_i+H_r	$(H_i+H_r)/H_i$	H_t	H_t/H_i
0.445	0.710	31.9	0.0222	0.893	1.256	0.680	0.958
	1.210	31.6	0.0383	1.400	1.157	1.170	0.968
	0.860	18.9	0.0455	0.900	1.047	0.820	0.953
	1.310	19.4	0.0675	1.430	1.092	1.170	0.894
0.556	0.710	31.9	0.0222	0.912	1.283	0.674	0.949
	1.210	31.6	0.0383	1.415	1.169	1.145	0.947
	0.860	18.9	0.0455	0.953	1.108	0.807	0.938
	1.310	19.4	0.0675	1.475	1.126	1.101	0.842
0.667	0.710	31.9	0.0222	0.935	1.317	0.665	0.936
	1.210	31.6	0.0383	1.452	1.200	1.120	0.927
	0.860	18.9	0.0455	1.010	1.174	0.796	0.926
	1.310	19.4	0.0675	1.515	1.156	1.047	0.799
0.778	0.710	31.9	0.0222	0.958	1.349	0.651	0.917
	1.210	31.6	0.0383	1.461	1.209	1.087	0.898
	0.860	18.9	0.0455	1.030	1.198	0.785	0.913
	1.310	19.4	0.0675	1.535	1.171	0.988	0.754
0.889	0.710	31.9	0.0222	0.980	1.380	0.650	0.916
	1.210	31.6	0.0383	1.493	1.233	1.010	0.835
	0.860	18.9	0.0455	1.048	1.218	0.712	0.828
	1.310	19.4	0.0675	1.545	1.179	0.953	0.727

TABLE III

EXPERIMENTAL DATA - SUBMERGENCE RATIO
BREAKWATER C

h/d	H_i	L	H_i/L	H_i+H_r	$(H_i+H_r)H_i$	H_t	H_t/H_i
0.445	0.710	31.9	0.0222	0.917	1.291	0.670	0.944
	1.210	31.6	0.0383	1.310	1.082	1.120	0.926
	0.860	18.9	0.0455	0.905	1.051	0.810	0.942
	1.310	19.4	0.0675	1.440	1.100	1.110	0.848
0.556	0.710	31.9	0.0222	0.946	1.332	0.665	0.937
	1.210	31.6	0.0383	1.331	1.101	1.110	0.918
	0.860	18.9	0.0455	0.955	1.100	0.763	0.887
	1.310	19.4	0.0675	1.495	1.141	1.075	0.821
0.667	0.710	31.9	0.0222	0.955	1.344	0.646	0.911
	1.210	31.6	0.0383	1.415	1.169	1.058	0.874
	0.860	18.9	0.0455	0.971	1.129	0.748	0.871
	1.310	19.4	0.0675	1.535	1.171	1.052	0.804
0.778	0.710	31.9	0.0222	0.980	1.380	0.617	0.869
	1.210	31.6	0.0383	1.460	1.208	0.989	0.817
	0.860	18.9	0.0455	1.000	1.162	0.643	0.747
	1.310	19.4	0.0675	1.560	1.190	1.012	0.773
0.889	0.710	31.9	0.0222	1.048	1.475	0.606	0.854
	1.210	31.6	0.0383	1.560	1.288	0.943	0.780
	0.860	18.9	0.0455	1.009	1.172	0.629	0.720
	1.310	19.4	0.0675	1.587	1.210	0.996	0.760

TABLE IV

EXPERIMENTAL DATA - SUBMERGENCE RATIO
BREAKWATER D

h/d	H_i	L	H_i/L	H_i+H_r	$(H_i+H_r)/H_i$	H_t	H_t/H_i
0.445	0.710	31.9	0.0222	0.810	1.140	0.690	0.973
	1.210	31.6	0.0383	1.300	1.074	1.190	0.984
	0.860	18.9	0.0455	0.900	1.047	0.830	0.965
	1.310	19.4	0.0675	1.420	1.083	1.120	0.855
0.556	0.710	31.9	0.0222	0.903	1.270	0.686	0.967
	1.210	31.6	0.0383	1.429	1.180	1.160	0.958
	0.860	18.9	0.0455	0.963	1.119	0.860	0.938
	1.310	19.4	0.0675	1.432	1.094	1.062	0.812
0.667	0.710	31.9	0.0222	0.935	1.316	0.679	0.956
	1.210	31.6	0.0383	1.508	1.245	1.137	0.939
	0.860	18.9	0.0455	0.976	1.134	0.801	0.932
	1.310	19.4	0.0675	1.486	1.131	1.044	0.798
0.778	0.710	31.9	0.0222	0.980	1.380	0.660	0.930
	1.210	31.6	0.0383	1.512	1.250	1.090	0.901
	0.860	18.9	0.0455	0.990	1.151	0.710	0.826
	1.310	19.4	0.0675	1.565	1.193	1.042	0.797
0.889	0.710	31.9	0.0222	1.000	1.409	0.654	0.919
	1.210	31.6	0.0383	1.545	1.276	1.070	0.884
	0.860	18.9	0.0455	1.032	1.201	0.662	0.769
	1.310	19.4	0.0675	1.612	1.231	1.012	0.774

TABLE V

EXPERIMENTAL DATA - SUBMERGENCE RATIO
BREAKWATER HEIGHT EQUALS STILLWATER DEPTH

BREAKWATER	h/d	H_i	L	H_i/L	H_i+H_r	$(H_i+H_r)/H_i$
A	1.00	0.710	31.9	0.0222	0.890	1.252
		1.210	31.6	0.0383	1.460	1.207
		0.860	18.9	0.0455	0.960	1.118
		1.310	19.4	0.0675	1.420	1.082
B	1.00	0.710	31.9	0.0222	0.870	1.226
		1.210	31.6	0.0383	1.320	1.091
		0.860	18.9	0.0455	0.920	1.070
		1.310	19.4	0.0675	1.410	1.077
C	1.00	0.710	31.9	0.0222	0.825	1.162
		1.210	31.6	0.0383	1.315	1.086
		0.860	18.9	0.0455	0.930	1.081
		1.310	19.4	0.0675	1.380	1.052
D	1.00	0.710	31.9	0.0222	0.835	1.176
		1.210	31.6	0.0383	1.300	1.075
		0.860	18.9	0.0455	0.935	1.088
		1.310	19.4	0.0675	1.400	1.069

TABLE VI

EXPERIMENTAL DATA - EFFECTIVE WAVE MOTION RATIO
BREAKWATER A

h	(d-h)/0.5L	H_i	L	H_i/L	$(H_i+H_r)/H_i$	H_t/H_i
12.0	0.940	0.710	31.9	0.0222	1.252	0.949
	0.950	1.210	31.6	0.0383	1.140	0.958
	1.588	0.860	18.9	0.0455	1.047	0.953
	1.547	1.310	19.4	0.0675	1.083	0.909
15.0	0.753	0.710	31.9	0.0222	1.340	0.955
	0.760	1.210	31.6	0.0383	1.170	0.947
	1.270	0.860	18.9	0.0455	1.107	0.923
	1.238	1.310	19.4	0.0675	1.117	0.902
18.0	0.564	0.710	31.9	0.0222	1.411	0.937
	0.570	1.210	31.6	0.0383	1.214	0.932
	0.953	0.860	18.9	0.0455	1.130	0.873
	0.928	1.310	19.4	0.0675	1.132	0.848
21.0	0.376	0.710	31.9	0.0222	1.431	0.891
	0.380	1.210	31.6	0.0383	1.262	0.906
	0.635	0.860	18.9	0.0455	1.142	0.829
	0.619	1.310	19.4	0.0675	1.150	0.794
24.0	0.188	0.710	31.9	0.0222	1.472	0.864
	0.190	1.210	31.6	0.0383	1.348	0.827
	0.318	0.860	18.9	0.0455	1.182	0.792
	0.309	1.310	19.4	0.0675	1.157	0.727

TABLE VII

EXPERIMENTAL DATA - EFFECTIVE WAVE MOTION RATIO
BREAKWATER B

h	(d-h)/0.5L	H_i	L	H_i/L	$(H_i+H_r)/H_i$	H_t/H_i
12.0	0.940	0.710	31.9	0.0222	1.256	0.358
	0.950	1.210	31.6	0.0383	1.157	0.968
	1.583	0.860	18.9	0.0455	1.047	0.953
	1.547	1.310	19.4	0.0675	1.092	0.894
15.0	0.753	0.710	31.9	0.0222	1.283	0.349
	0.760	1.210	31.6	0.0383	1.169	0.947
	1.270	0.860	18.9	0.0455	1.108	0.938
	1.233	1.310	19.4	0.0675	1.125	0.842
18.0	0.564	0.710	31.9	0.0222	1.317	0.936
	0.570	1.210	31.6	0.0383	1.200	0.927
	0.953	0.860	18.9	0.0455	1.174	0.926
	0.923	1.310	19.4	0.0675	1.155	0.799
21.0	0.376	0.710	31.9	0.0222	1.349	0.917
	0.380	1.210	31.6	0.0383	1.209	0.898
	0.635	0.860	18.9	0.0455	1.198	0.913
	0.619	1.310	19.4	0.0675	1.171	0.754
24.0	0.188	0.710	31.9	0.0222	1.380	0.916
	0.190	1.210	31.6	0.0383	1.233	0.835
	0.318	0.860	18.9	0.0455	1.218	0.828
	0.309	1.310	19.4	0.0675	1.179	0.727

TABLE VIII

EXPERIMENTAL DATA - EFFECTIVE WAVE MOTION RATIO
BREAKWATER C

h	h/y	H_i	L	H_i/L	$(H_i+H_r)/H_i$	H_t/H_i
12.0	0.940	0.710	31.9	0.0222	1.291	0.944
	0.950	1.210	31.6	0.0383	1.082	0.926
	1.588	0.860	18.9	0.0455	1.051	0.942
	1.547	1.310	19.4	0.0675	1.100	0.848
15.0	0.753	0.710	31.9	0.0222	1.332	0.937
	0.760	1.210	31.6	0.0383	1.101	0.918
	1.270	0.860	18.9	0.0455	1.100	0.887
	1.238	1.310	19.4	0.0675	1.141	0.821
18.0	0.564	0.710	31.9	0.0222	1.344	0.911
	0.570	1.210	31.6	0.0383	1.169	0.874
	0.953	0.860	18.9	0.0455	1.129	0.871
	0.928	1.310	19.4	0.0675	1.171	0.804
21.0	0.376	0.710	31.9	0.0222	1.380	0.869
	0.380	1.210	31.6	0.0383	1.280	0.817
	0.635	0.860	18.9	0.0455	1.162	0.747
	0.619	1.310	19.4	0.0675	1.190	0.773
24.0	0.188	0.710	31.9	0.0222	1.475	0.854
	0.190	1.210	31.6	0.0383	1.288	0.780
	0.318	0.860	18.9	0.0455	1.172	0.720
	0.309	1.310	19.4	0.0675	1.210	0.760

TABLE IX

EXPERIMENTAL DATA - EFFECTIVE WAVE MOTION RATIO
BREAKWATER D

h	(d-h)/0.5L	H_i	L	H_i/L	$(H_i+H_r)/H_i$	H_t/H_i
12.0	0.940	0.710	31.9	0.0222	1.140	0.973
	0.950	1.210	31.6	0.0383	1.074	0.984
	1.588	0.860	18.9	0.0455	1.047	0.965
	1.547	1.310	19.4	0.0675	1.083	0.855
15.0	0.753	0.710	31.9	0.0222	1.270	0.967
	0.760	1.210	31.6	0.0383	1.180	0.958
	1.270	0.860	18.9	0.0455	1.119	0.938
	1.238	1.310	19.4	0.0675	1.094	0.812
18.0	0.564	0.710	31.9	0.0222	1.316	0.956
	0.570	1.210	31.6	0.0383	1.245	0.939
	0.953	0.860	18.9	0.0455	1.134	0.932
	0.923	1.310	19.4	0.0675	1.131	0.798
21.0	0.376	0.710	31.9	0.0222	1.380	0.930
	0.380	1.210	31.6	0.0383	1.250	0.901
	0.635	0.860	18.9	0.0455	1.151	0.826
	0.619	1.310	19.4	0.0675	1.193	0.797
24.0	0.188	0.710	31.9	0.0222	1.409	0.919
	0.190	1.210	31.6	0.0383	1.276	0.884
	0.318	0.860	18.9	0.0455	1.201	0.769
	0.309	1.310	19.4	0.0675	1.231	0.774

TABLE X

EXPERIMENTAL DATA - EFFECTIVE WAVE MOTION RATIO
BREAKWATER HEIGHT EQUALS STILLWATER DEPTH

BREAKWATER	h	(d-h)/0.5L	H_i	L	H_i/L	$(H_i+H_r)/H_i$
A	27.0	0.000	0.710	31.9	0.0222	1.252
		0.000	1.210	31.6	0.0383	1.207
		0.000	0.860	18.9	0.0455	1.118
		0.000	1.310	19.4	0.0675	1.082
B	27.0	0.000	0.710	31.9	0.0222	1.226
		0.000	1.210	31.6	0.0383	1.091
		0.000	0.860	18.9	0.0455	1.070
		0.000	1.310	19.4	0.0675	1.077
C	27.0	0.000	0.710	31.9	0.0222	1.162
		0.000	1.210	31.6	0.0383	1.082
		0.000	0.860	18.9	0.0455	1.081
		0.000	1.310	19.4	0.0675	1.052
D	27.0	0.000	0.710	31.9	0.0222	1.176
		0.000	1.210	31.6	0.0383	1.075
		0.000	0.860	18.9	0.0455	1.088
		0.000	1.310	19.4	0.0675	1.069

TABLE XI

LIST OF SYMBOLS

H_i = Height of incident wave

H_t = Height of transmitted wave

$H_i + H_r$ = Measured height of superimposed incident and reflected waves

L = Wave length

d = Stillwater depth

h = Height of breakwater

W = Width (parallel to tank walls) of breakwater

h/d = Submergence ratio

$(H_i + H_r)/H_i$ = Reflection coefficient

H_t/H_i = Transmission coefficient

H_i/L = Wave steepness

W/L = Relative breakwater width

d/L = Relative depth

(d-h)/0.5L = Effective wave motion ratio

SWL = Still Water Level

BIBLIOGRAPHY

BIBLIOGRAPHY

1. Beach Erosion Board, Corps of Engineers, U. S. Army. "A Model Study of the Effects of Submerged Breakwaters on Wave Action". War Department, Technical Memorandum No. 1, Washington: May 15, 1940.

2. Beach Erosion Board, Corps of Engineers, U. S. Army. "A Wave Method for Determining Depths over Bottom Discontinuities". War Department, Military Intelligence Division, Technical Memorandum No. 5, Washington: May, 1944.

3. Hamilton, W. S. "Forces Exerted by Waves on a Sloping Board". Transactions, American Geophysical Union, Vol. XXXI (1950), pages 849-855.

4. Johnson, J. W., R. A. Fuchs, and J. R. Morison. "The Damping Action of Submerged Breakwaters". Transactions, American Geophysical Union, Vol. XXXII, No. 5 (1951), pages 704-718.

5. Priest, Melville S. "Reduction of Wave Heights by Submerged Offshore Structures". Engineering Experiment Station, Bulletin No. 34, Alabama Polytechnic Institute, Auburn, Alabama, Nov., 1958.

6. May, Gerald W. "Transmission and Reflection of Deep Water Waves From a Submerged Sill"., unpublished Master of Science Thesis, Department of Civil Engineering, University of Colorado, 1964.

7. Le Mehaute, B., and A. Brebner. "An Introduction to the Mathematical Theories of Two-Dimensional Periodic Progressive Waves". Queen's University at Kingston, Civil Engineering Report No. 11, Kingston, Ontario, July 1960.

8. Le Mehaute, B. and J. I. Collins. "Clapotis and Wave Reflection." Queen's University at Kingston, Civil Engineering Report No. 13, Kingston, Ontario, January 1961.

9. Dean, W. R. "On the Reflexion of Surface Waves by a Submerged Circular Cylinder". Proceedings, Cambridge Philosophical Society, Vol. 44 (1948), pages 483-491.

10. Dean, W. R. "On the Reflexion of Surface Waves by a Submerged Plane Barrier". Proceedings, Cambridge Philosophical Society, Vol. 41 (1945), pages 231-238.

11. Ursell, F. "Fixed Vertical Barrier Effect on Surface Waves in Deep Water". Proceedings, Cambridge Philosophical Society, Vol. 43, (1947), pages 374-382.

12. Johnson, Fuchs and Morison. "The Damping Action of Submerged Breakwaters". Trans., AGU, Vol. XXXII, No. 5 (1951), Page 715.

13. Lamb, Horace. Hydrodynamics. Fourth Edition. New York: Dover Publications, 1945.

14. Coyer, C. B. "A Multipurpose Wave Generator". Proceedings, International Hydraulic Convention, Minneapolis, Minnesota, Sept. 1953, pages 281-291.

15. Stoker, J. J. Water Waves. Interscience Publishers, Inc., New York, 1957.

16. Johnson, Fuchs and Morison, "The Damping Action of Submerged Breakwaters". Trans., AGU, Vol. XXXII, No. 5 (1951), Page 712.

thesM655
Transmission and reflection of deep wate
3 2768 001 89136 9
DUDLEY KNOX LIBRARY